LA-NUREG-6896-MS

Informal Report

NRC-1 and UC-34c

Comparisons of Calculated and Experimental Delayed Fission-Product Beta and Gamma Spectra from ^{235}U Thermal Fission

Issued: July 1977

los alamos
scientific laboratory
of the University of California
LOS ALAMOS, NEW MEXICO 87545

UNITED STATES
ENERGY RESEARCH AND DEVELOPMENT ADMINISTRATION
CONTRACT W-7405-ENG. 36

This work was supported by the US Nuclear Regulatory Commission,
Division of Safeguards, Fuel Cycle and Environmental Research.

Printed in the United States of America. Available from
National Technical Information Service
U.S. Department of Commerce
5285 Port Royal Road
Springfield, VA 22161
Price: Printed Copy $4.50 Microfiche $3.00

LA-NUREG-6896-MS
Informal Report
NRC-1 and UC-34c

los alamos
scientific laboratory
of the University of California
LOS ALAMOS, NEW MEXICO 87545

Comparisons of Calculated and Experimental Delayed Fission-Product Beta and Gamma Spectra from ^{235}U Thermal Fission

T. R. England
M. G. Stamatelatos

Manuscript completed: July 1977
Issued: July 1977

Prepared for the US Nuclear Regulatory Commission
Office of Nuclear Regulatory Research

COMPARISONS OF CALCULATED AND EXPERIMENTAL DELAYED FISSION-PRODUCT BETA AND GAMMA SPECTRA FROM ^{235}U THERMAL FISSION

by

T. R. England and M. G. Stamatelatos

ABSTRACT

Delayed fission-product beta and gamma spectra following short and long ^{235}U thermal neutron irradiations (0.015 s, 1 s, 10 s, 100 s, 5.56 h, and 8 h) were calculated for a number of cooling periods. The results of these calculations, based on ENDF/B-IV fission-product data, are compared with corresponding experimental data available recently from several research establishments (Los Alamos Scientific Laboratory, Oak Ridge National Laboratory, and the University of Illinois). These comparisons show generally good agreement between calculations and experiments and indicate the adequacy of ENDF/B-IV data for such calculations.

I. INTRODUCTION

Considerable national and international effort has been placed in recent years on obtaining a reliable computational and experimental basis for determining accurate fission-product decay heat and spectral source terms. These data are needed for a number of fissionable nuclides important in nuclear reactor safety, safeguards, and other studies. Some of this research has been motivated by the need to predict and avoid the occurrence of a hypothetical loss-of-coolant accident (LOCA). From the nuclear regulatory standpoint, accurate evaluations of decay-heat sources have been needed for the improvement of standards governing the design and operation of nuclear reactors.

The computational results reported here cover an important component of fission-product decay sources, namely delayed beta and gamma spectra. Comparisons have been made between computed spectra and beta and gamma spectra measured at the Los Alamos Scientific Laboratory (LASL), Oak Ridge National Laboratory (ORNL), and the University of Illinois (UI). Results of these comparisons are reported here in graphic form for delayed beta and gamma spectra and in tabular form for corresponding total energy release rates. In this report, these comparisons, like the measured spectra, are limited to ^{235}U thermal fission; however, the results tend to qualify the data base for all fuels because differences arise only due to fission product yields (for the same irradiation history).

The irradiation times used in the various calculational and experimental comparisons in this report may be of limited direct interest. The purpose of this report is to examine the adequacy of the data base used in the calculations; the calculational models can then be used for irradiation and cooling times of more specific interest to users.

II. DECAY SPECTRA

The primary requirements for calculating reliable fission-product decay spectra are a complete and accurate input data base and adequate computational methods.

The starting point for our computational procedure has been the use of the fission-product Evaluated Nuclear Data Files (ENDF/B) Version IV;[1] these data and corrections are extensively summarized in Refs. 2 and 3. These files, which are among the most complete sources of information of this kind in the world, contain fission yields, neutron cross sections below 20 MeV, and decay data for 824 fission products. Beta and gamma spectral data are included for 180 important nuclides.

The computational tools at LASL include a code system consisting of three computer programs, CINDER-10, FPDCYS, and FPSPEC. In the spectral calculations, CINDER-10 is used to calculate fission-product activities and total beta and gamma decay energies at the desired irradiation and cooling times. The FPDCYS code calculates multigroup spectra of the individual fission products using the gamma energies and intensities and beta end-point energies and intensities contained in ENDF/B-IV. The FPSPEC code combines the outputs of CINDER-10 and FPDCYS in any desired multigroup structure to calculate the aggregate fission-product spectra. Details on these computer programs can be found in Refs. 4-6.

The experimental beta spectra compared in this report with our calculations are from the University of Illinois[7] and from the Oak Ridge National Laboratory.[8,9] The experimental gamma spectra are from the Los Alamos Scientific Laboratory,[10,11] and the Oak Ridge National Laboratory.[8,9]

A. Data Libraries and Details of the Calculations

The CINDER-10 library contains all decay parameters (half-lives, branching ratios, total β and γ decay energies), yields, and cross sections necessary to compute the coupled buildup of nuclide densities, activities, energies, etc., for all 824 nuclides in ENDF/B-IV. The basic spectral library produced by FPDCYS that is used in this report consists of multigroup spectra for the 180 nuclides having spectral data in ENDF/B-IV. For beta energies, we have used 75 groups in a uniform 100-keV binning between 0 and 7.5 MeV. The beta spectra are derived from the end-point energies and intensities using the accurate procedure described in Ref. 4; the resulting spectra are listed in Ref. 5.

The gamma spectra are in 150 groups in a uniform 50 keV binning between 0 and 7.5 MeV. When comparing calculated and experimental gamma spectra it is necessary to broaden the lines before grouping when using a fine group structure in order to match the finite resolution and energy dependence of the gamma spectrometer used by each experimenter. Two gamma libraries were therefore generated --one for the LASL and one for the ORNL comparisons. Each gamma line at energy E_0 was assumed to be a Gaussian having an area equal to the line intensity, I:[4]

$$G = \frac{I}{\sqrt{2\pi}\,\sigma} \exp\left[-\frac{(E-E_0)^2}{2\sigma^2} \right] .$$

The value of σ at E_0 was prescribed by the experimenter. The unbroadened 150-group spectra are listed in Ref. 5.

In this report we have compared the total energy in each bin rather than total yield per bin. This has the advantage of visually displaying the energy release over the energy axis; a division of the energy plots by the abscissa energy would provide the more conventional spectra in terms of yields. The actual plots are for the quantity

$$\text{MeV/Fission/bin} \equiv \frac{\text{MeV/s/bin}}{\text{Fission/s}} \quad .$$

The quantity MeV/s/bin is the energy release rate per bin at the specified mean cooling (decay) time (or, as will be noted, an average over the measurement count time). The quantity Fissions/s is the fission rate prior to initiation of the cooling interval; this rate was held constant in each experiment. To the extent that neutron absorption can be ignored, the decay energy release rate is simply the plotted value times any user-specified fission rate.

For most cooling times of interest to users of the ENDF/B-IV based data, the 180 nuclides account for >90% of the total decay energy. As will be noted in the tabular comparisons of integral energy release rates, some of the experiments have very short cooling times wherein the 180 nuclides do not account for the bulk of the energy. In all comparisons we have multiplied the calculated spectra by the ratio of the calculated energy from all nuclides to the integrated energy calculated from the 180 nuclides. That is, the spectral shape determined from the 180 nuclides having spectral data is assumed to define the shape of all nuclides. This will be improved as more spectral data are added to future versions of ENDF/B; in the meantime, we are augmenting the ENDF/B-IV library with other spectral data.

There is one other problem in using ENDF/B-IV data in the tabular comparisons of energy-integrated data. The ENDF/B-IV files contain internal electron conversion coefficients for only 38 nuclides. In tabular comparisons of integral gamma data, we have shown the comparison with and without electron conversion energies; this comparison is based only on the electron conversion coefficients contained in ENDF/B-IV. (Spectral comparisons do not include the electron conversion energies).

All measured spectra are necessarily based on a finite counting time. We have examined the difference between using an integration of the calculated values over the counting interval and that obtained using the rate at the mid-point of the interval. For the spectral comparison plots, there is no observable difference. For the energy integrated values, the difference is ~1% (i.e., the energy release rate at the mid-point or mean time is ~1% lower than the average over the counting interval). In the ORNL tabular comparisons, we have used the time average of the integrated values over the counting interval because these data will be used in defining a new decay heat standard. For the UI and LASL comparisons we have used calculated rates at the tabulated mean time. The ~1% difference in the two methods is considerably smaller than the uncertainty in the experimental values.

For the tabular comparisons with the ORNL data, we have used the most recent data tabulated in Ref. 9, a draft report subject to change. The units of MeV/fission used in the present report and in the draft form of Ref. 9 are different quantities. In effect, the values in Ref. 9 are an integration of MeV/s over the counting interval divided by the number of fissions. Therefore, the values extracted from that reference were multiplied by the ratio of the fission time

to the counting time in order to obtain the same type of quantity tabulated for the other experiments. This results in the conventional quantity

$$\text{MeV/fission} \equiv \frac{\text{MeV/s}}{\text{Fissions/s}} \quad ,$$

where MeV/s is, in this case, an average over the counting interval. Reference 9 in draft form also tabulates an "average time" which is defined there as the cooling time up to the start of the counting period plus 1/2 of the sum of the fission and counting times. In the present report, the mean and decay times always refer the decay time (subsequent to the fission interval) up to the mid-point of the counting interval.

The irradiation times of all experiments are too brief to cause significant effects due to the coupling of nuclides by neutron absorption; however, individual nuclide densities produced directly in fission or by decay coupling will be lowered by a significant cross section. Therefore, the cross sections were included for these comparisons using the flux levels (10^{12} to 10^{13} n cm^2-s) specified for the experiments. The less significant effects of neutron absorption coupling are also included.

B. Results

Tables I, II, and III provide comparisons of energy integrated values (total beta and gamma MeV/fission) and the fraction of total energy due to those nuclides having spectral data; as previously noted, these determine the calculated spectral shape. Uncertainties in integral data have been tabulated only for the ORNL data. The reader interested in these integral comparisons should also consult Refs. 7, 9, and 10; the latter two references were only in draft form as this report was being prepared and are subject to minor changes. The LASL gamma experiment will likely be repeated; however, there is no reason at this time to expect any significant change.

The most obvious conclusion from the integral comparisons is that the LASL and ORNL measured gamma energy release rates both indicate that the calculated value is too large at a cooling time on the order of 4000 s. This is most pronounced in the ORNL data. To a much lesser extent, it is also evident in the total (beta plus gamma) heating comparison noted in Ref. 10. While the experimental data do not agree on the degree of the difference, they do agree that the calculated gamma energy is ~5 to 20% too large at this cooling time (however, an accurate experiment[10] suggests that the difference is likely less than 10%). Attempts to find errors in the ENDF/B-IV files to explain this difference have so far been negative. The difference may be due to fission yields rather than to decay parameters.

Comparisons with the LASL gamma spectra are included in Figs. 1 through 13. The decay times follow a 20000-s (5.56-h) irradiation.

The ORNL gamma spectra are shown in Figs. 14 through 51 for the 1, 10, and 100 s irradiation cases. Corresponding beta spectra are compared in Figs. 52 through 90.

The University of Illinois beta spectra are compared in Figs. 91 through 102. The decay times follow an 8-h irradiation, (comparable to the 5.56-h irradiation time of the LASL gamma measurements). Also provided are spectra following a 15-ms fission pulse.

For each experiment, the plots are arranged to run from the shortest to the longest cooling time, and for ORNL and UI comparisons, each set begins with the shortest irradiation time.

III. DISCUSSION

The agreement between calculated and experimental results varies, but overall, it is seen to be good in both spectra and integrated energy releases. Since the degree of agreement varies even among experimental results, it is difficult to pinpoint specific shortcomings of the ENDF/B-IV fission-product files. Nevertheless, general conclusions can be drawn.

The most stringent test on the ENDF/B-IV data is revealed by comparison at short irradiation and short cooling times. At these times, the fission products with spectral data on the ENDF/B-IV file are not represented as well as at longer irradiation and cooling times. This is evident from the tabular comparisons of integral data. At longer cooling times, however, the fission products with spectral data on ENDF/B-IV account for most of the energy release. At these times, also, the agreement between experimental and calculated data is seen to be better, particularly for the gamma spectra.

The primary intent of this report is to document the spectral comparisons. However, the tabular data on integral comparisons may mislead those readers who are also concerned with the adequacy of ENDF/B-IV data in calculations of total (beta plus gamma) energy release rates. The LASL and ORNL measurements are part of a larger program involving several laboratories and measurements to accurately define a new standard for decay heating;[9,10] preliminary unpublished results from that program indicate that, for more extended irradiation times, the calculated heating will be within 3% of the best estimate of a standard for cooling times of 15-10^5 s.

In conclusion, while it is seen that the ENDF/B-IV file could be expanded to include more spectral data for short-lived fission products, it is adequate, in its present form, for predicting fission-product source terms at both short and long irradiation and cooling times with a large degree of accuracy.

ACKNOWLEDGMENTS

We appreciate the generosity of E. T. Jurney (LASL) and J. K. Dickens (ORNL) in making their preliminary data available to us in a most useful form prior to other publication. We also appreciate the helpful discussions with J. L. Yarnell (LASL) and B. W. Wehring (UI), and the assistance of N. L. Whittemore and D. George in preparing the graphical comparisons and H. Holleman in typing and compiling the report.

REFERENCES

1. Fission-product decay library compiled by a task force chaired by R. E. Schenter. These data are part of the Evaluated Nuclear Data File (ENDF/B-IV) available from the National Nuclear Data Center (NNDC) at the Brookhaven National Laboratory, Upton, New York. (The spectral data in these files were compiled by C. W. Reich.)

2. T. R. England and R. E. Schenter, "ENDF/B-IV Fission Product Files: Summary of Major Nuclide Data," Los Alamos Scientific Laboratory report LA-6116-MS [ENDF-223], (October 1975).

3. P. F. Rose and T. W. Burrows, "ENDF/B Fission Product Decay Data," Brookhaven National Laboratory report, BNL-NCS-50545 [ENDF-243], Vols. 1 and 2, (August 1976).

4. M. G. Stamatelatos and T. R. England, "FPDCYS and FPSPEC, Computer Programs for Calculating Fission-Product Beta and Gamma Multigroup Spectra from ENDF/B-IV Data," Los Alamos Scientific Laboratory report LA-NUREG-6818-MS (May 1977).

5. T. R. England and M. G. Stamatelatos, "Multigroup Beta and Gamma Spectra of Individual ENDF/B-IV Fission-Product Nuclides," Los Alamos Scientific Laboratory report LA-NUREG-6622-MS (December 1976).

6. T. R. England, M. G. Stamatelatos, and N. L. Whittemore, in "Applied Nuclear Data Research and Development," Los Alamos Scientific Laboratory report LA-6472-PR (August 1976) p. 13.

7. N. Tsoulfanidis, B. W. Wehring, and M. E. Wyman, "Measurements of Time-Dependent Energy Spectra of Beta Rays from Uranium-235 Fission Fragments," Nucl. Sci. and Eng. 43, 42 (1971).

8. Data supplied by J. K. Dickens and to be published in an Oak Ridge National Laboratory report in preparation, "Delayed Beta- and Gamma-Ray Production Due to Thermal-Neutron Fission of ^{235}U, Spectral Distributions for Times After Fission Between 2 and 14400 sec: Tabular Data".

9. J. K. Dickens, J. F. Emery, T. A. Love, J. W. McConnell, K. J. Northcutt, R. W. Peelle, and H. Weaver, "Fission-Product Energy Release of ^{235}U Between 2 and 14000 sec.," Oak Ridge National Laboratory report ORNL/NUREG-14, (Draft April 22, 1977).

10. J. L. Yarnell and P. J. Bendt, "Decay Heat from Products of ^{235}U Thermal Fission by Fast-Response Boil-off Colorimetry," Los Alamos Scientific Laboratory report LA-NUREG-6713 (Draft January 15, 1977).

11. T. R. England and M. G. Stamatelatos, "Beta and Gamma Spectra and Total Decay Energies from Fission Products," Trans. Am. Nucl. Soc. 23, 493 (1976).

(Refs. 10 and 11 include preliminary and otherwise unpublished LASL measurements of gamma spectra made by E. T. Jurney).

TABLE I

COMPARISONS OF TOTAL CALCULATED GAMMA RELEASE RATES WITH LASL EXPERIMENTS[a]

Mean Cooling Time (s)	MeV/Fission Experimental	Ratio Cal/Exp	% of Energy in 180 Nuclides[c]
70	2.741	0.991 (0.989)[b]	87.6
199	2.058	1.002 (0.999)	93.5
388	1.724	1.000 (1.003)	95.5
660	1.429	1.038 (1.035)	96.6
1524	1.021	1.077 (1.073)	99.8
2214	0.8422	1.091 (1.087)	98.7
3234	0.6712	1.100 (1.094)	99.3
5000	0.4981	1.095 (1.089)	99.7
21845	0.1328	0.991 (0.978)	99.8
EARLIER RESULT FROM PILOT EXPERIMENT[d]			
62136	0.0352	1.078 (1.053)	99.9
151200	0.0122	1.084 (1.045)	99.8

[a]The LASL Measurements were made in 1976 by E. Jurney in support of the LASL decay heat experiment Ref. (10). These results are for a 20000-s constant thermal fission rate of ^{235}U.

[b]Ratios in parentheses exclude the internal conversion energy calculated from ENDF/B-IV files (see text; the files contain internal conversion coefficients for only 38 nuclides).

[c]See text; this column shows the fraction of total gamma energy resulting from the 180 nuclides having spectral data.

[d]The pilot experiment is believed to be accurate at these longer cooling times.

TABLE II

COMPARISON OF TOTAL CALCULATED BETA AND GAMMA ENERGY RELEASE RATES WITH ORNL EXPERIMENTS[a]

Mean Cooling Time (s)	Counting Times (s)	BETA MeV/Fission Experimental	BETA Ratio Cal/Exp	BETA % of Energy in 180 Nuclides[c]	GAMMA MeV/Fission Experimental	GAMMA Ratio Cal/Exp	GAMMA % of Energy in 180 Nuclides[c]
1 s Irradiation							
2.2[b]	1	0.241 ± 0.020	0.871	34.4	0.188 ± 0.010	0.799 (0.798)[d]	19.3
3.2	1	0.194 ± 0.012	0.865	35.8	0.146 ± 0.007	0.816 (0.815)	20.5
4.2	1	0.161 ± 0.009	0.871	36.9	0.119 ± 0.005	0.833 (0.832)	21.5
5.7	2	0.127 ± 0.006	0.890	38.3	0.094 ± 0.004	0.852 (0.850)	22.9
8.2	3	0.0940 ± 0.0043	0.909	39.9	0.0700 ± 0.0027	0.877 (0.876)	25.0
12.2	5	0.0610 ± 0.0028	1.000	42.1	0.0496 ± 0.0016	0.918 (0.917)	28.1
17.2	5	0.0412 ± 0.0018	1.065	42.5	0.0364 ± 0.0012	0.950 (0.949)	31.4
22.2	5	0.0310 ± 0.0014	1.090	43.3	0.0286 ± 0.0010	0.976 (0.975)	34.5
29.7	10	0.0223 ± 0.0009	1.124	44.6	0.0223 ± 0.0007	0.975 (0.974)	38.9
39.7	10	0.0159 ± 0.0007	1.153	46.9	0.0170 ± 0.0005	0.980 (0.979)	44.4
52.2	15	0.0117 ± 0.0005	1.171	50.2	0.0133 ± 0.0004	0.968 (0.967)	50.5
67.2	15	0.00873 ± 0.0003	1.187	54.3	0.0103 ± 0.0003	0.970 (0.969)	56.5
82.2	15	0.00695 ± 0.0003	1.184	58.1	0.00827 ± 0.00027	0.976 (0.976)	61.5
99.7	20	0.00547 ± 0.00021	1.200	61.9	0.00655 ± 0.00020	0.995 (0.995)	66.2
10 s Irradiation							
13.7	6	0.410 ± 0.020	1.037	42.6	0.360 ± 0.011	0.939 (0.938)	31.7
20.7	8	0.273 ± 0.014	1.105	43.7	0.264 ± 0.009	0.960 (0.959)	36.1
29.7	10	0.192 ± 0.009	1.130	45.5	0.198 ± 0.006	0.971 (0.970)	41.3
39.7	10	0.142 ± 0.006	1.156	48.0	0.156 ± 0.005	0.968 (0.968)	46.6
49.7	10	0.114 ± 0.005	1.153	50.7	0.127 ± 0.004	0.976 (0.975)	51.2
64.7	20	0.0870 ± 0.0040	1.158	54.8	0.0985 ± 0.003	0.988 (0.988)	57.2
84.7	20	0.0645 ± 0.0030	1.163	59.7	0.0745 ± 0.0020	0.993 (0.992)	63.5
104.7	20	0.0486 ± 0.0019	1.211	63.6	0.0585 ± 0.0020	1.004 (1.003)	68.2
134.7	40	0.0368 ± 0.0015	1.194	68.2	0.0438 ± 0.0013	1.009 (1.008)	73.4
184.7	60	0.0257 ± 0.0010	1.166	73.2	0.0295 ± 0.0008	1.023 (1.022)	78.7
254.7	80	0.0169 ± 0.0006	1.197	77.6	0.0198 ± 0.0006	1.020 (1.019)	82.8
344.7	100	0.0122 ± 0.0005	1.154	81.5	0.0137 ± 0.0004	1.016 (1.015)	86.0
494.7	200	0.00850 ± 0.00030	1.104	85.9	0.00930 ± 0.00030	1.003 (1.002)	88.9
694.7	200	0.00630 ± 0.00025	1.016	89.3	0.00660 ± 0.00025	0.992 (0.990)	91.1

TABLE II (continued)

100 s Irradiation									
90	40	0.420	± 0.018	1.108	66.6	0.455	± 0.020	1.024 (1.023)	71.6
140	60	0.277	± 0.012	1.118	72.5	0.302	± 0.013	1.031 (1.030)	77.9
210	80	0.185	± 0.008	1.111	77.4	0.196	± 0.009	1.048 (1.047)	82.5
300	100	0.129	± 0.005	1.101	81.4	0.134	± 0.006	1.048 (1.047)	85.7
450	200	0.0890	± 0.0035	1.058	85.9	0.090	± 0.004	1.040 (1.039)	88.9
650	200	0.0640	± 0.0025	1.002	89.2	0.0625	± 0.0025	1.050 (1.048)	91.1
950	400	0.0458	± 0.0030	0.960	91.5	0.0442	± 0.0018	1.074 (1.072)	92.6
1350	400	0.0320	± 0.0012	0.947	92.6	0.0315	± 0.0012	1.116 (1.114)	93.7
1750	400	0.0240	± 0.0008	0.946	93.2	0.0242	± 0.0010	1.157 (1.154)	94.5
2200	500	0.0186	± 0.0006	0.931	93.8	0.0191	± 0.0008	1.184 (1.181)	95.4
2700	500	0.0141	± 0.0005	0.946	94.4	0.0154	± 0.0007	1.195 (1.192)	96.2
3450	1000	0.0102	± 0.0004	0.949	95.3	0.0117	± 0.0006	1.209 (1.206)	97.3
4950	2000	0.00615	± 0.00025	0.974	96.5	0.00785	± 0.00050	1.185 (1.181)	98.5
7950	4000	0.00323	± 0.00020	1.015	97.5	0.00468	± 0.00038	1.089 (1.085)	99.3
11950	4000	0.00198	± 0.00014	1.001	NC[e]	0.00285	± 0.00033	0.979 (NC)[e]	NC

[a]Experimental data are preliminary results abstracted from Ref. (9). Values from this reference have been multiplied by the ratio of the irradiation to the counting time to convert to MeV/Fission (see text). The reader should consult Ref. (9) for any publication using the experimental data.

[b]This is the mid-point of the counting period. (Reference (9) tabulates an "average time" defined as the cooling time to the start of the counting period plus 1/2 of the sum of the irradiation and counting time.)

[c]See text; this column shows the fraction of total energy resulting from the 180 nuclides having spectral data in ENDF/B-IV.

[d]See text; ratios in parentheses exclude the internal conversion electron energy due to the 38 nuclides having internal conversion coefficients in ENDF/B-IV.

[e]Not calculated.

TABLE III

COMPARISONS OF TOTAL CALCULATED BETA RELEASE RATES WITH UI EXPERIMENTS[a]

Mean Cooling Time (s)	MeV/Fission Experimental	Ratio Cal/Exp	% of Energy in 180 Nuclides[b]
8 hour Irradiation			
6	4.98	0.860	67.8
21	3.51	0.952	75.2
66	2.58	0.968	82.9
210	1.87	0.947	92.3
960	1.09	0.967	97.1
3750	0.518	1.036	99.2
10950	0.267	1.050	99.7
Pulse (15 ms) Irradiation			
13	1.17E-03	0.760	NC[c]
66	1.58E-04	1.001	NC
204	3.78E-05	1.072	NC
960	6.99E-06	0.970	NC
3750	1.471E-06	0.884	NC

[a] Values based on Ref. 7.

[b] See text; this column shows the fraction of total calculated energy obtained from the 180 nuclides having spectral data in ENDF/B-IV.

[c] NC = not calculated. (Values in Table II at comparable cooling times apply.)

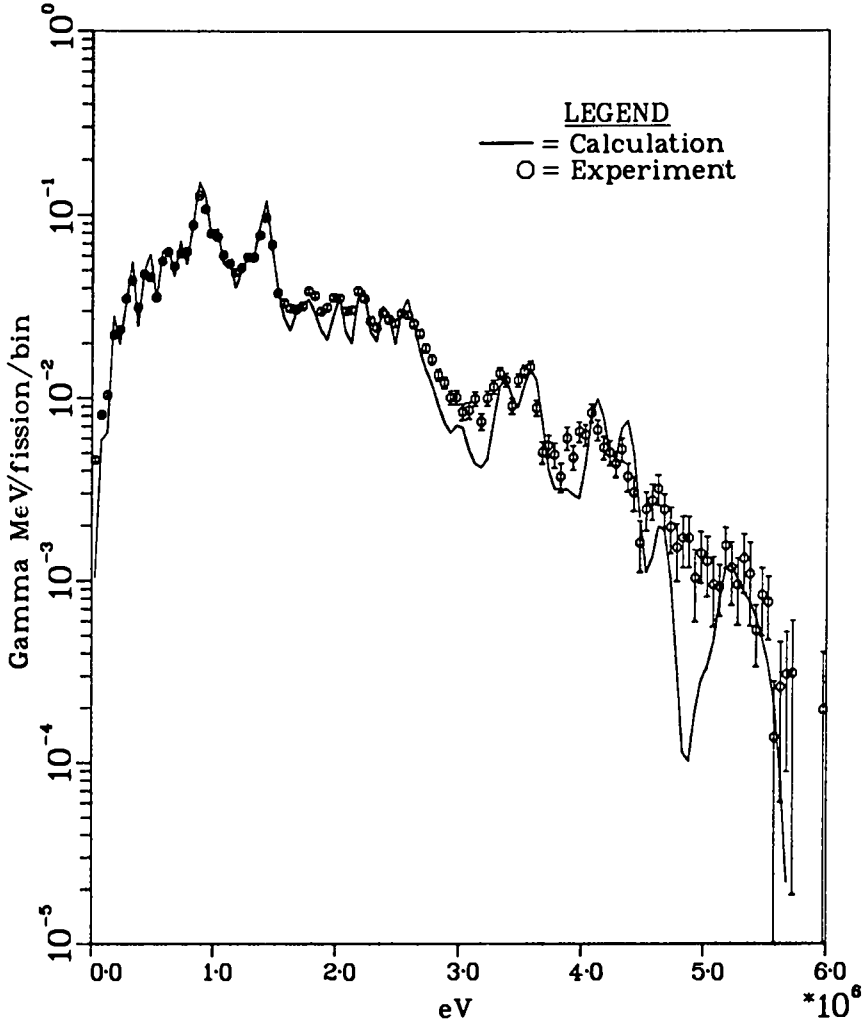

Fig. 1. Comparison of calculation with LASL 5.56-h irradiation, 70-s decay.

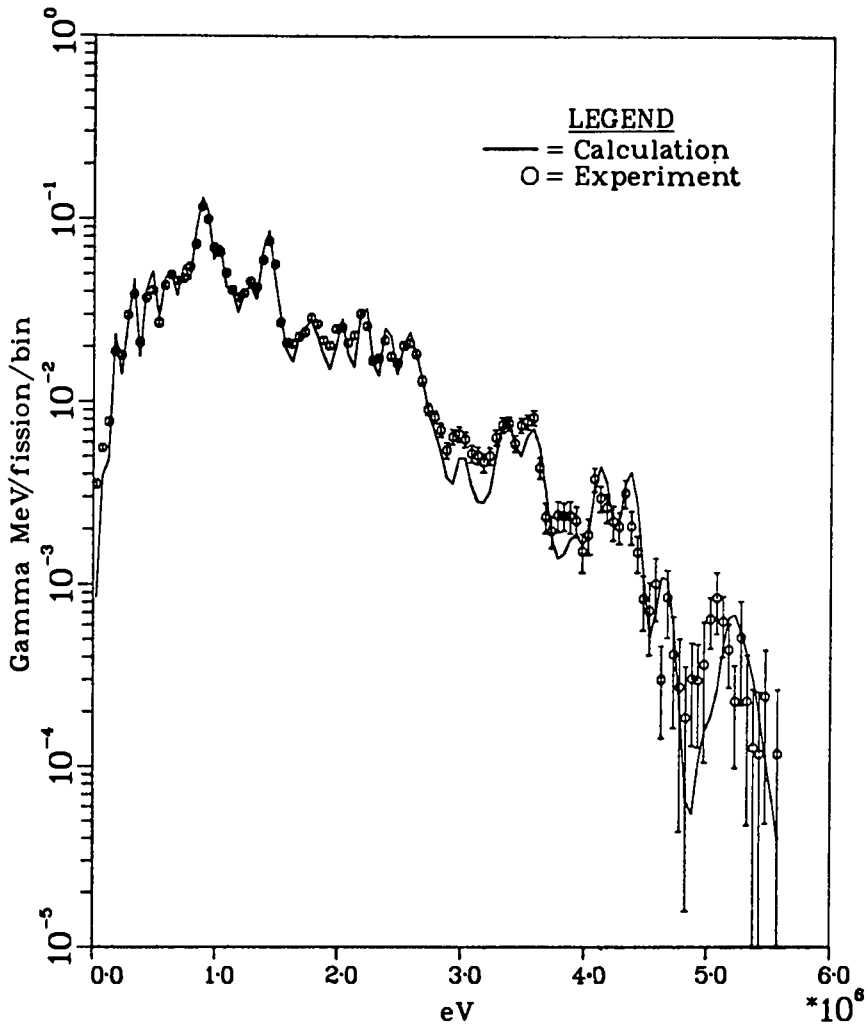

Fig. 2. Comparison of calculation with LASL 5.56-h irradiation, 199-s decay.

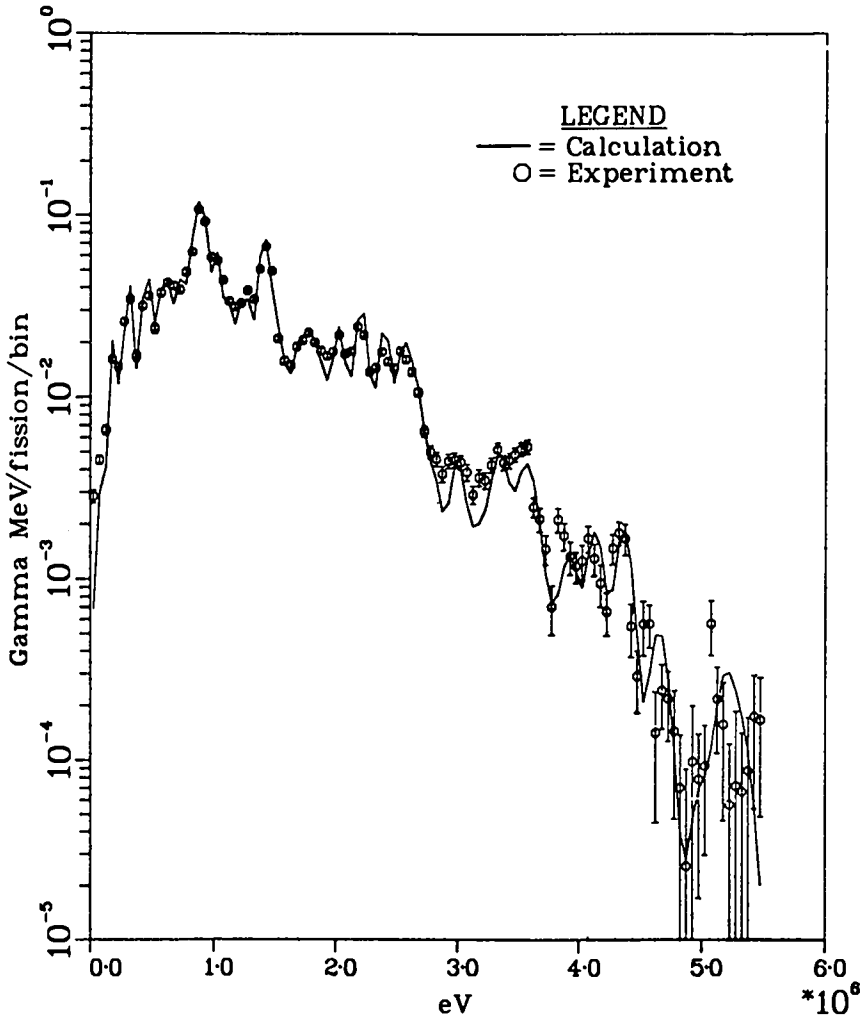

Fig. 3. Comparison of calculation with LASL 5.56-h irradiation, 388-s decay.

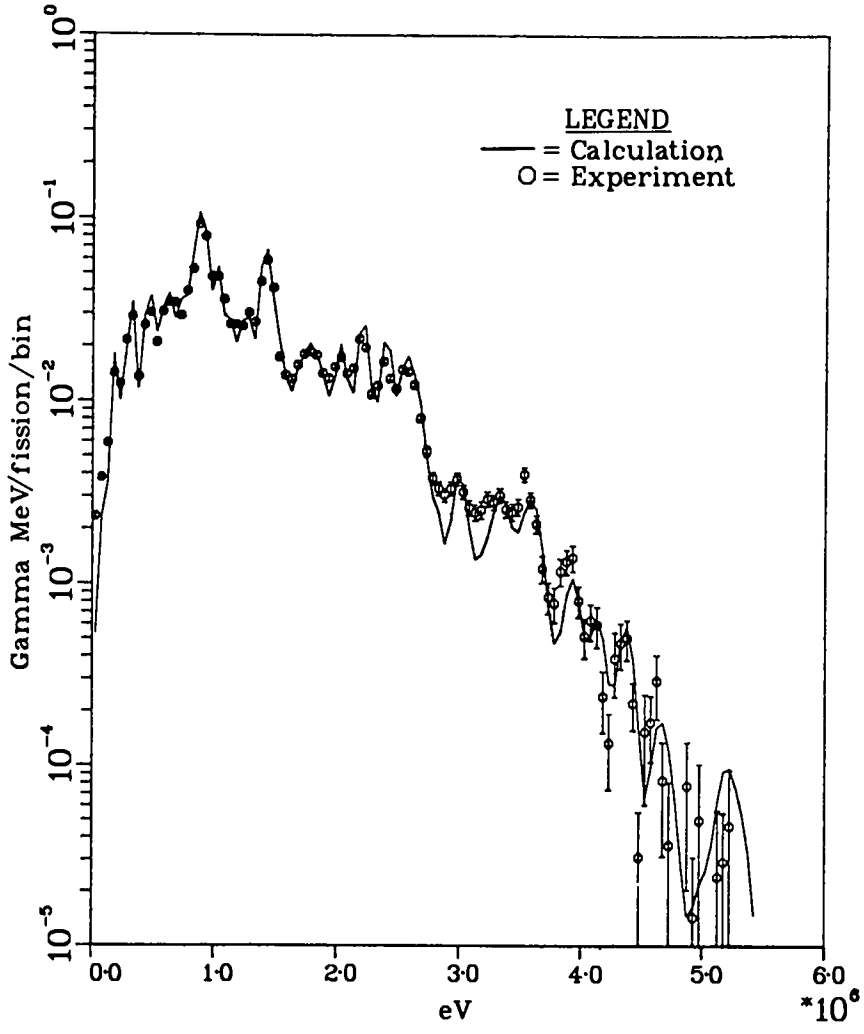

Fig. 4. Comparison of calculation with LASL 5.56-h irradiation, 660-s decay.

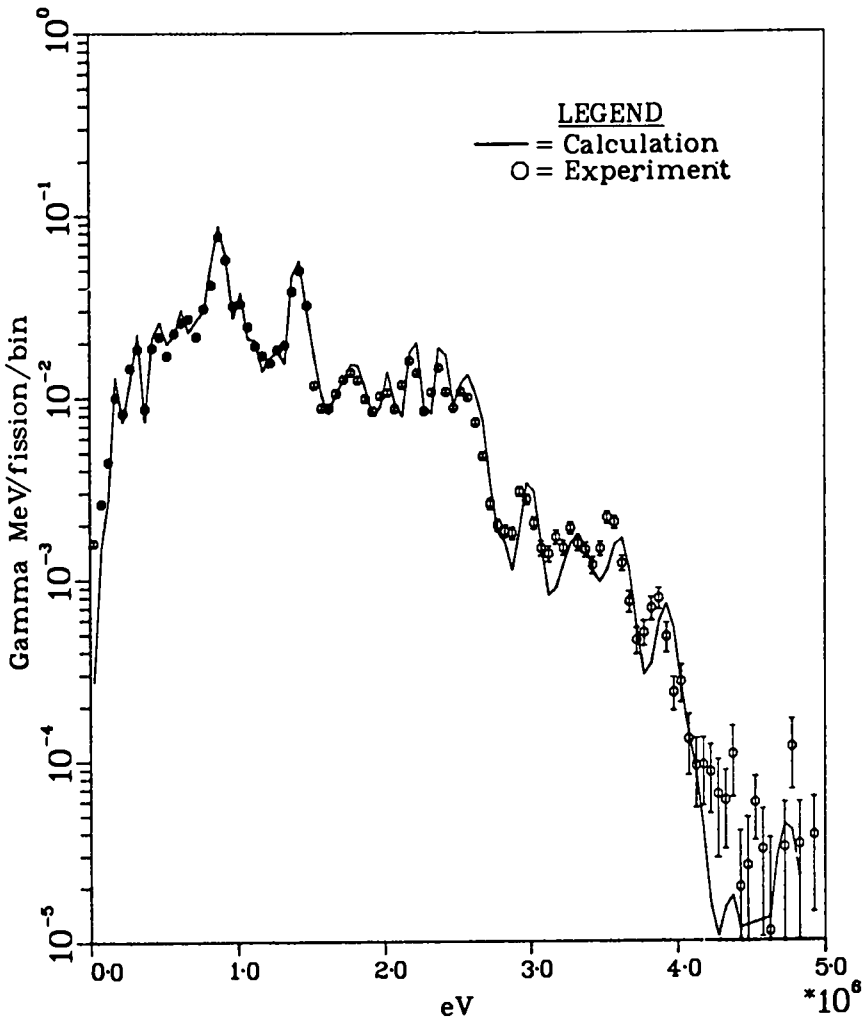

Fig. 5. Comparison of calculation with LASL 5.56-h irradiation, 1524-s decay.

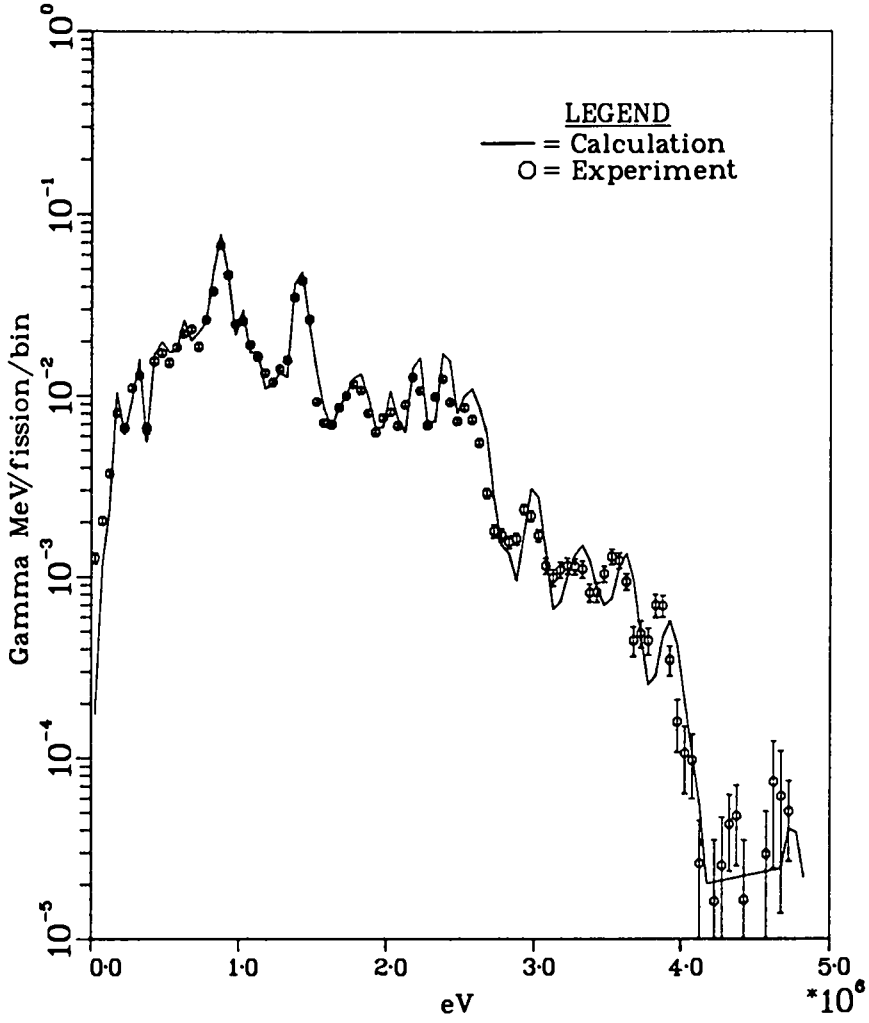

Fig. 6. Comparison of calculation with LASL 5.56-h irradiation, 2214-s decay.

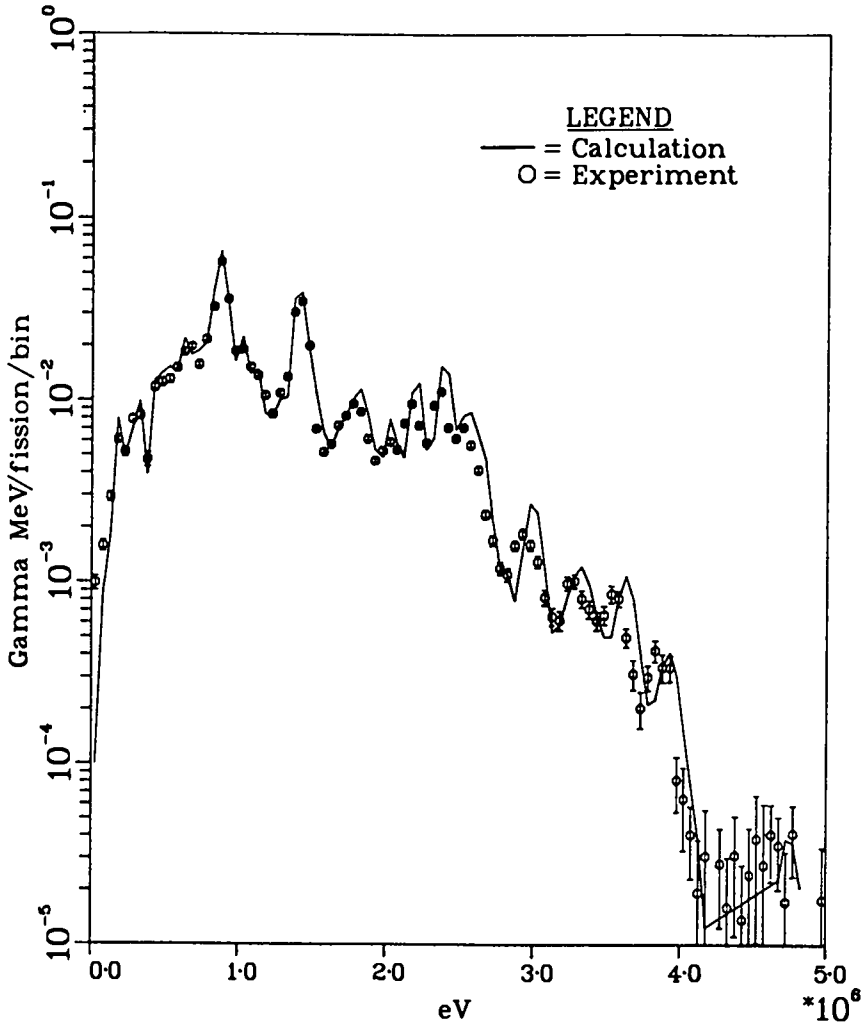

Fig. 7. Comparison of calculation with LASL 5.56-h irradiation, 3234-s decay.

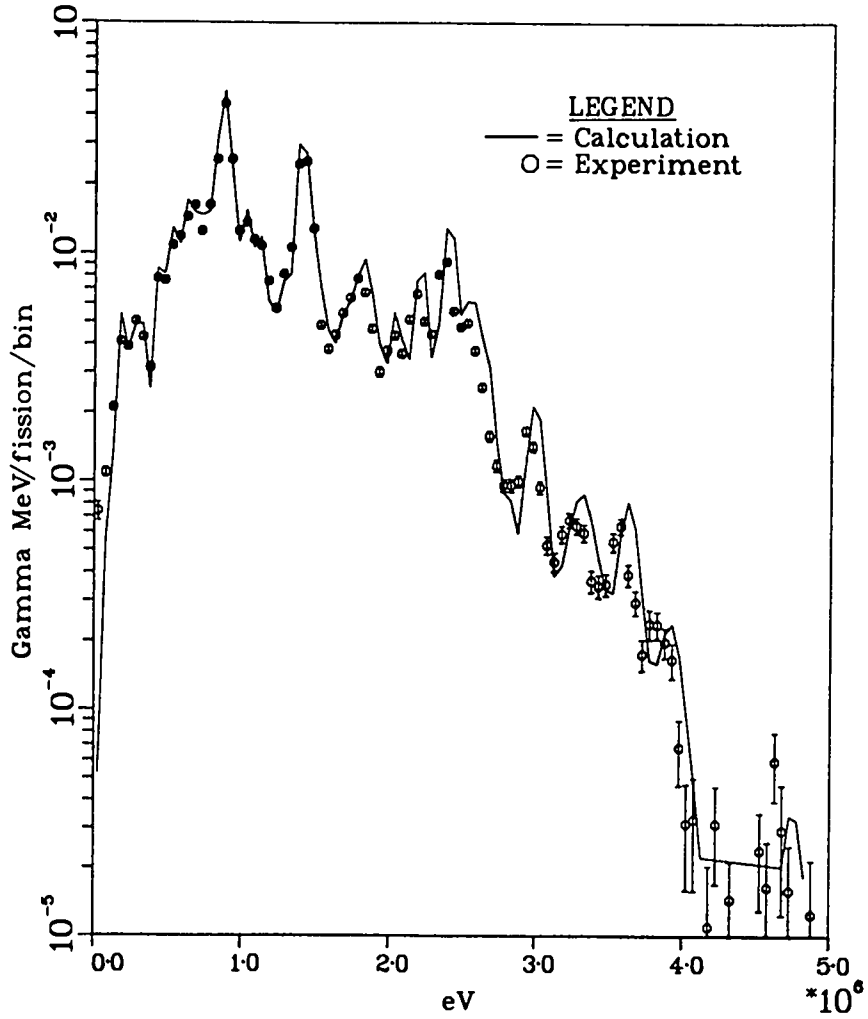

Fig. 8. Comparison of calculation with LASL 5.56-h irradiation, 5000-s decay.

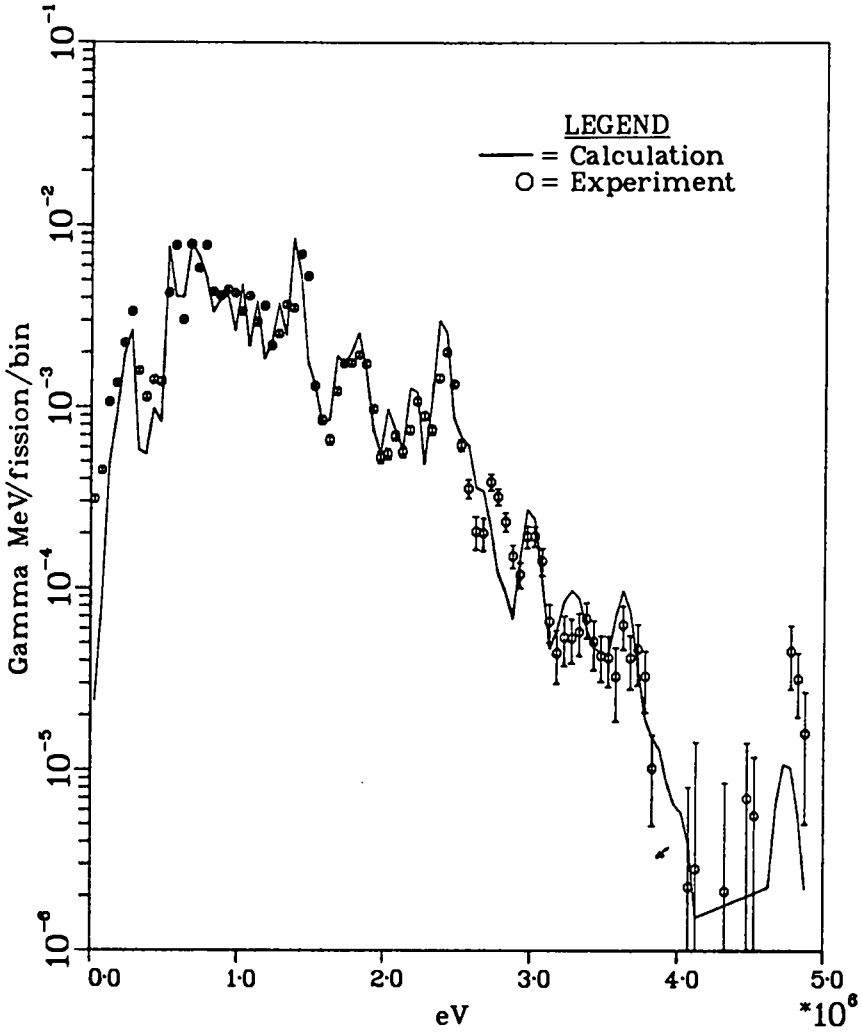

Fig. 9. Comparison of calculation with LASL 5.56-h irradiation, 21845-s decay.

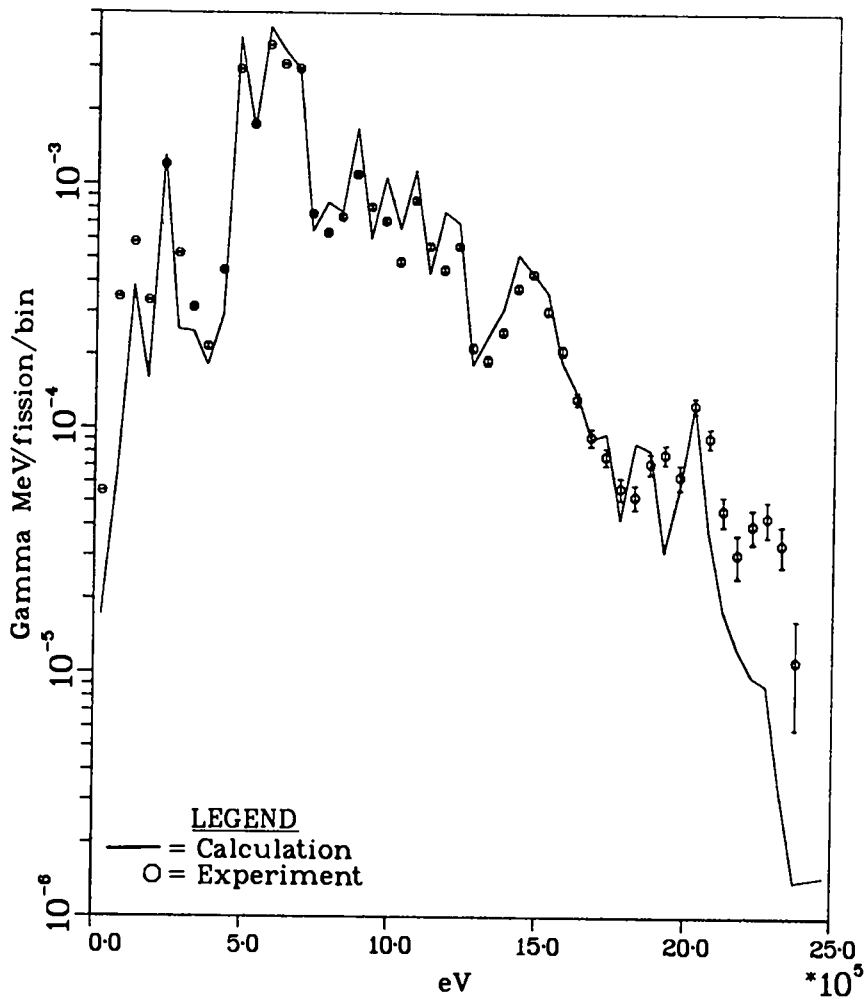

Fig.10. Comparison of calculation with LASL 5-h irradiation, 62136-s decay.

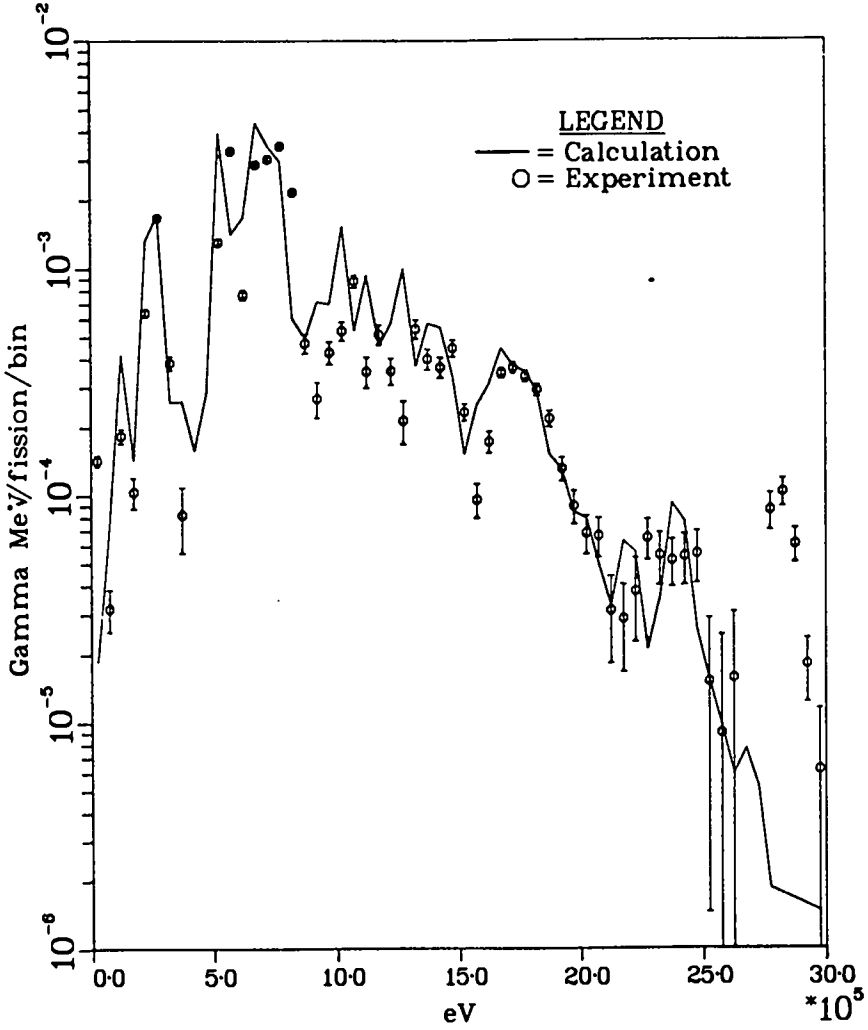

Fig.11. Comparison of calculation with LASL 5.56-h irradiation, 70550-s decay.

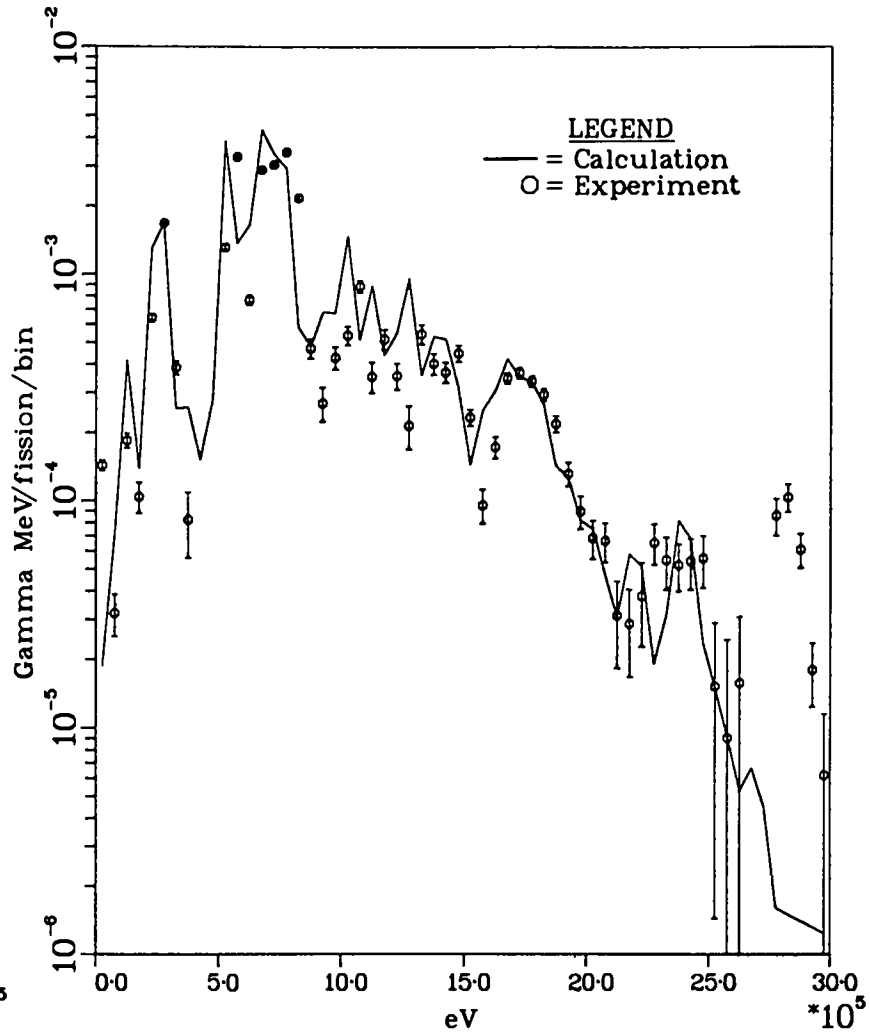

Fig. 12. Comparison of calculation with LASL 5.56-h irradiation, 72550-s decay.

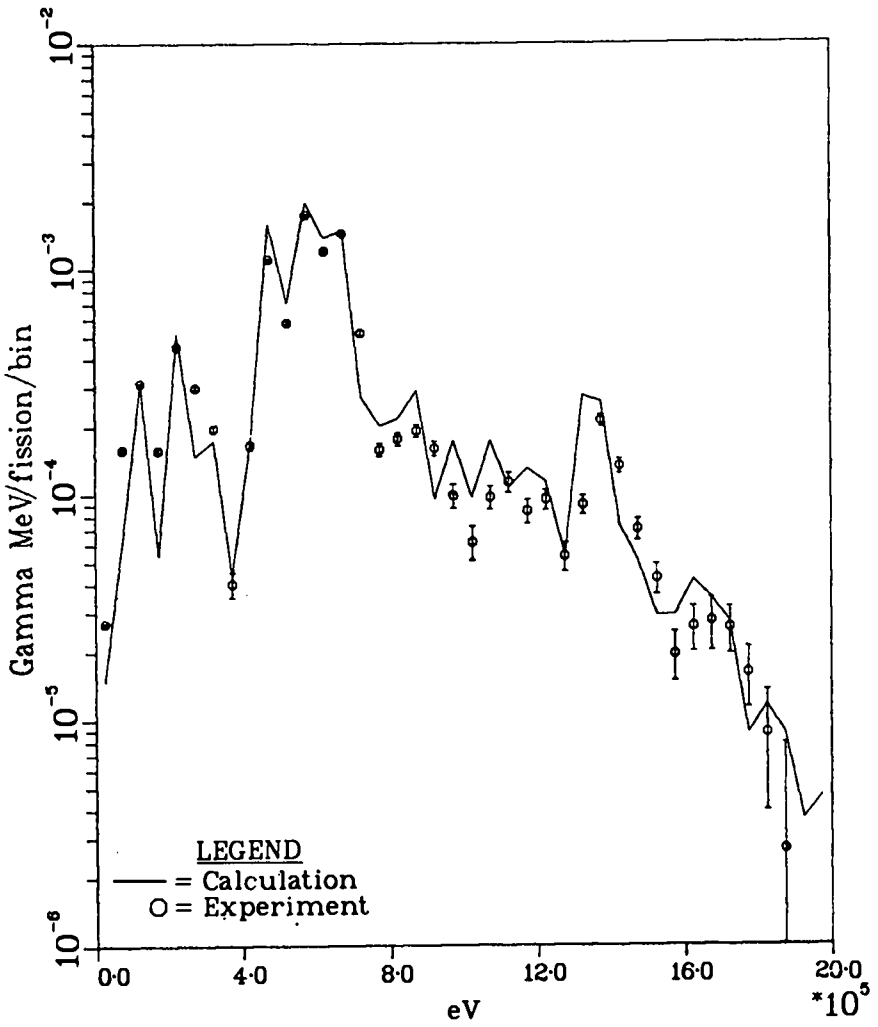

Fig.13. Comparison of calculation with LASL 5-h irradiation, 151200-s decay.

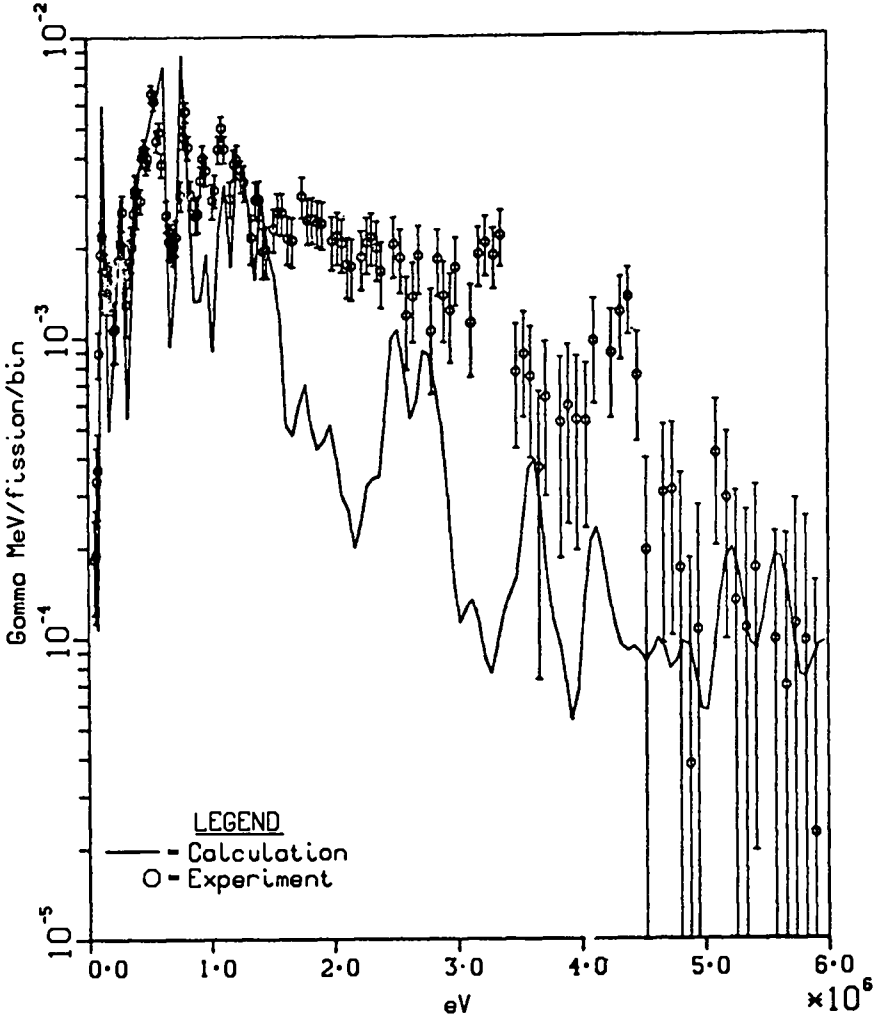

Fig.14. Comparison of calculation with ORNL 1-s irradiation experiment, 2.2-s decay.

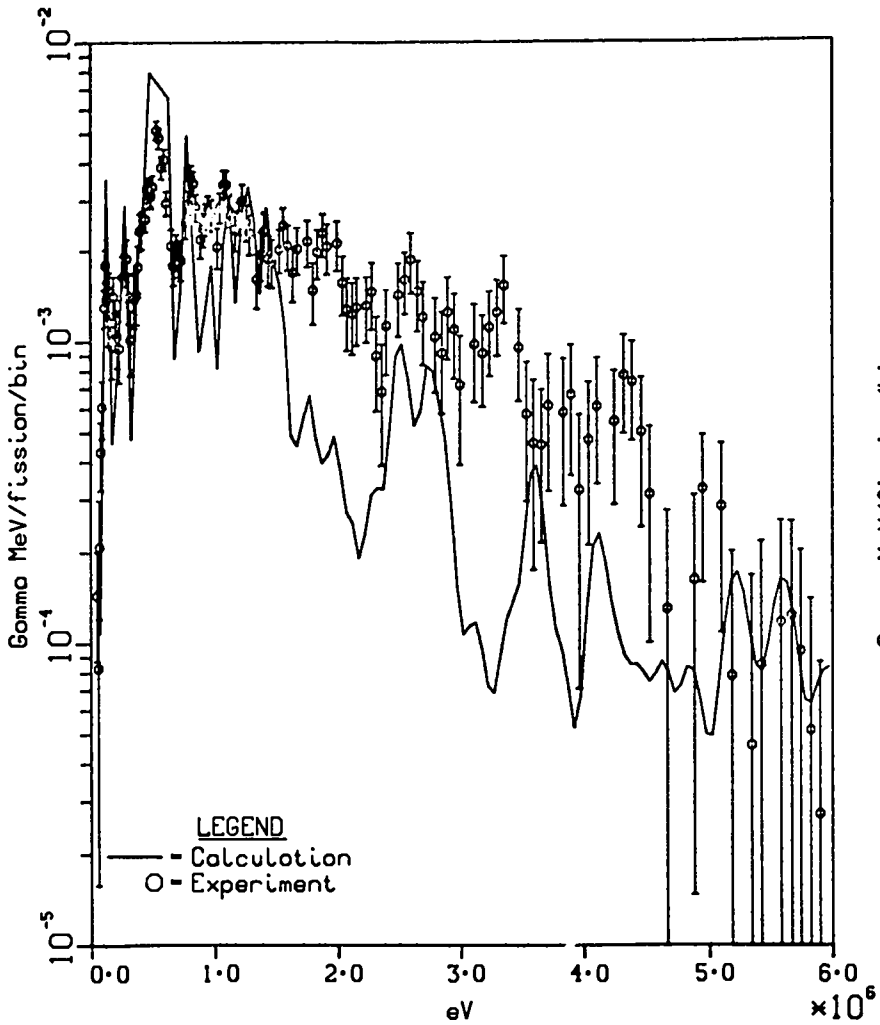

Fig. 15. Comparison of calculation with ORNL 1-s irradiation experiment, 3.2-s decay.

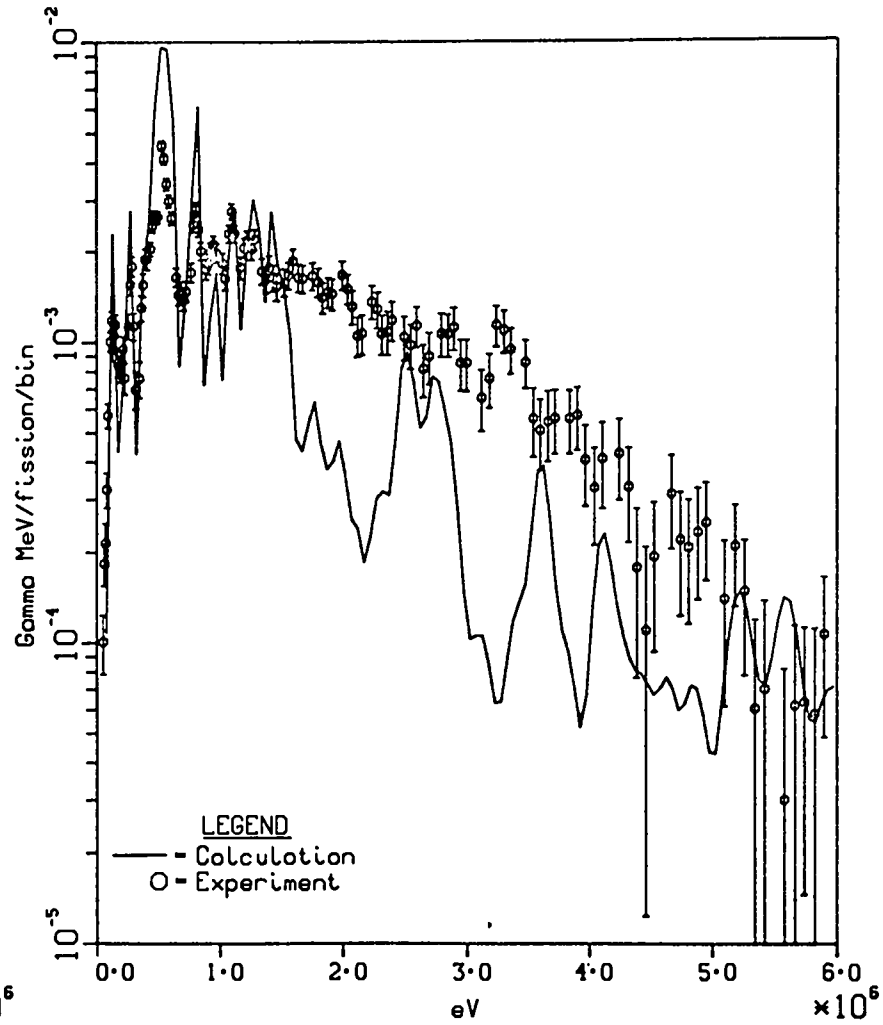

Fig.16. Comparison of calculation with ORNL 1-s irradiation experiment, 4.2-s decay.

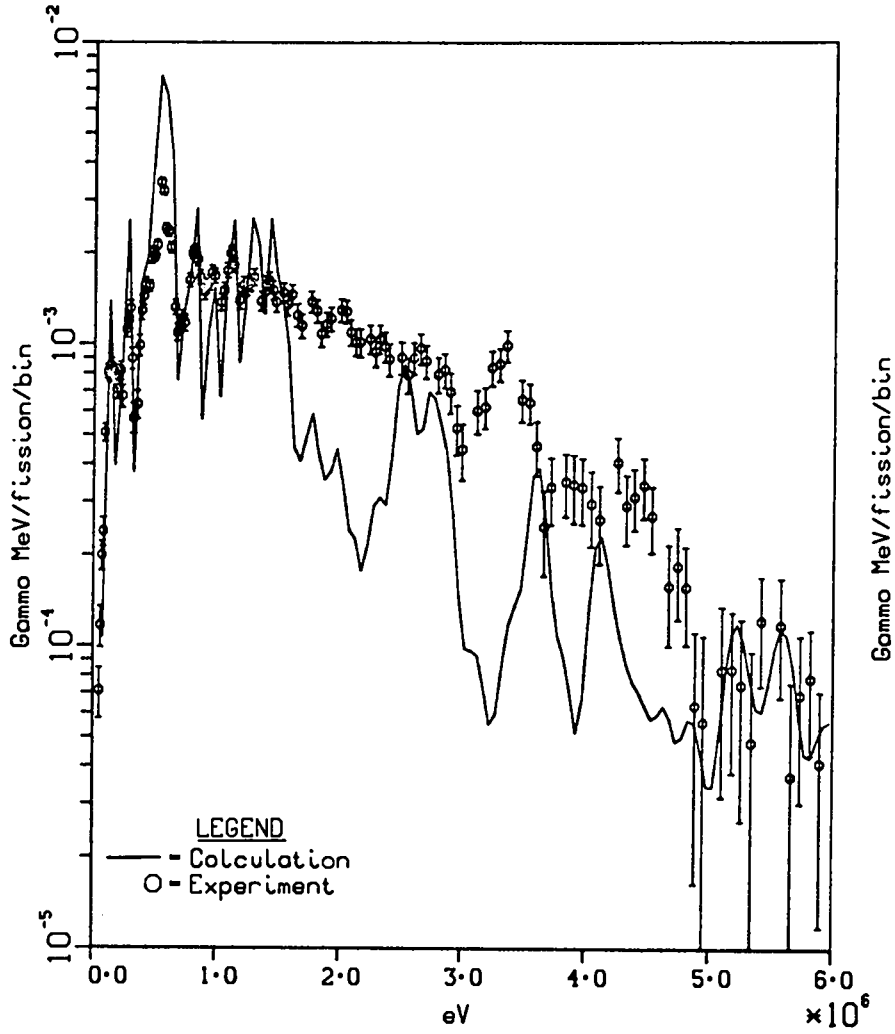

Fig.17. Comparison of calculation with ORNL 1-s irradiation experiment, 5.7-s decay.

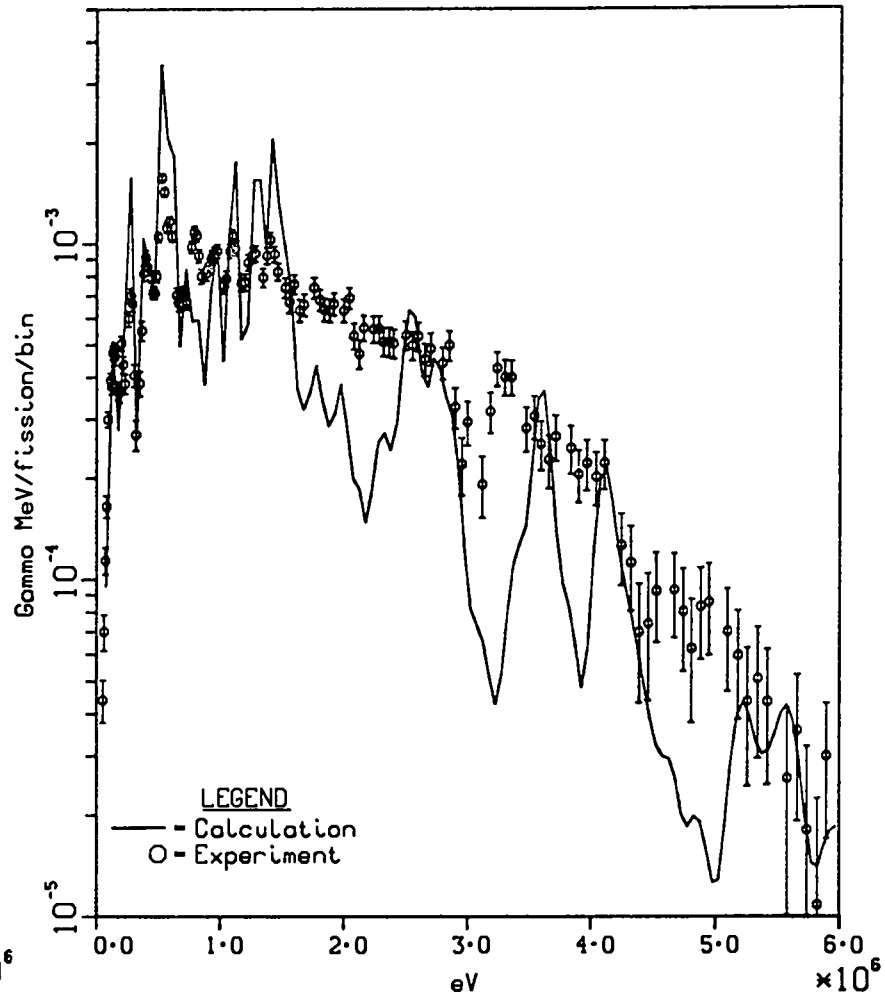

Fig.18. Comparison of calculation with ORNL 1-s irradiation experiment, 12.2-s decay.

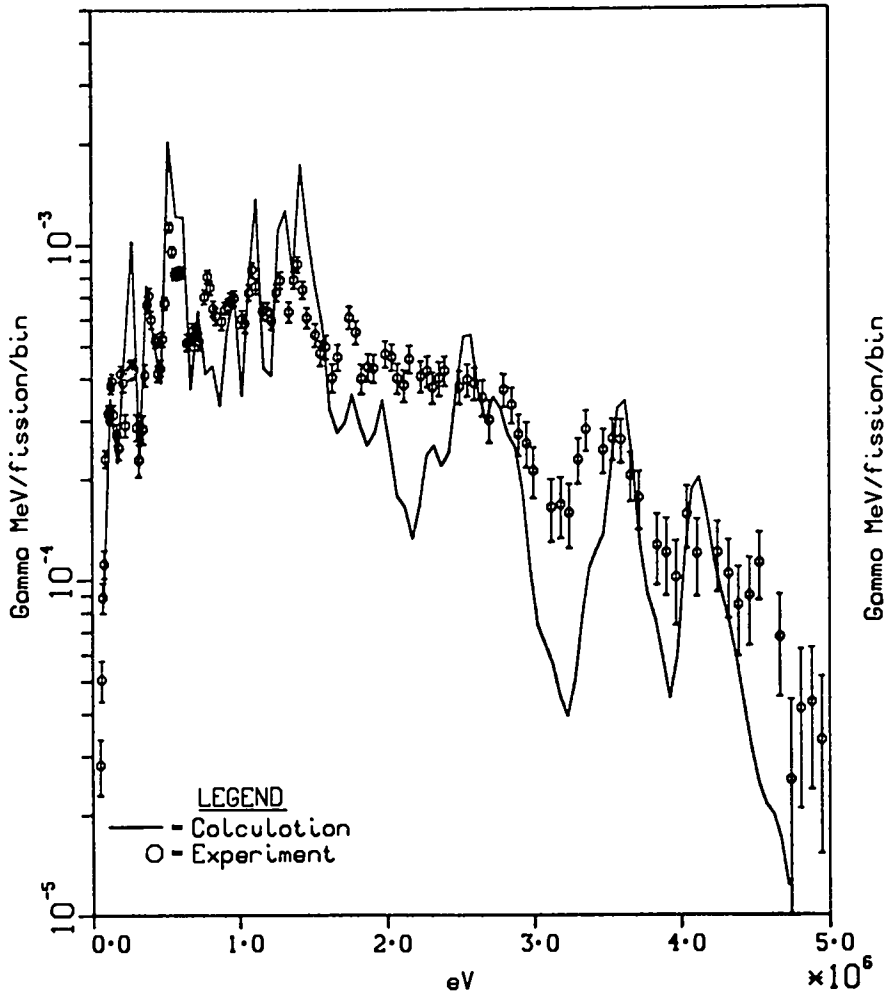

Fig.19. Comparison of calculation with ORNL 1-s irradiation experiment, 17.2-s decay.

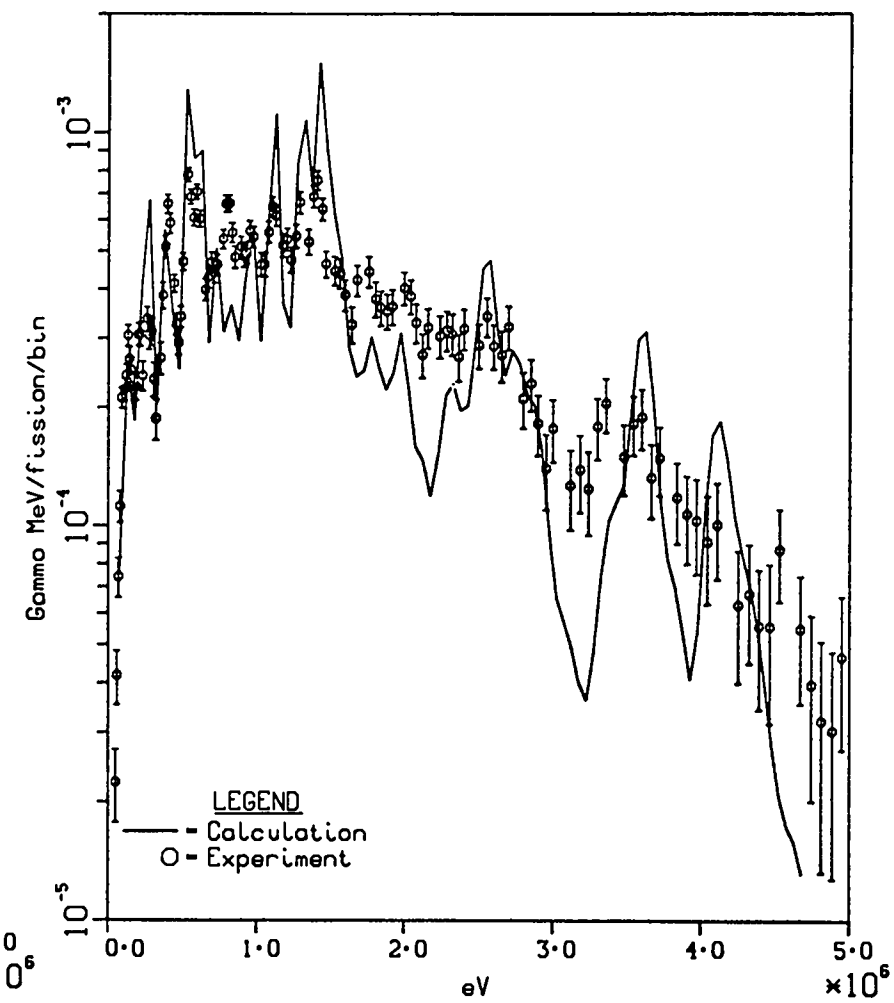

Fig.20. Comparison of calculation with ORNL 1-s irradiation experiment, 22.2-s decay.

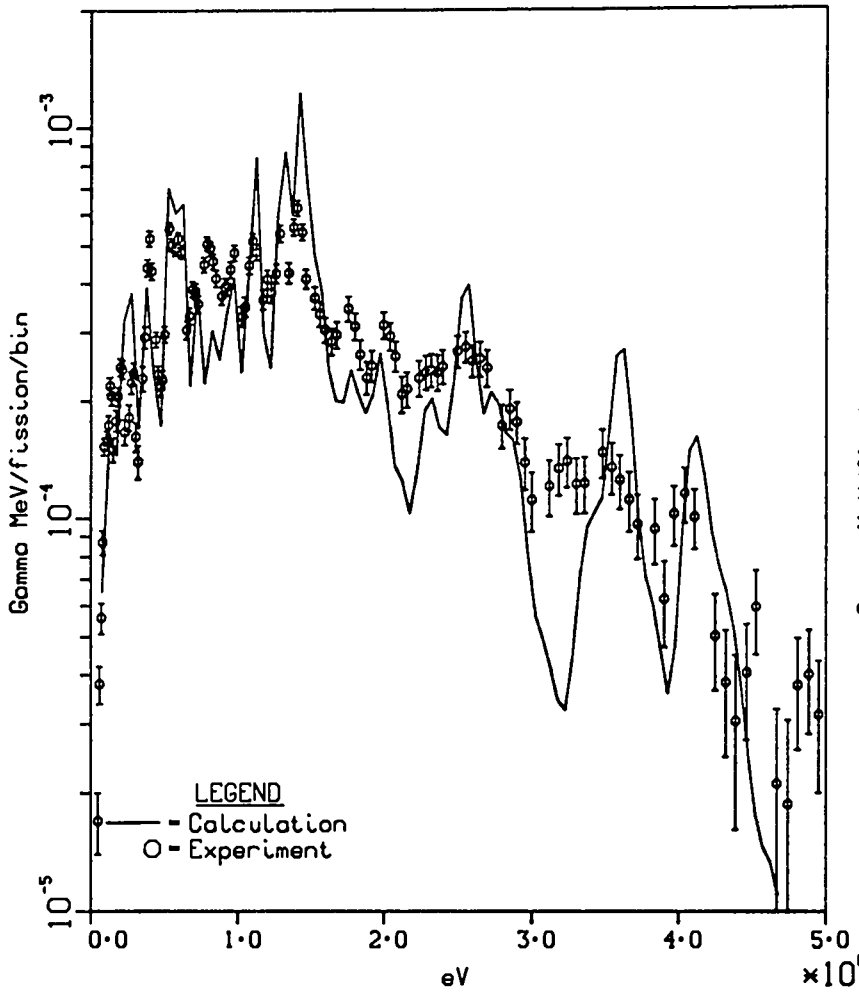

Fig. 21. Comparison of calculation with ORNL 1-s irradiation experiment, 29.7-s decay.

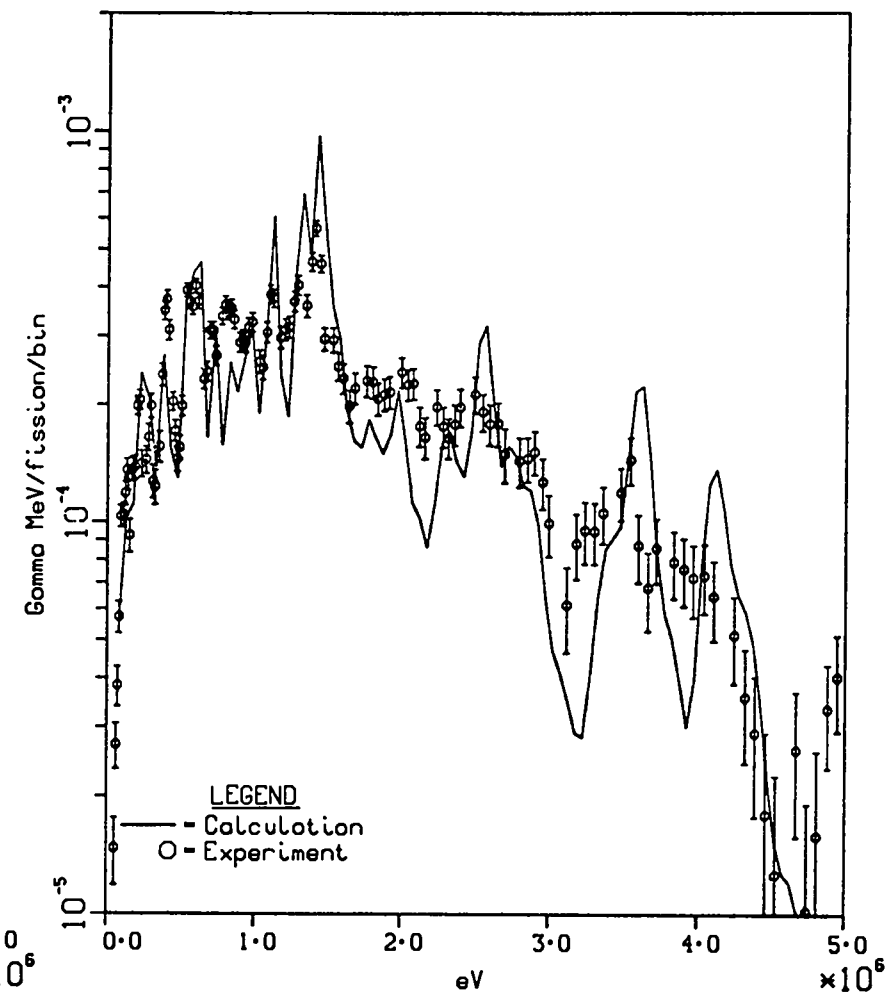

Fig. 22. Comparison of calculation with ORNL 1-s irradiation experiment, 39.7-s decay.

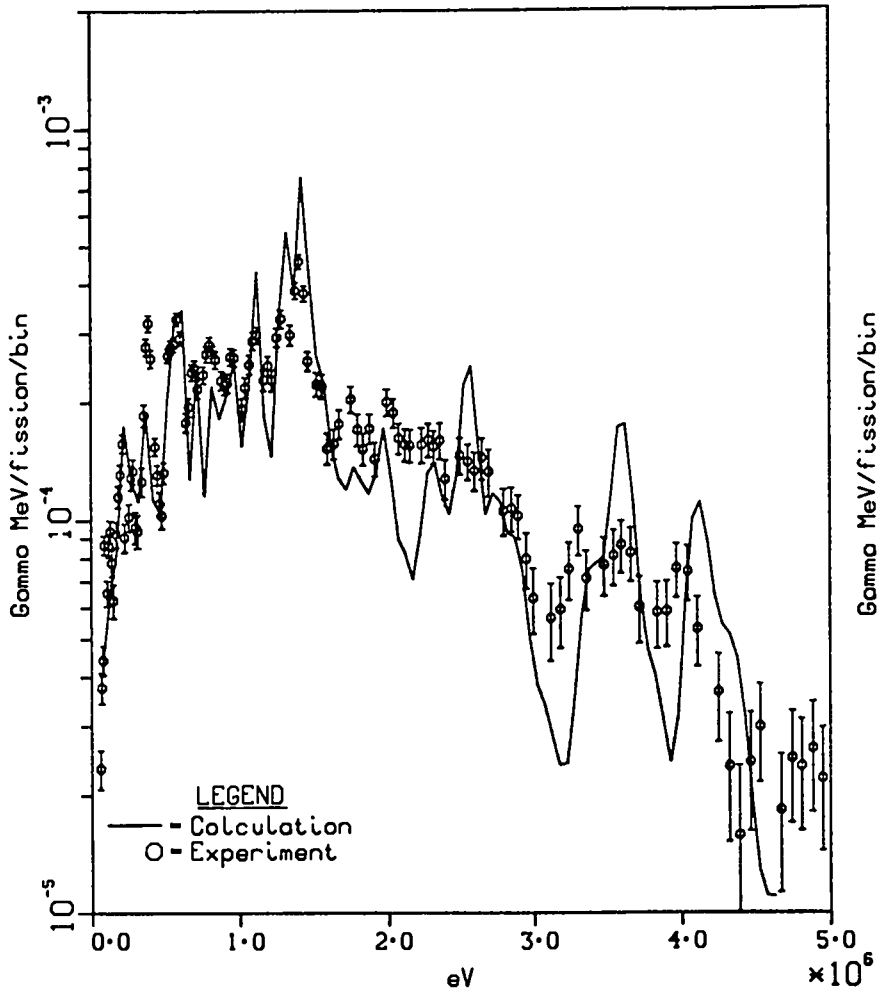

Fig. 23. Comparison of calculation with ORNL 1-s irradiation experiment, 52.2-s decay.

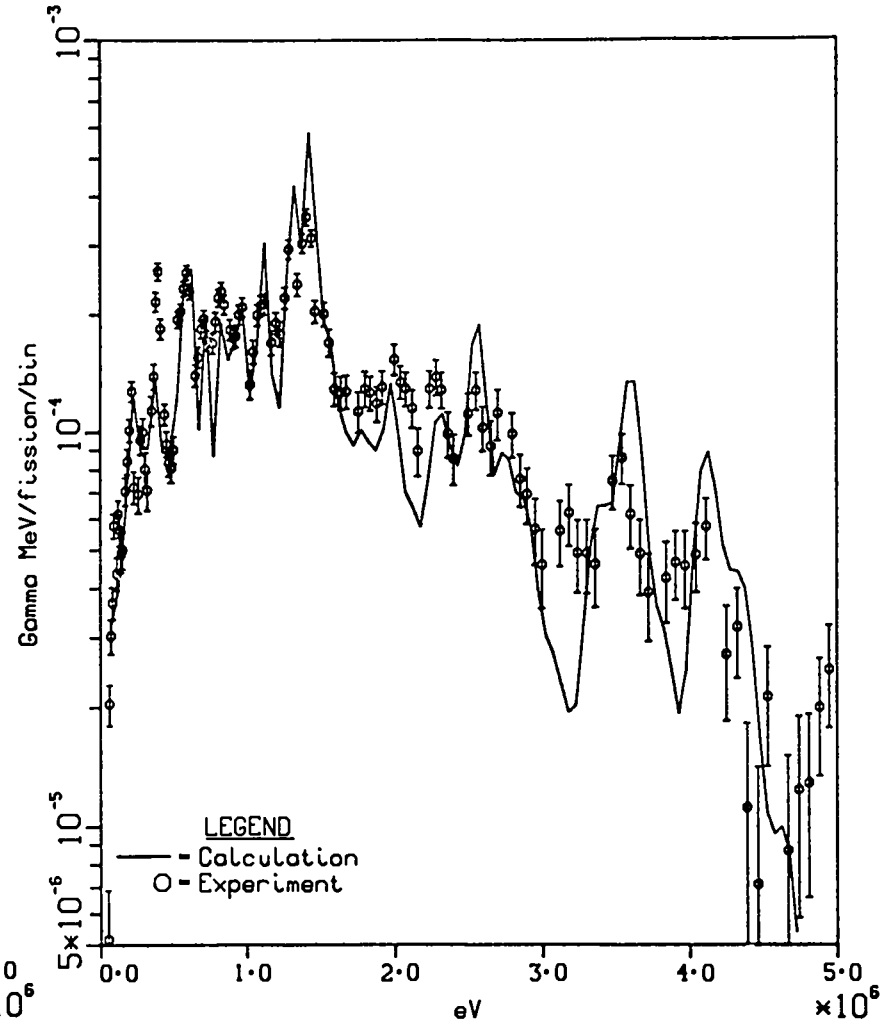

Fig. 24. Comparison of calculation with ORNL 1-s irradiation experiment, 67.2-s decay.

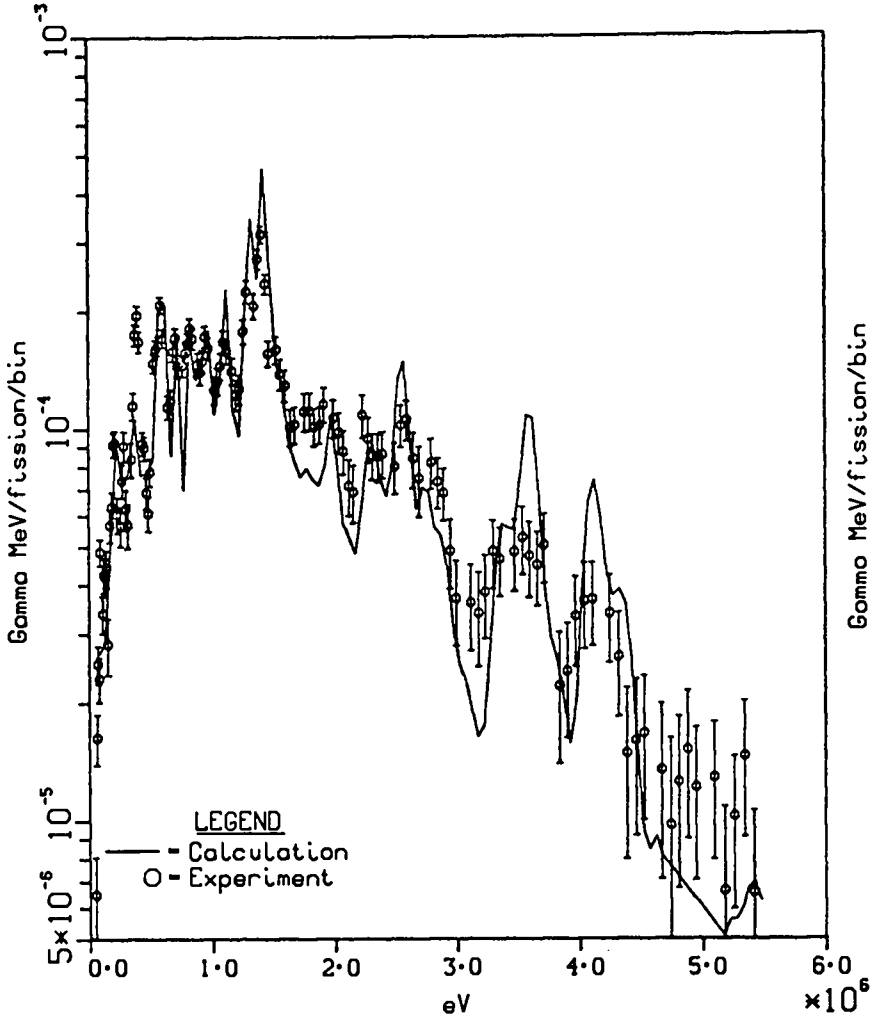

Fig.25. Comparison of calculation with ORNL 1-s irradiation experiment, 82.2-s decay.

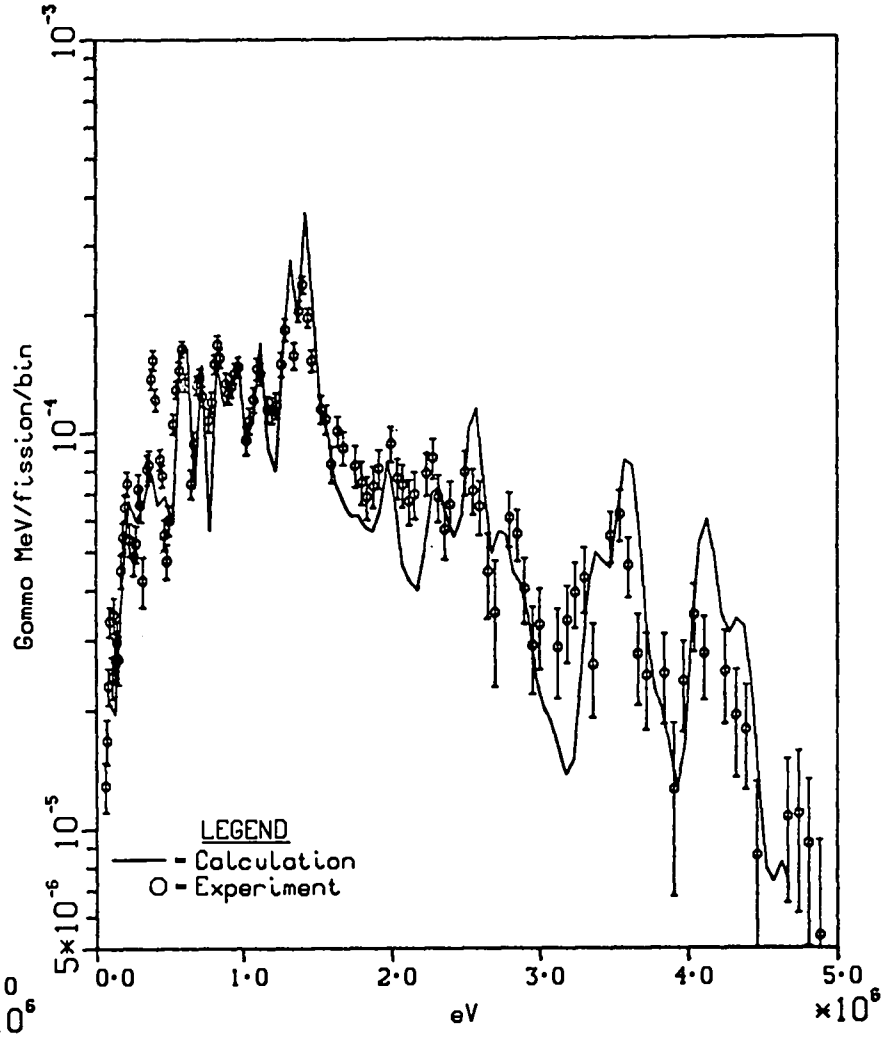

Fig. 26. Comparison of calculation with ORNL 1-s irradiation experiment, 99.7-s decay.

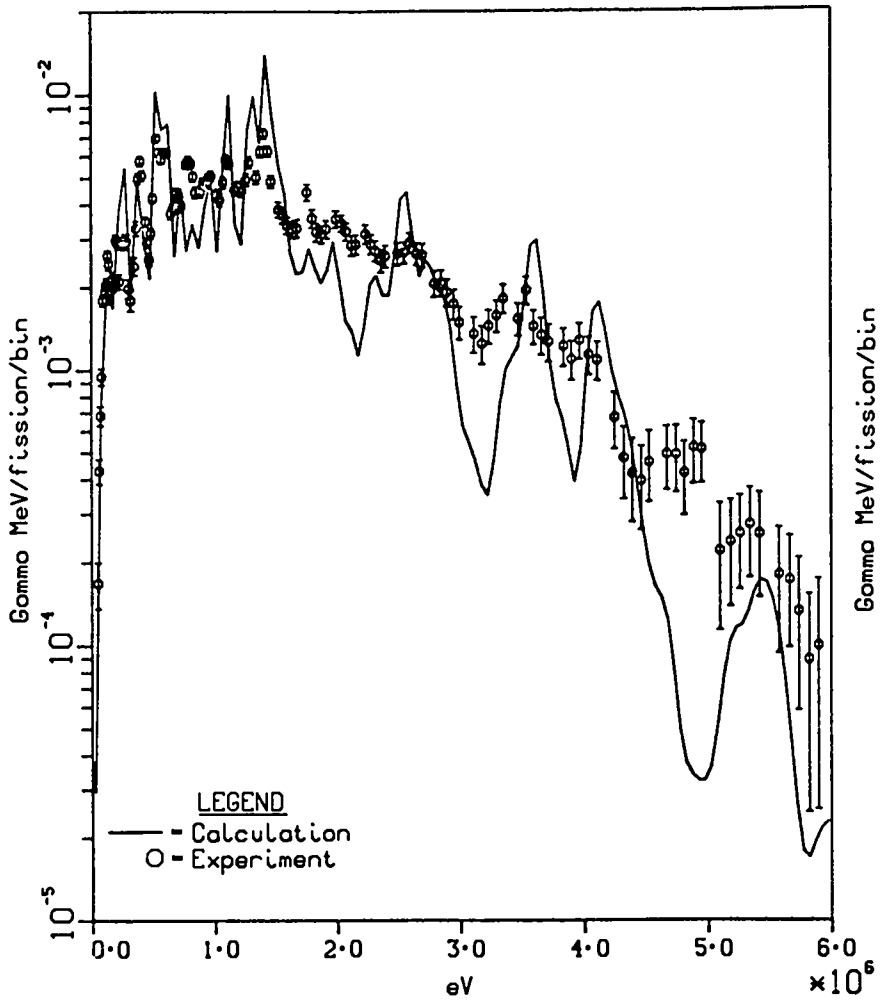

Fig. 27. Comparison of calculation with ORNL 10-s irradiation experiment, 20.7-s decay.

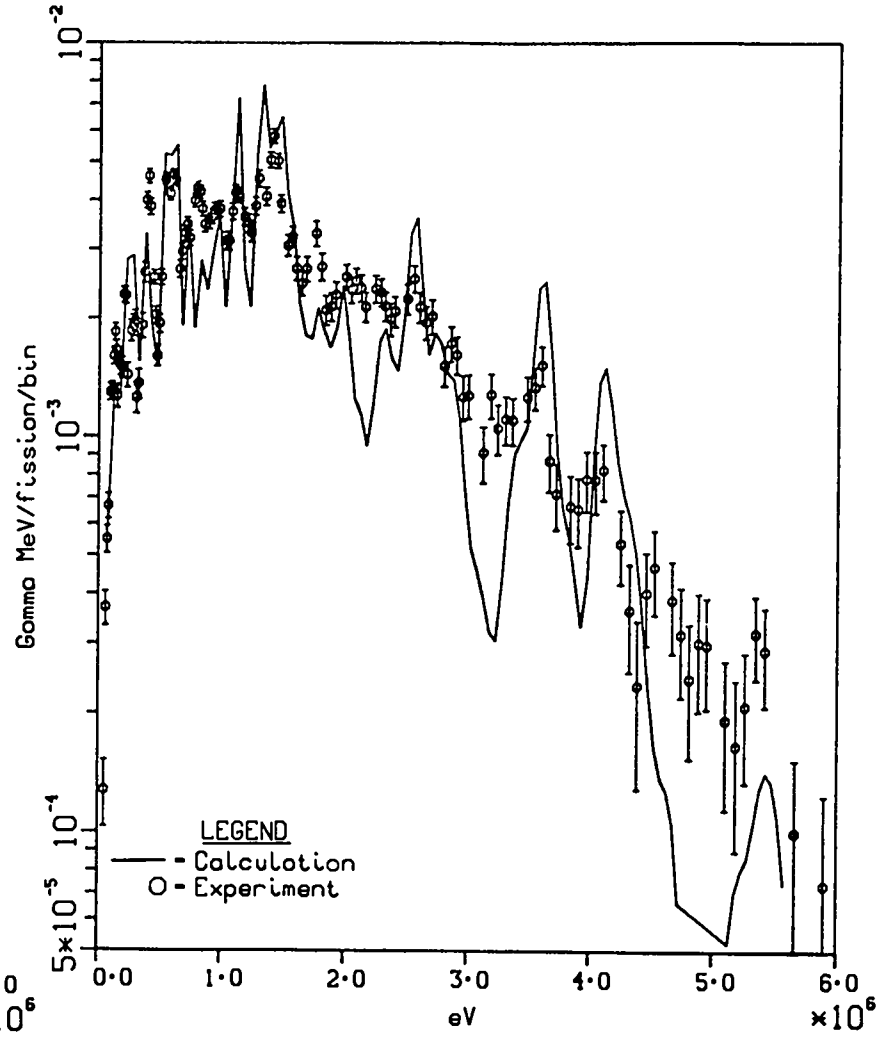

Fig. 28. Comparison of calculation with ORNL 10-s irradiation experiment, 29.7-s decay.

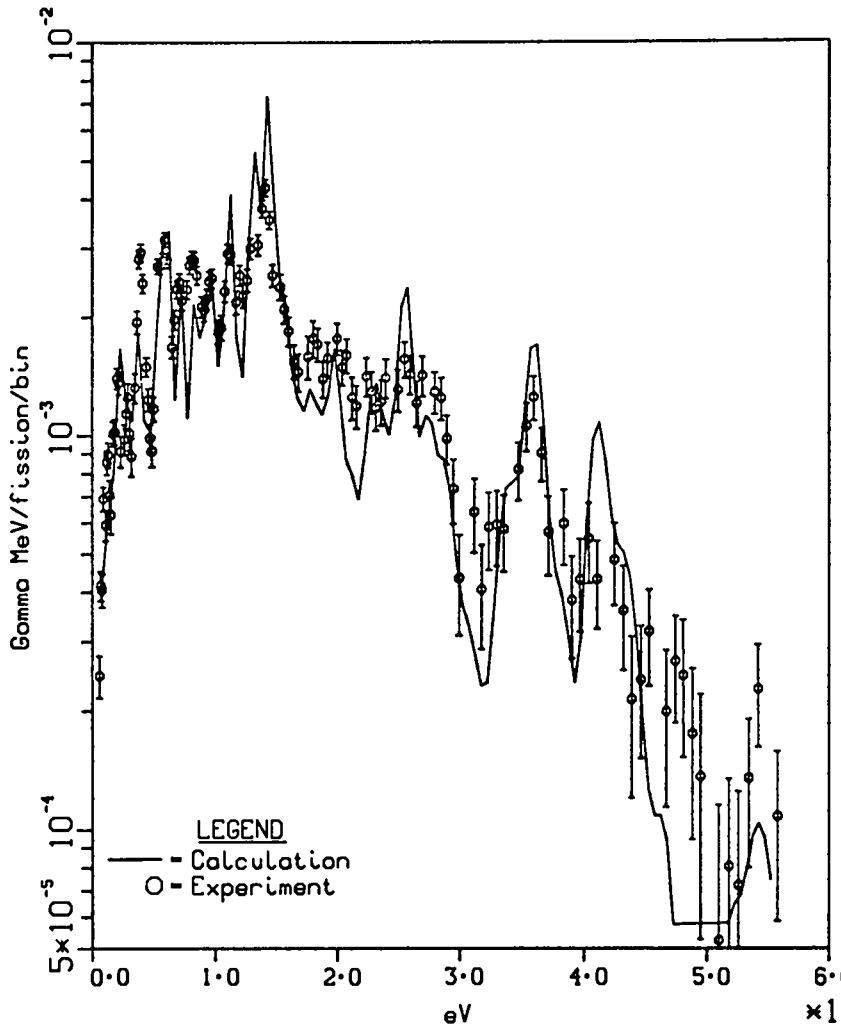

Fig.29. Comparison of calculation with ORNL 10-s irradiation experiment, 49.7-s decay.

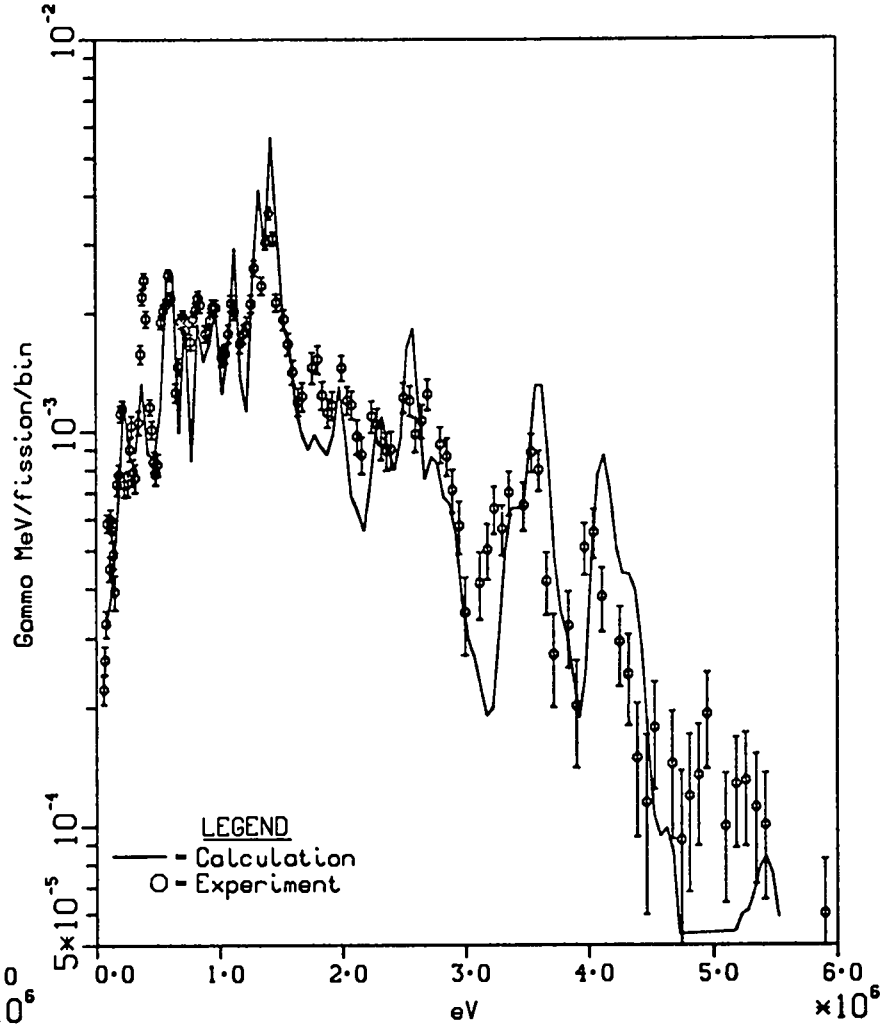

Fig.30. Comparison of calculation with ORNL 10-s irradiation experiment, 64.7-s decay.

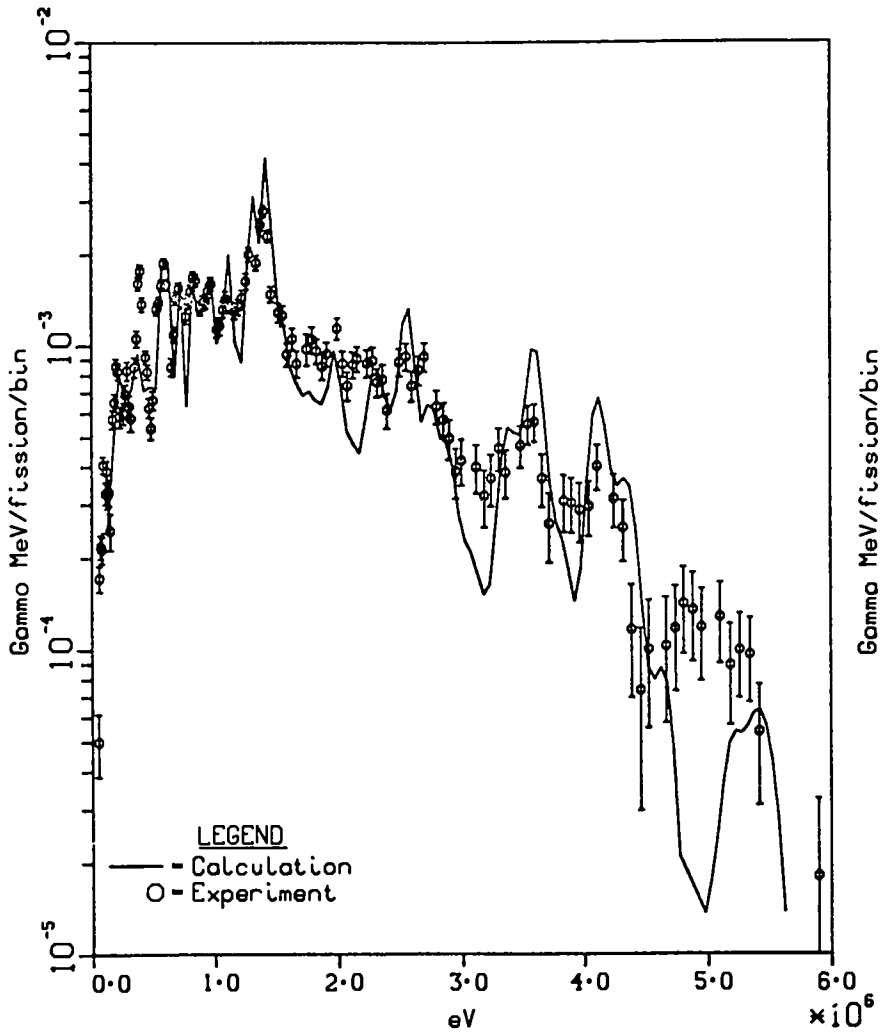

Fig. 31. Comparison of calculation with ORNL 10-s irradiation experiment, 84.7-s decay.

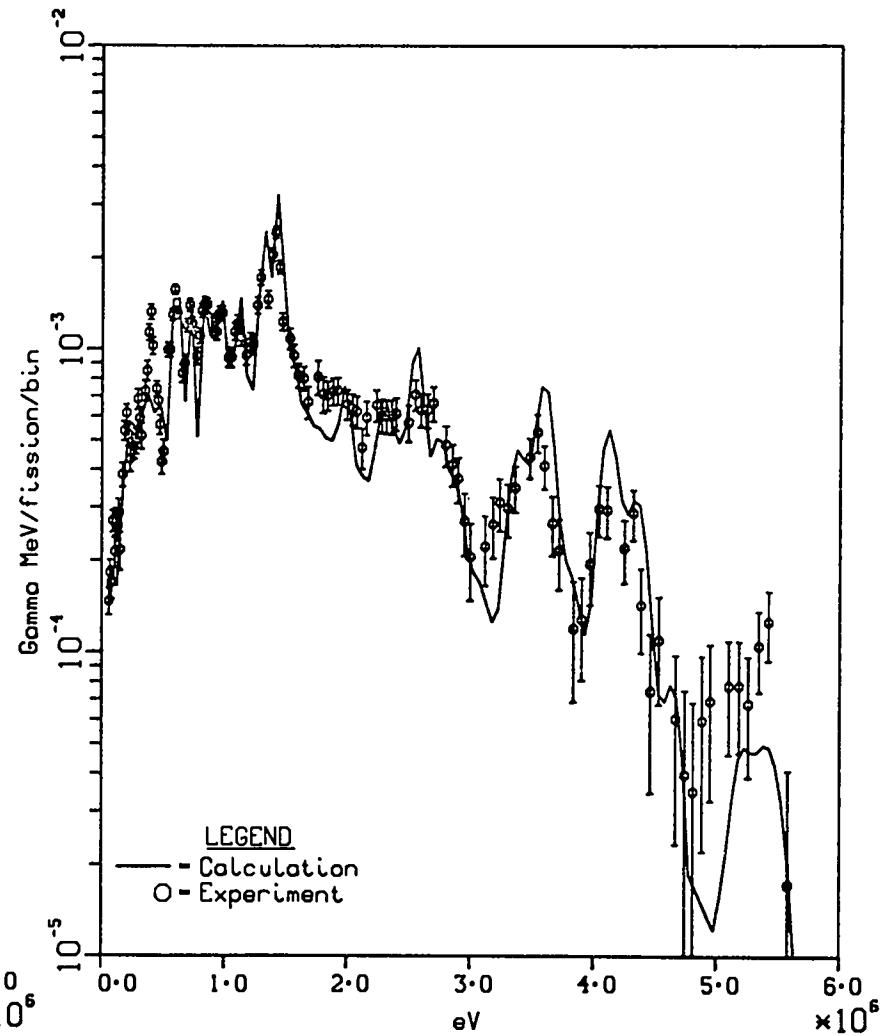

Fig. 32. Comparison of calculation with ORNL 10-s irradiation experiment, 104.7-s decay.

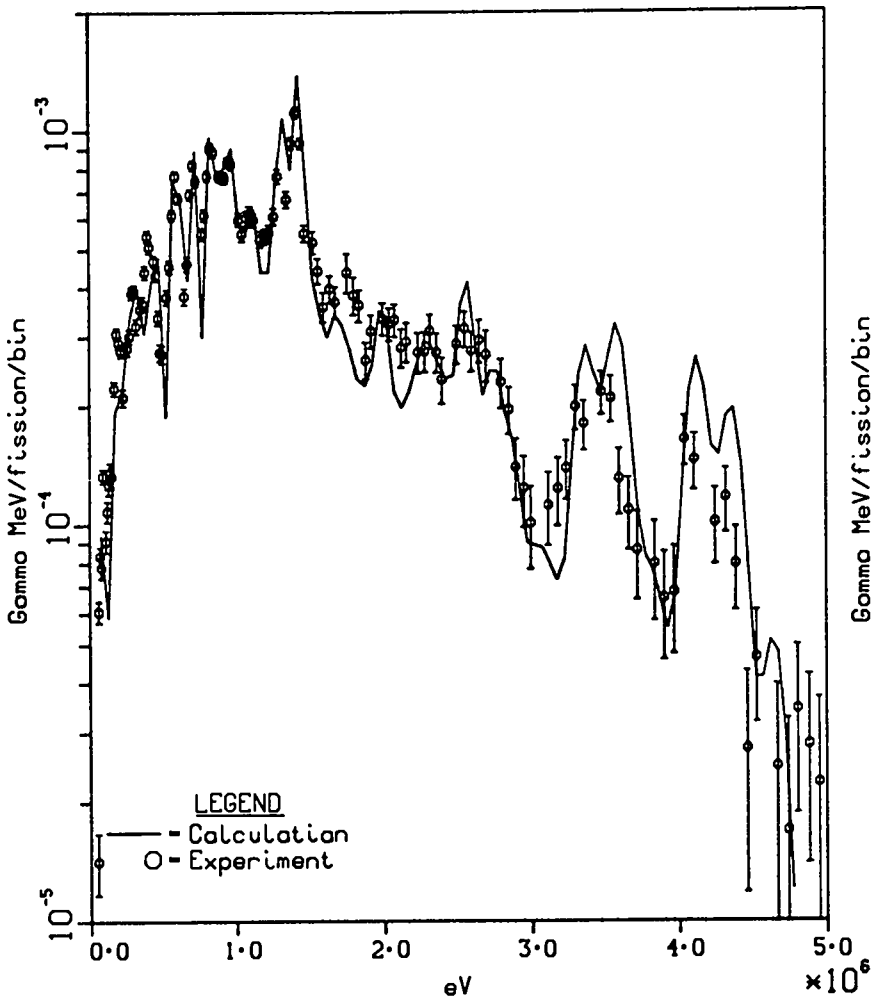

Fig.33. Comparison of calculation with ORNL 10-s irradiation experiment, 184.7-s decay.

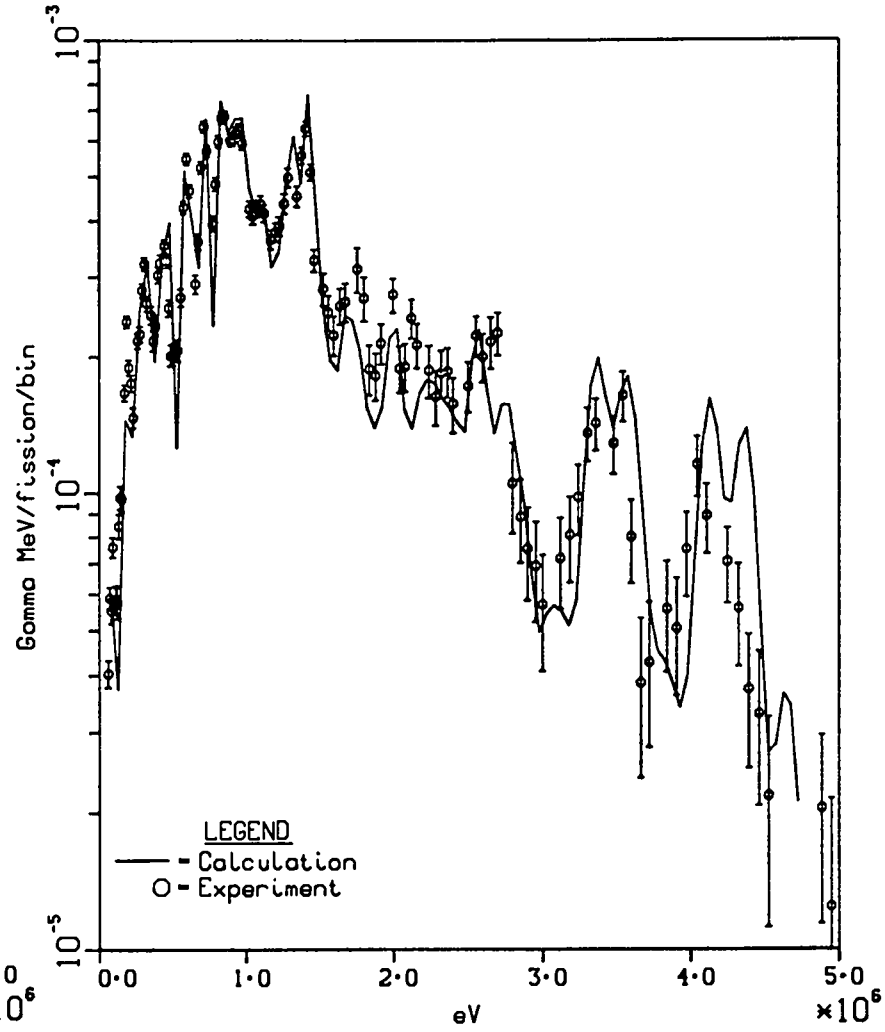

Fig.34. Comparison of calculation with ORNL 10-s irradiation experiment, 254.7-s decay.

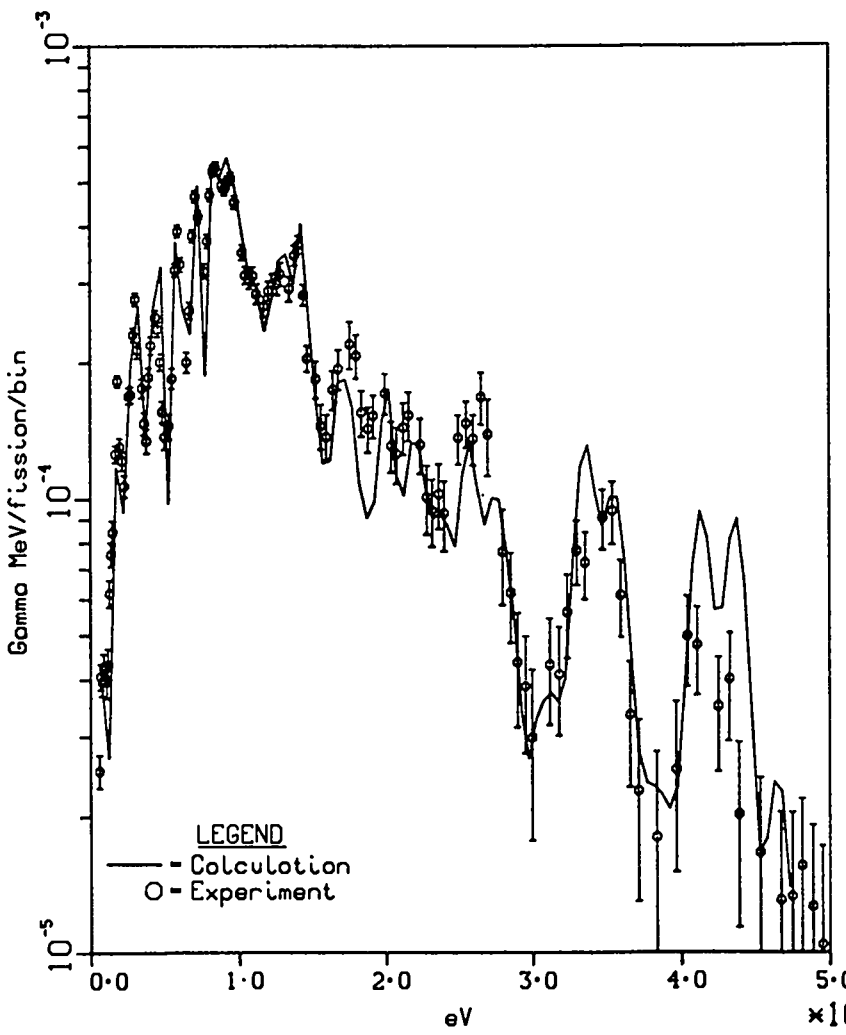

Fig.35. Comparisan of calculation with ORNL 10-s irradiation experiment, 344.7-s decay.

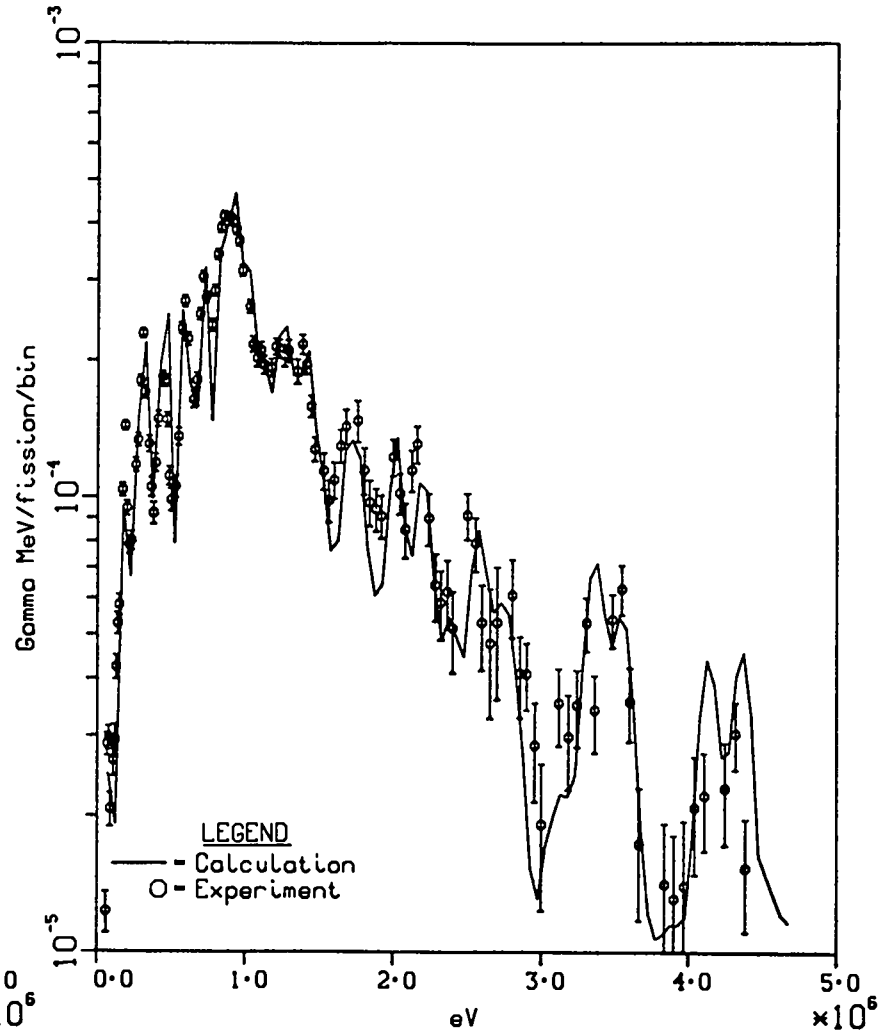

Fig.36. Comparison of calculation with ORNL 10-s irradiation experiment, 494.7-s decay.

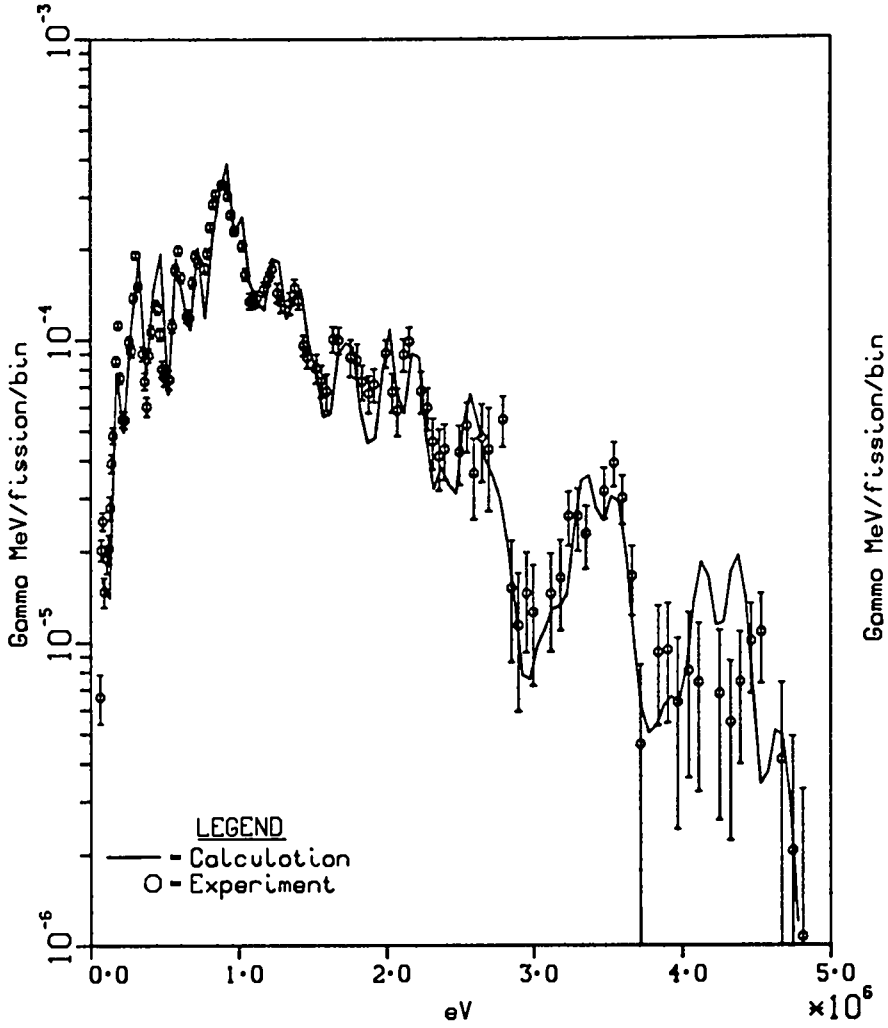

Fig.37. Comparison of calculation with ORNL 10-s irradiation experiment, 694.7-s decay.

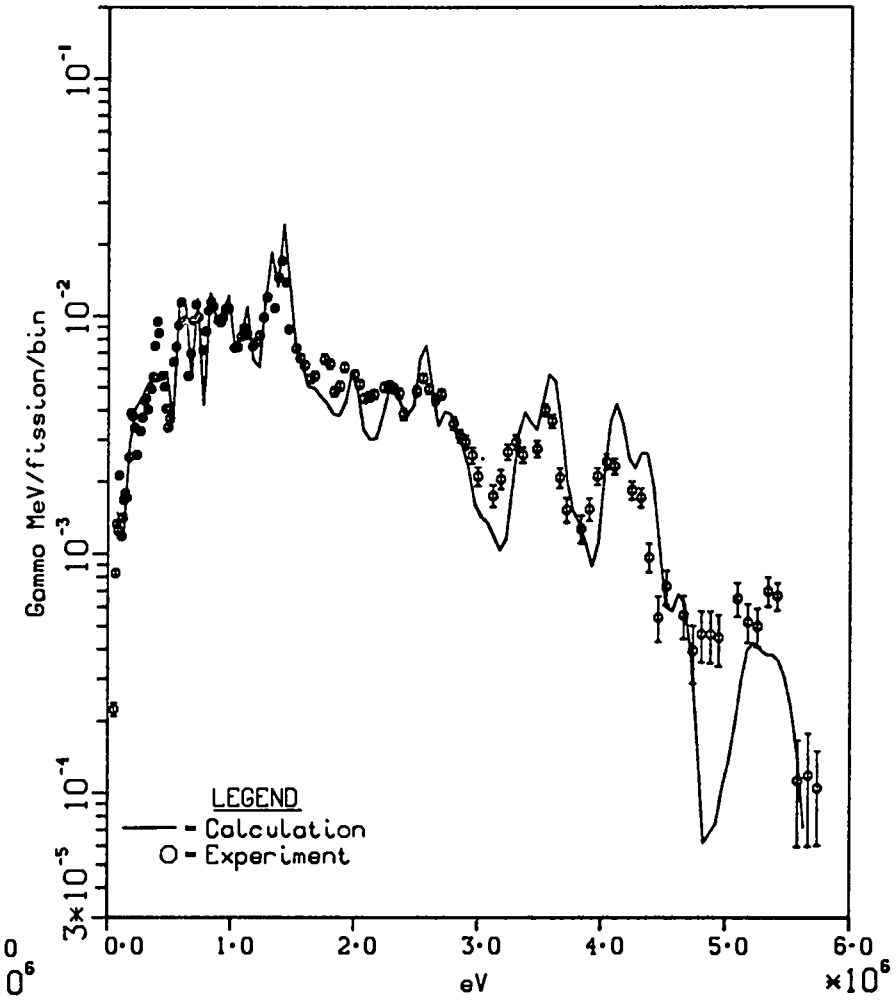

Fig.38. Comparison of calculation with ORNL 100-s irradiation experiment, 90.0-s decay.

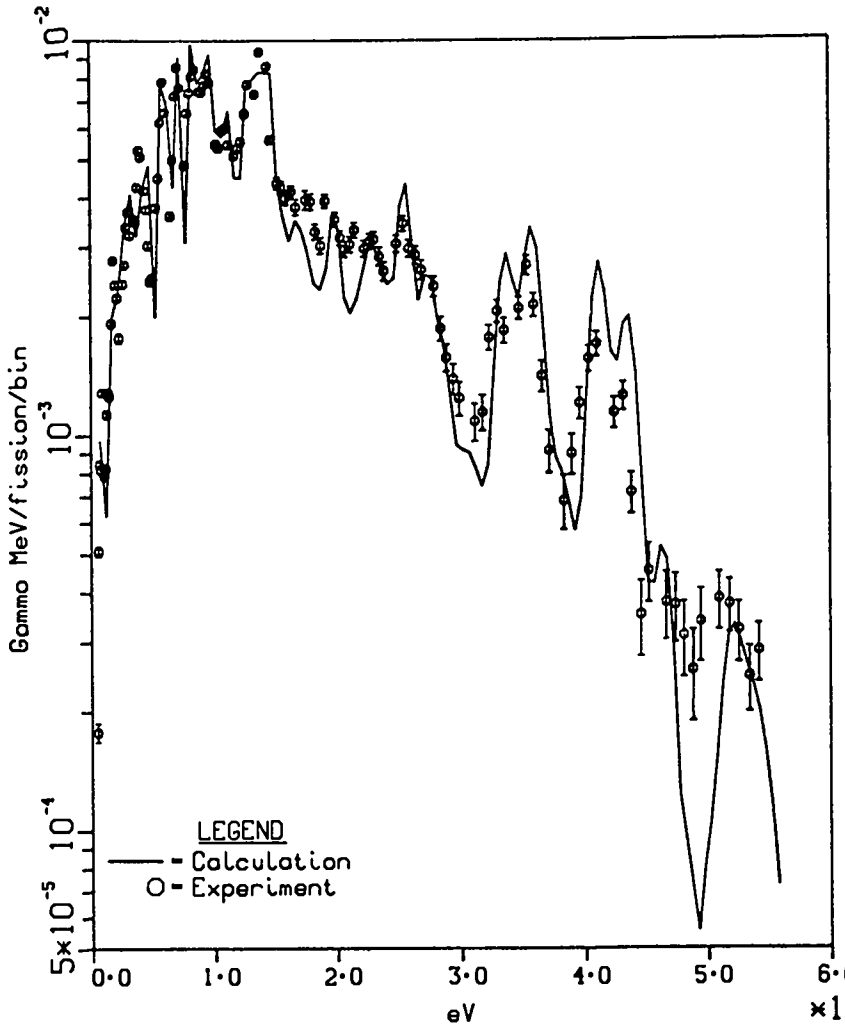

Fig.39. Comparison of calculation with ORNL 100-s irradiation experiment, 140.0-s decay.

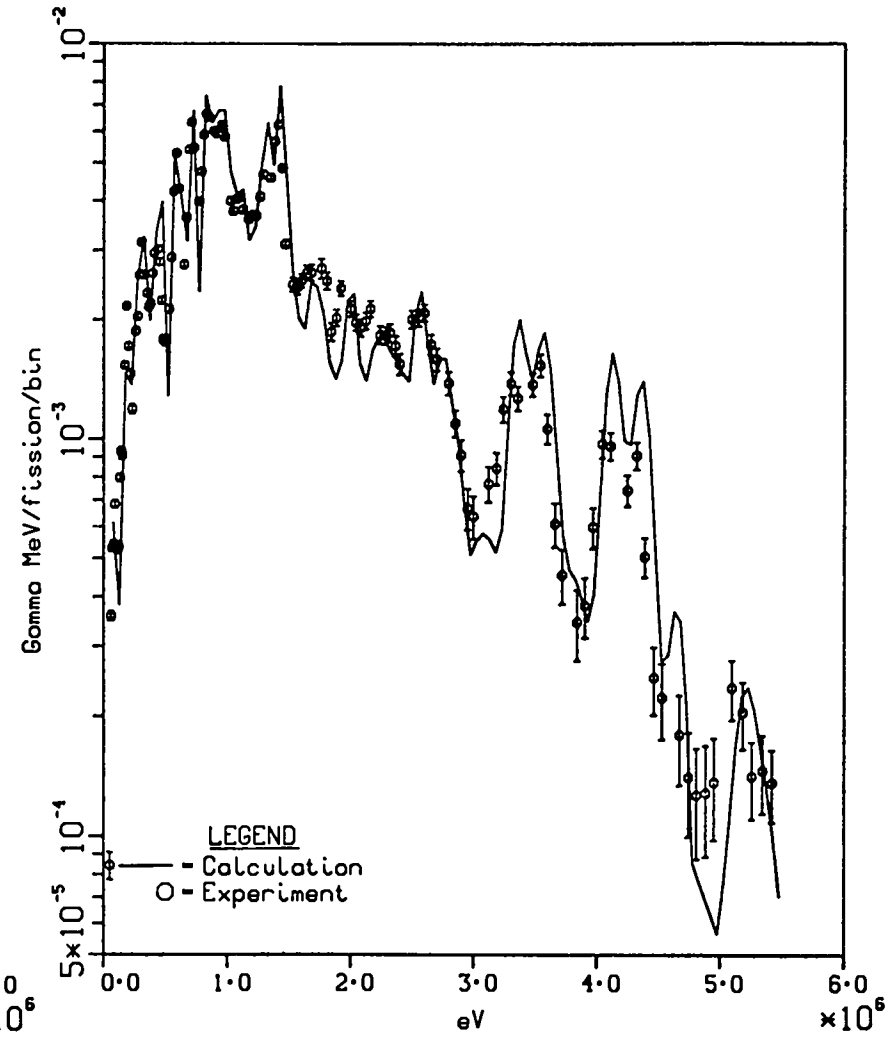

Fig.40. Comparison of calculation with ORNL 100-s irradiation experiment, 210.0-s decay.

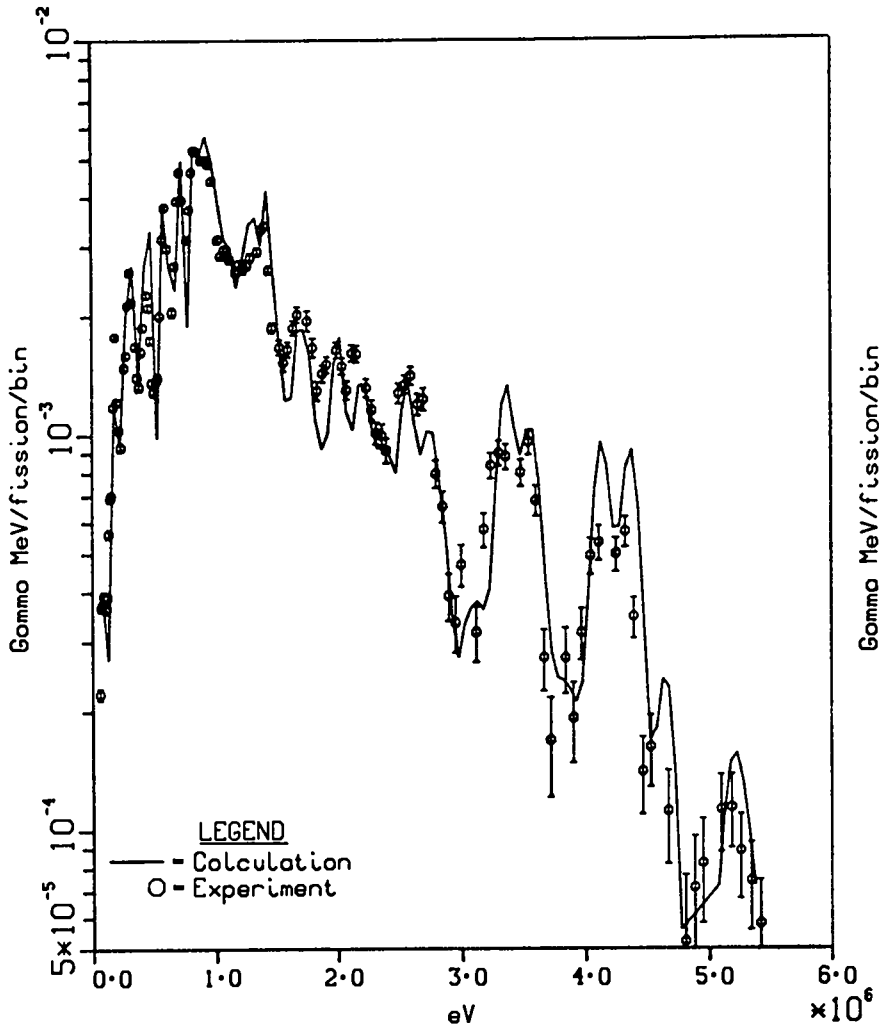

Fig.41. Comparison of calculation with ORNL 100-s irradiation experiment, 300.0-s decay.

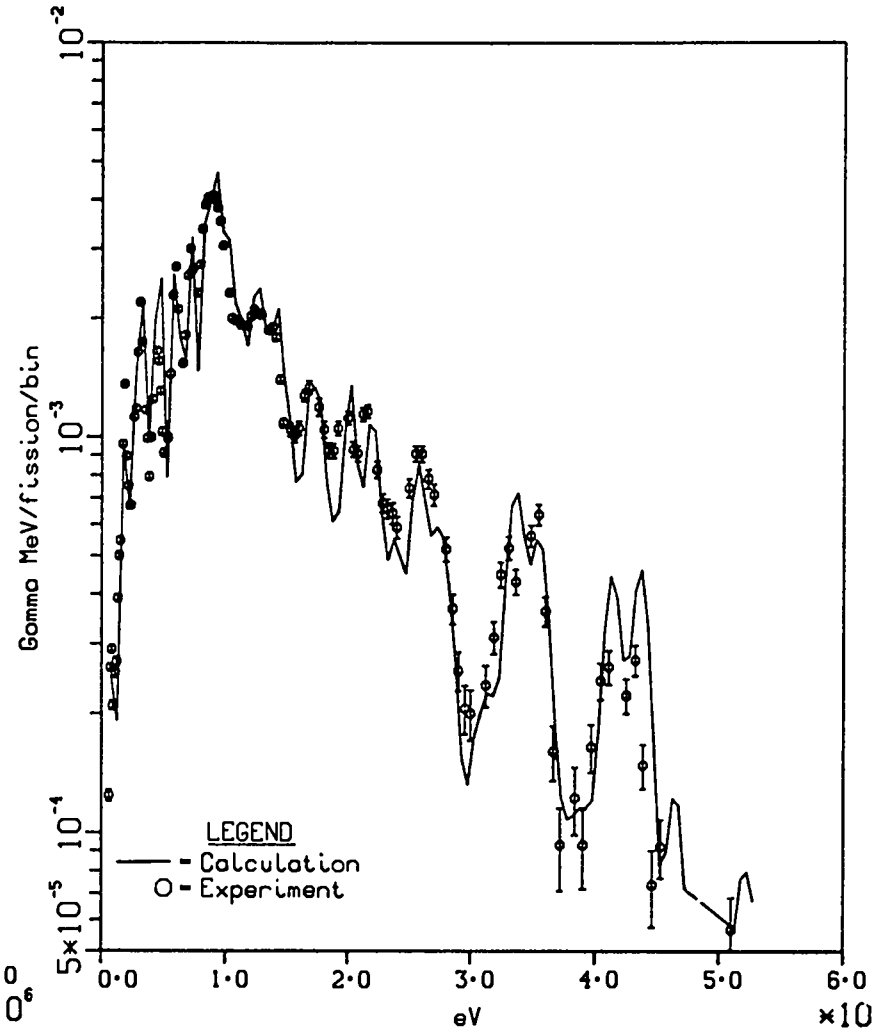

Fig.42. Comparison of calculation with ORNL 100-s irradiation experiment, 450.0-s decay.

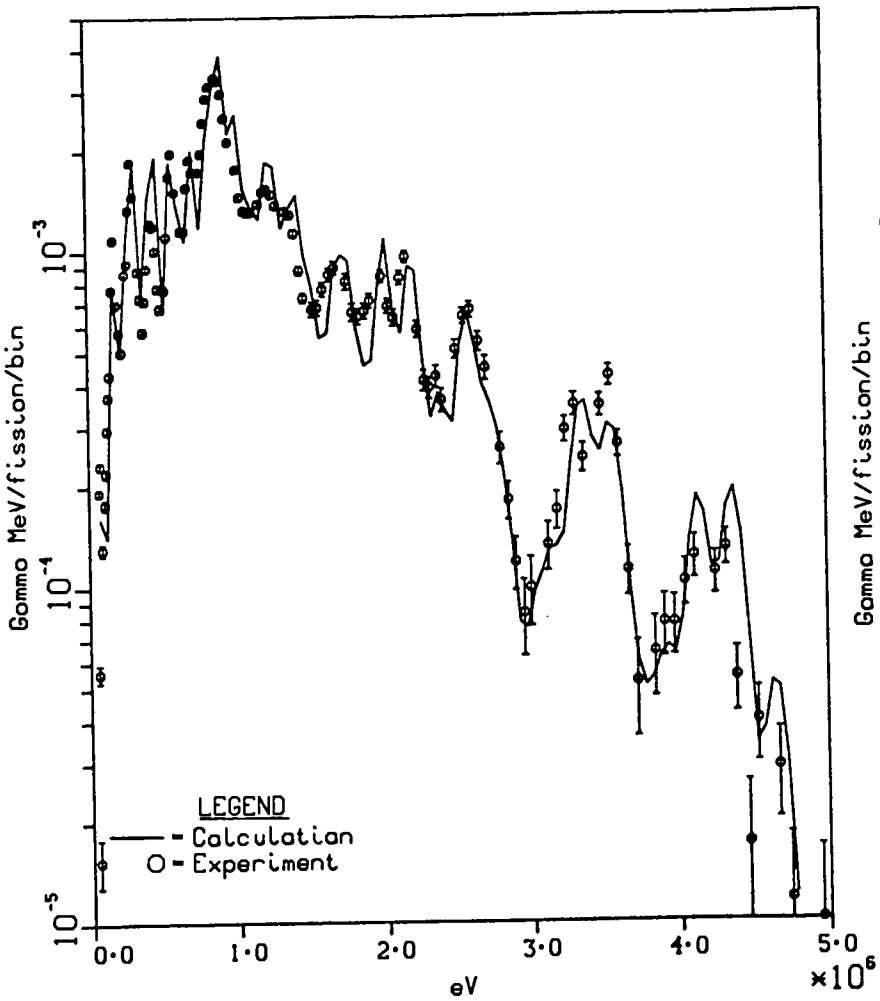

Fig.43. Comparison of calculation with ORNL 100-s irradiation experiment, 650.0-s decay.

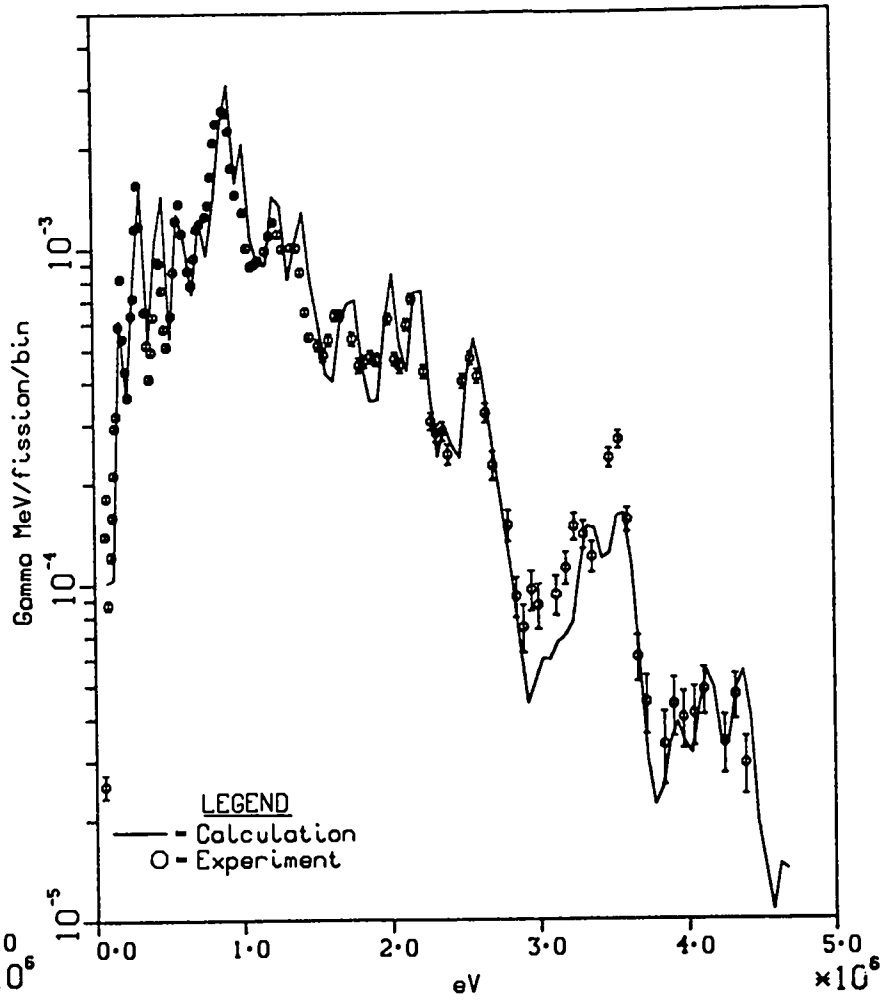

Fig.44. Comparisan of calculation with ORNL 100-s irradiation experiment, 950.0-s decay.

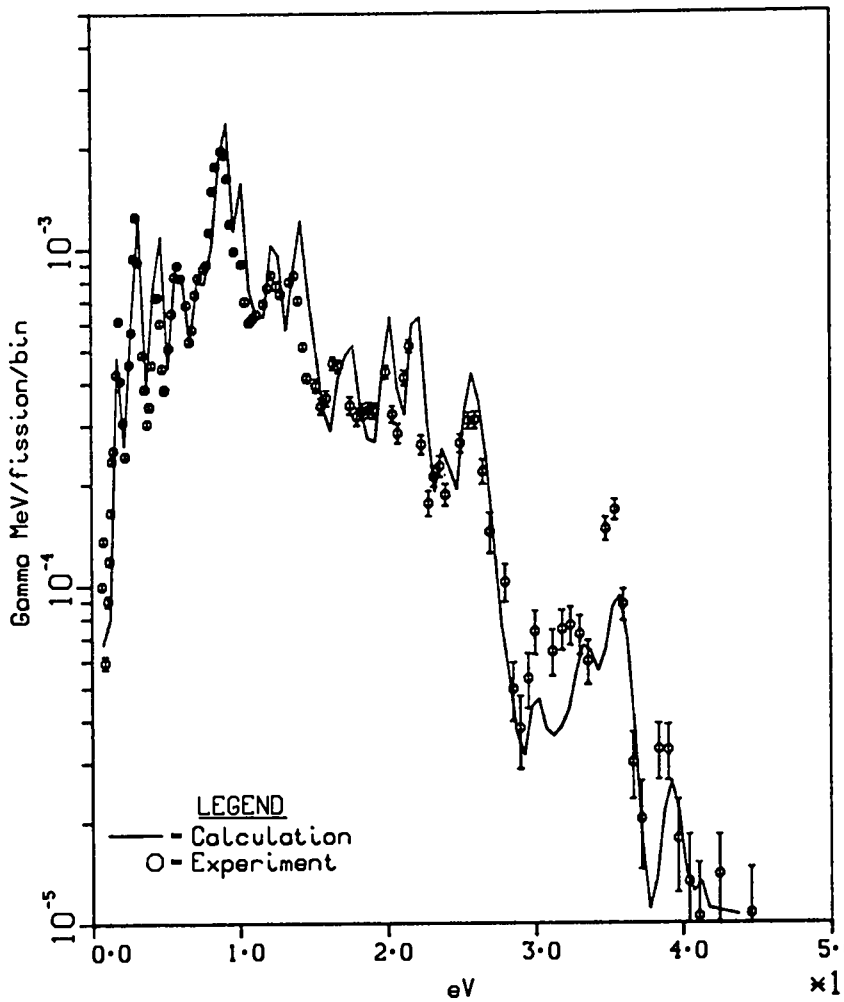

Fig.45. Comparison of calculation with ORNL 100-s irradiation experiment, 1350.0-s decay.

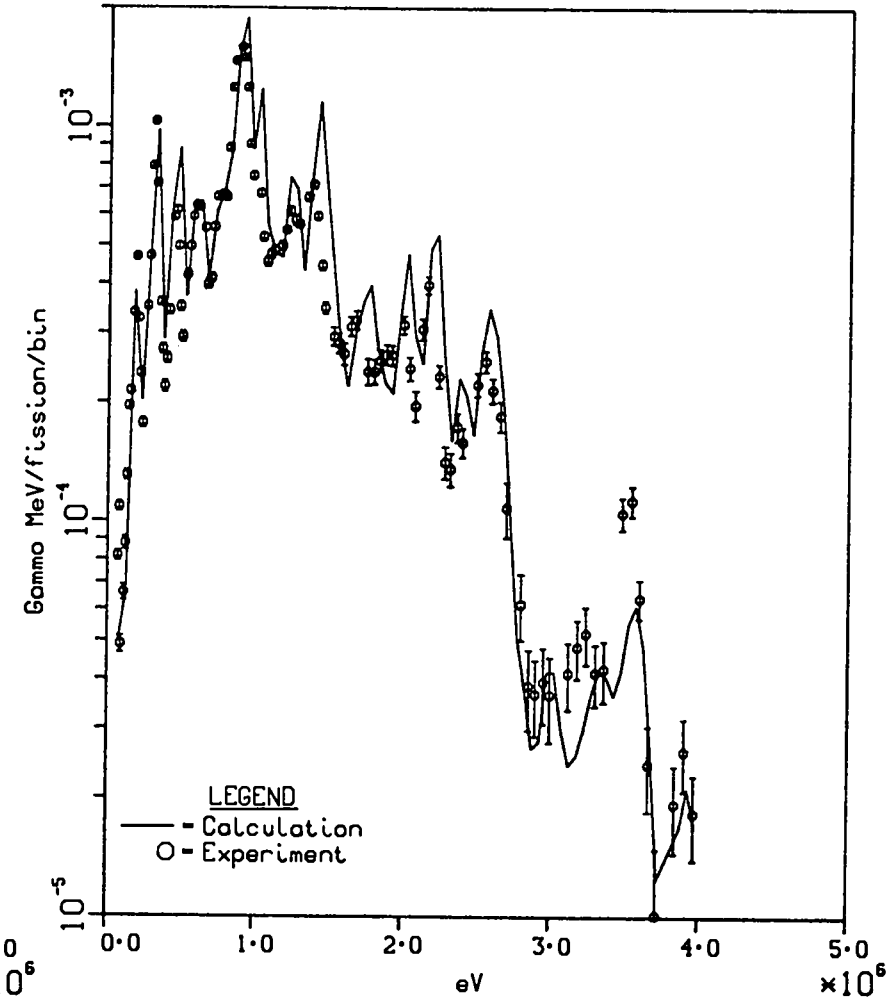

Fig.46. Comparison of calculation with ORNL 100-s irradiation experiment, 1750.0-s decay.

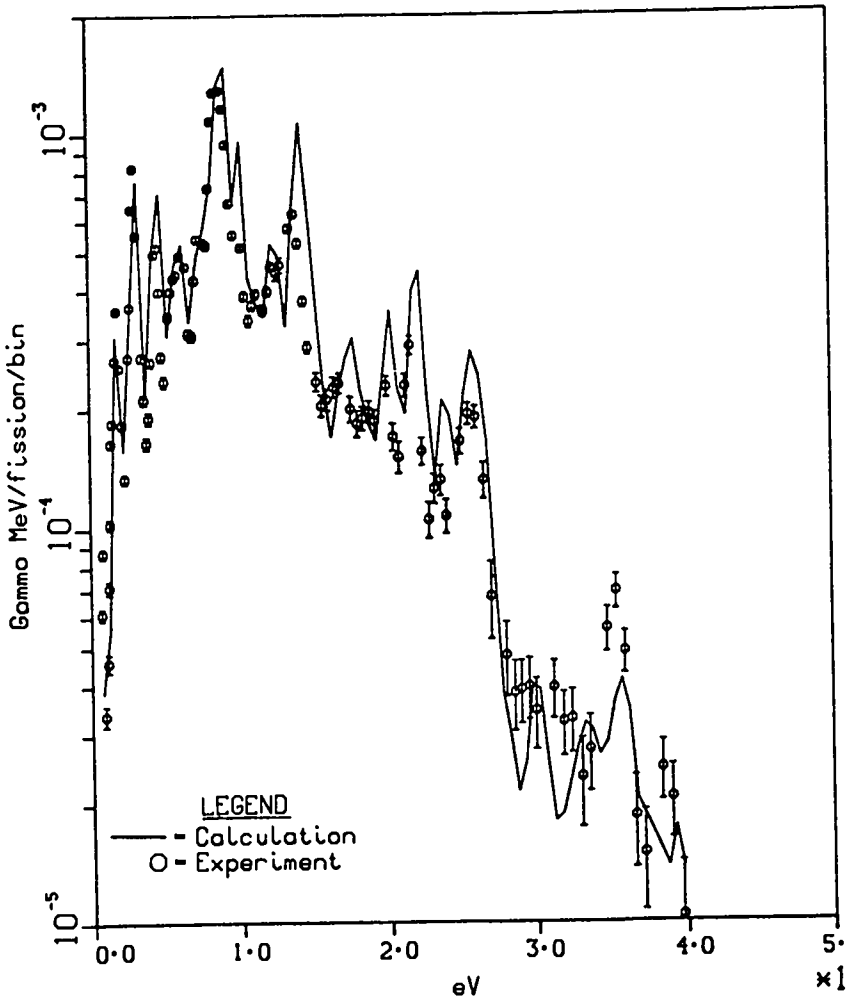

Fig.47. Comparison of calculation with ORNL 100-s irradiation experiment, 2200.0-s decay.

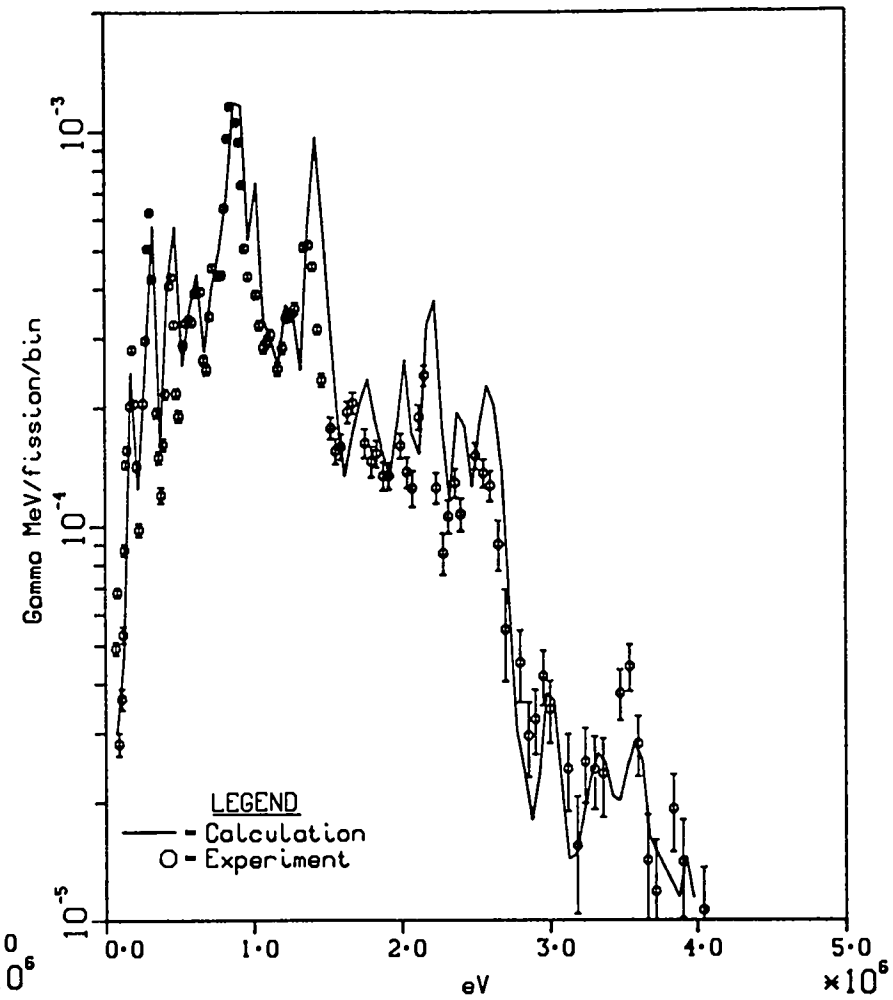

Fig.48. Comparison of calculation with ORNL 100-s irradiation experiment, 2700.0-s decay.

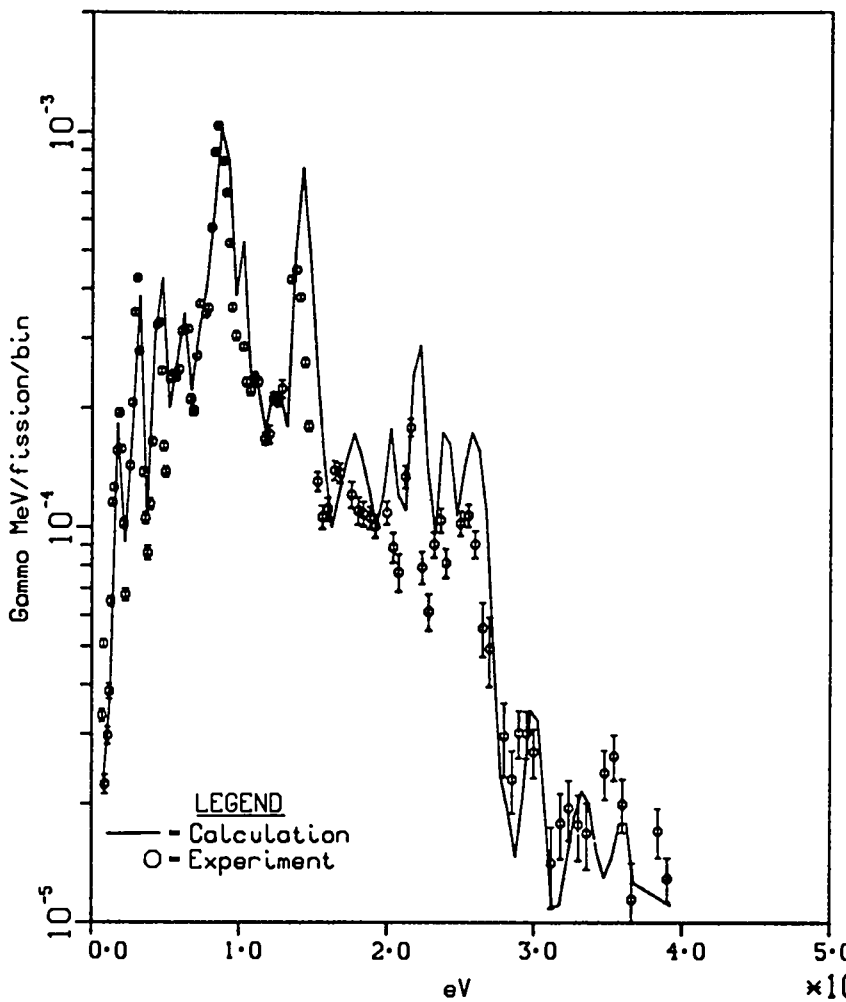

Fig.49. Comparison of calculation with ORNL 100-s irradiation experiment, 3450.0-s decay.

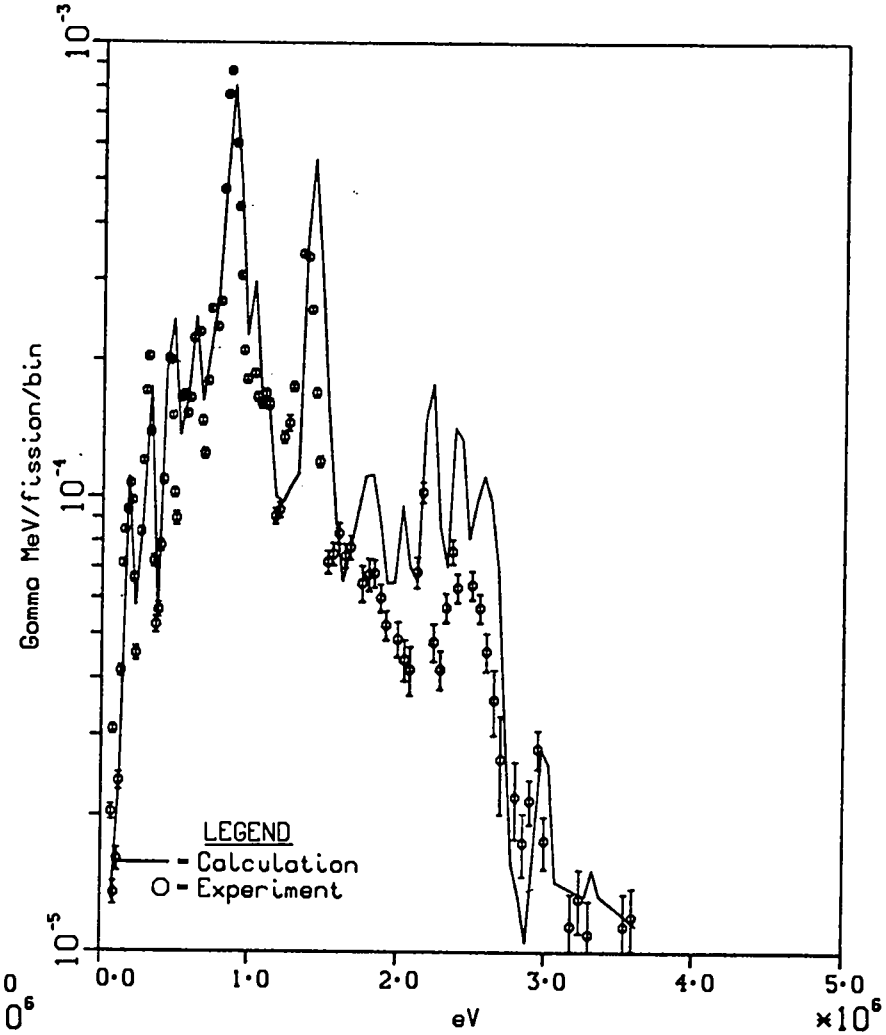

Fig.50. Comparison of calculation with ORNL 100-s irradiation experiment, 4950.0-s decay.

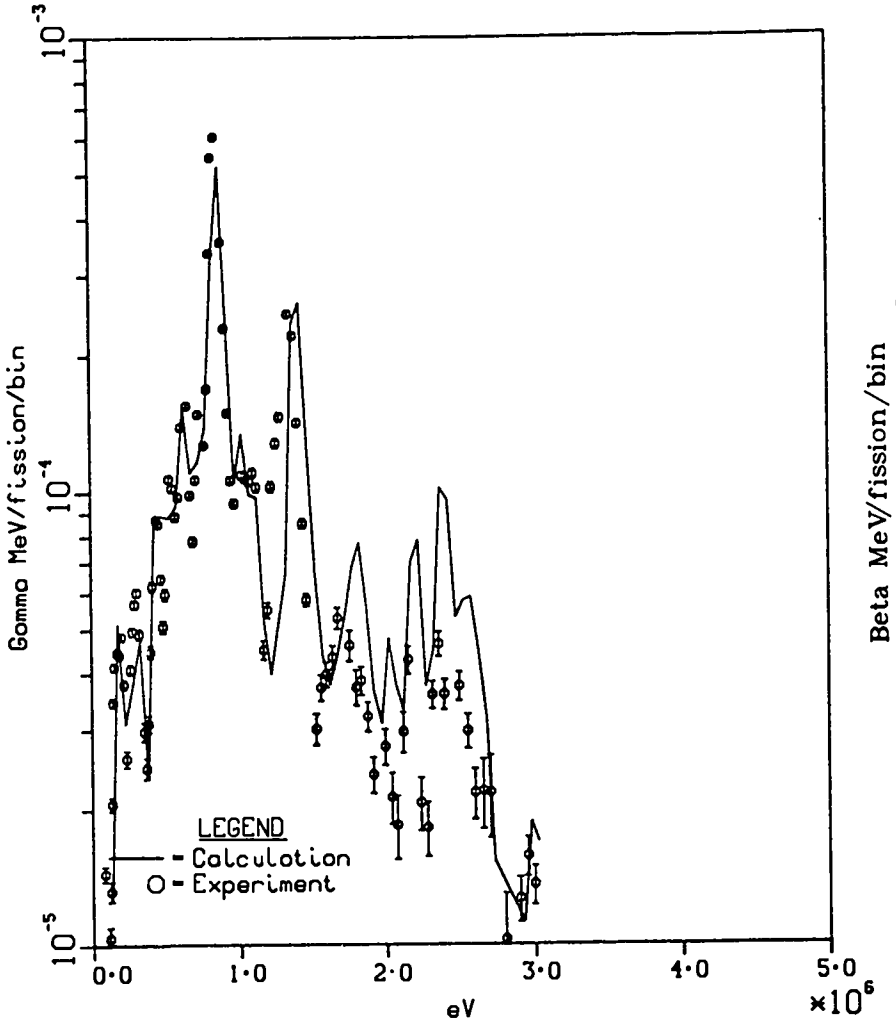

Fig.51. Comparison of calculation with ORNL 100-s irradiation experiment, 7950.0-s decay.

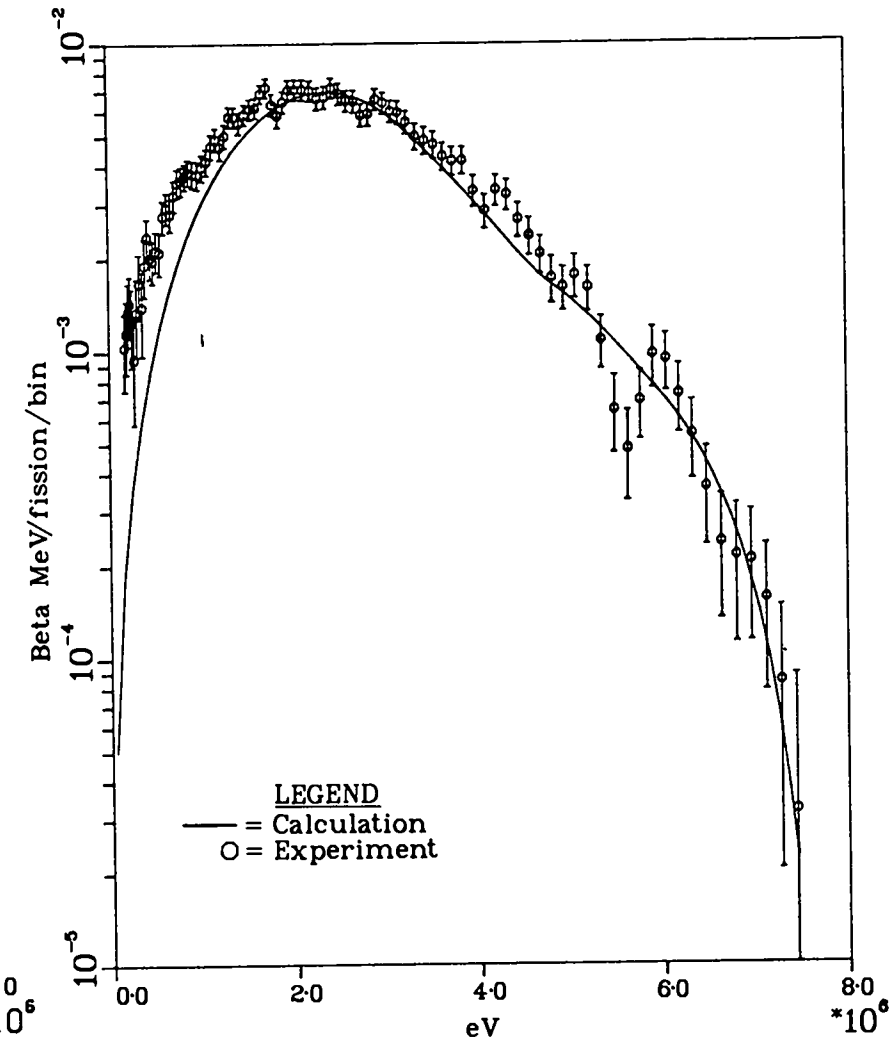

Fig. 52. Comparison of calculation with ORNL 1-s irradiation experiment, 2.2-s decay.

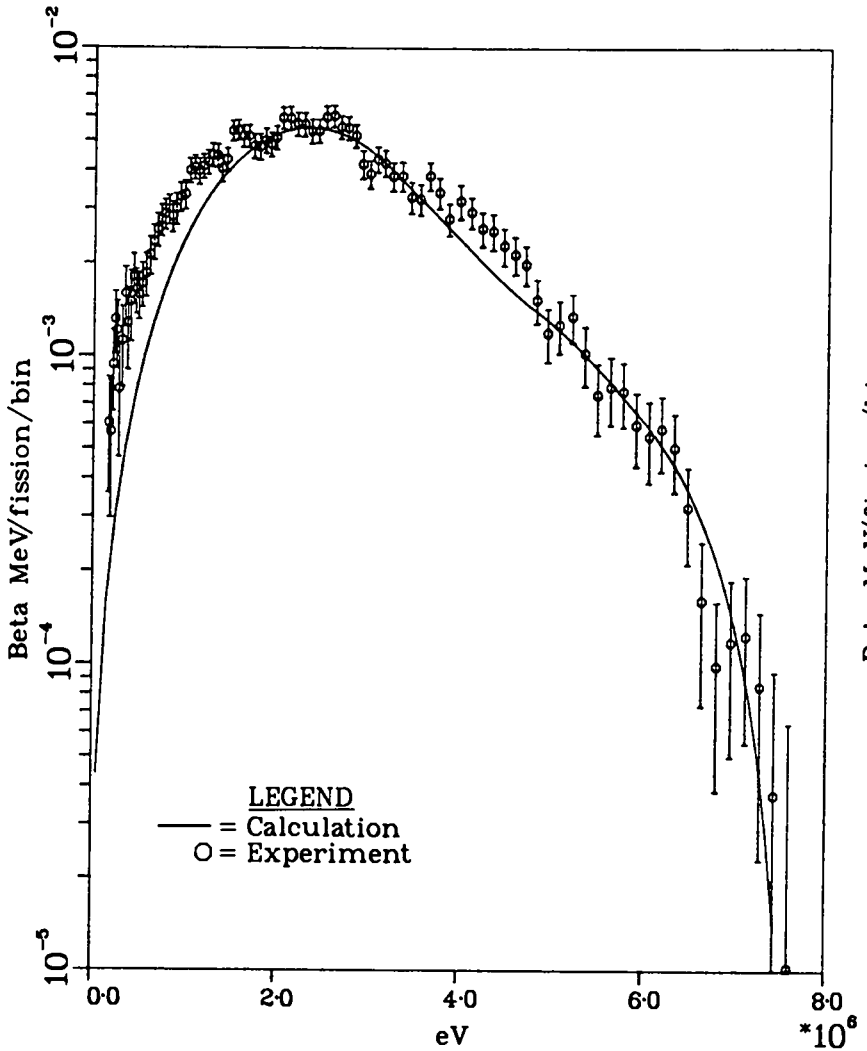

Fig. 53. Comparison of calculation with ORNL 1-s irradiation experiment, 3.2-s decay.

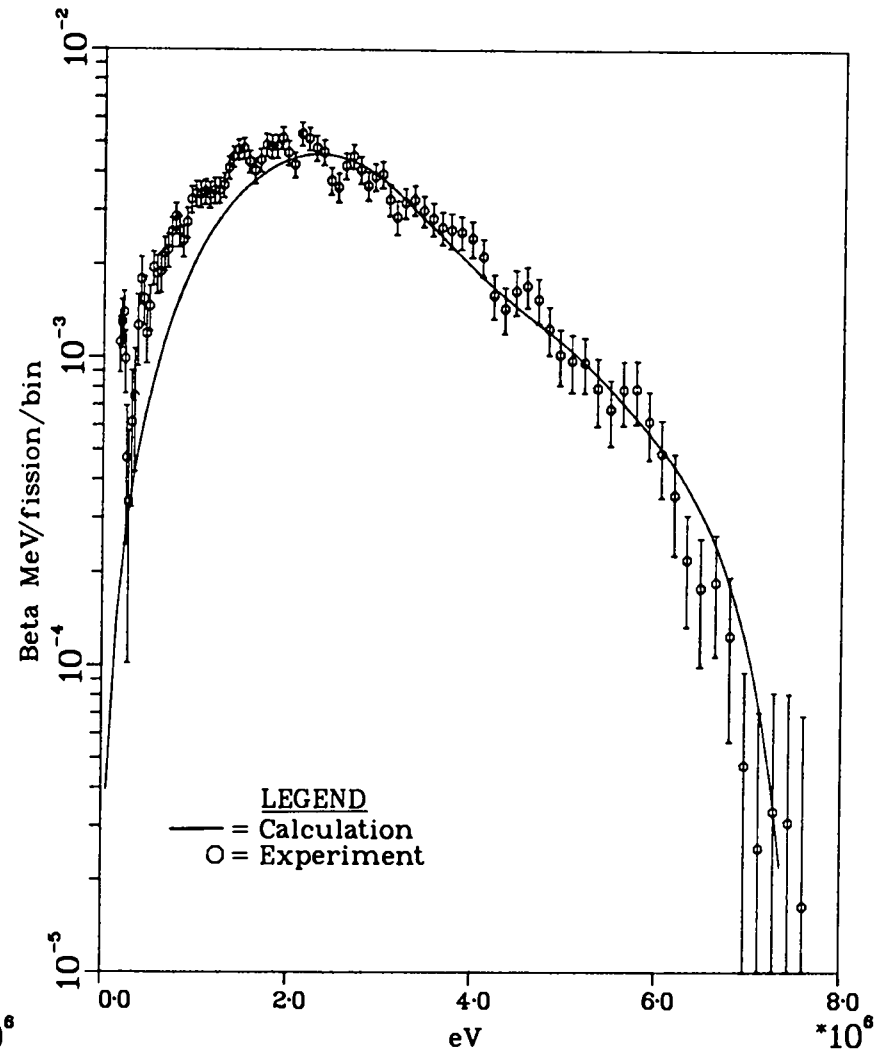

Fig. 54. Comparison of calculation with ORNL 1-s irradiation experiment, 4.2-s decay.

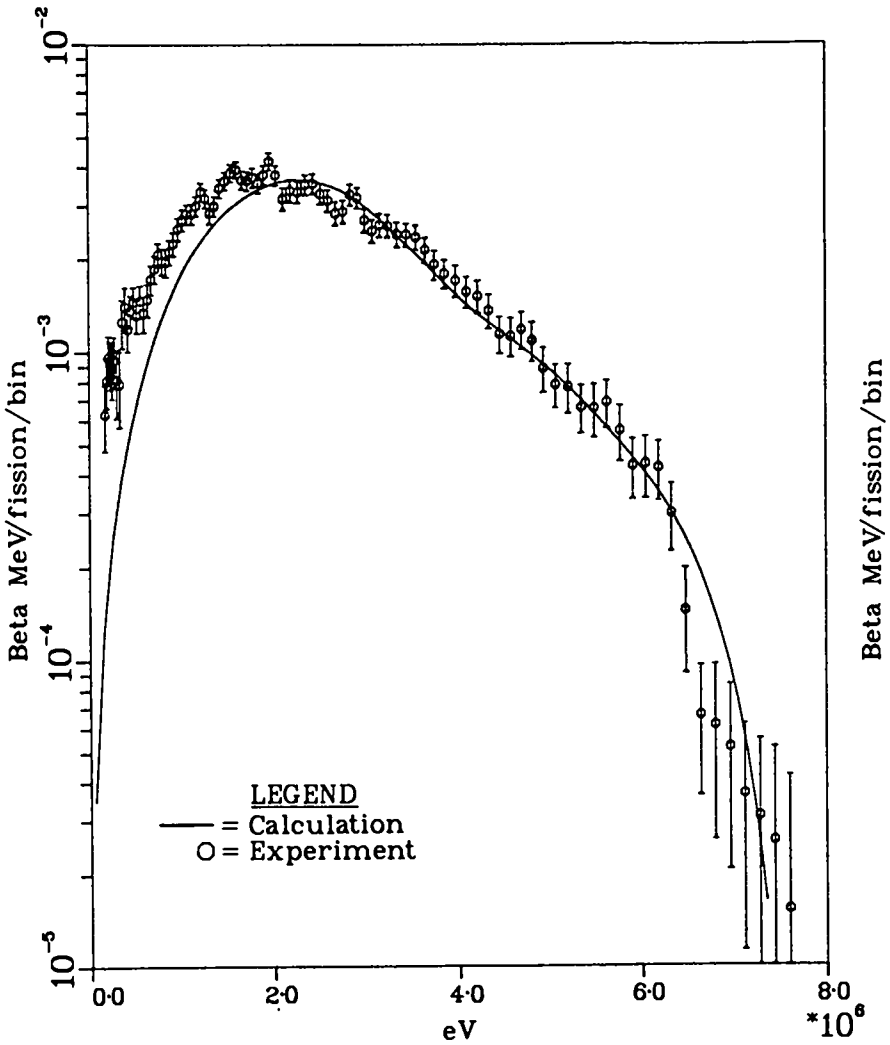

Fig. 55. Comparison of calculation with ORNL 1-s irradiation experiment, 5.2-s decay.

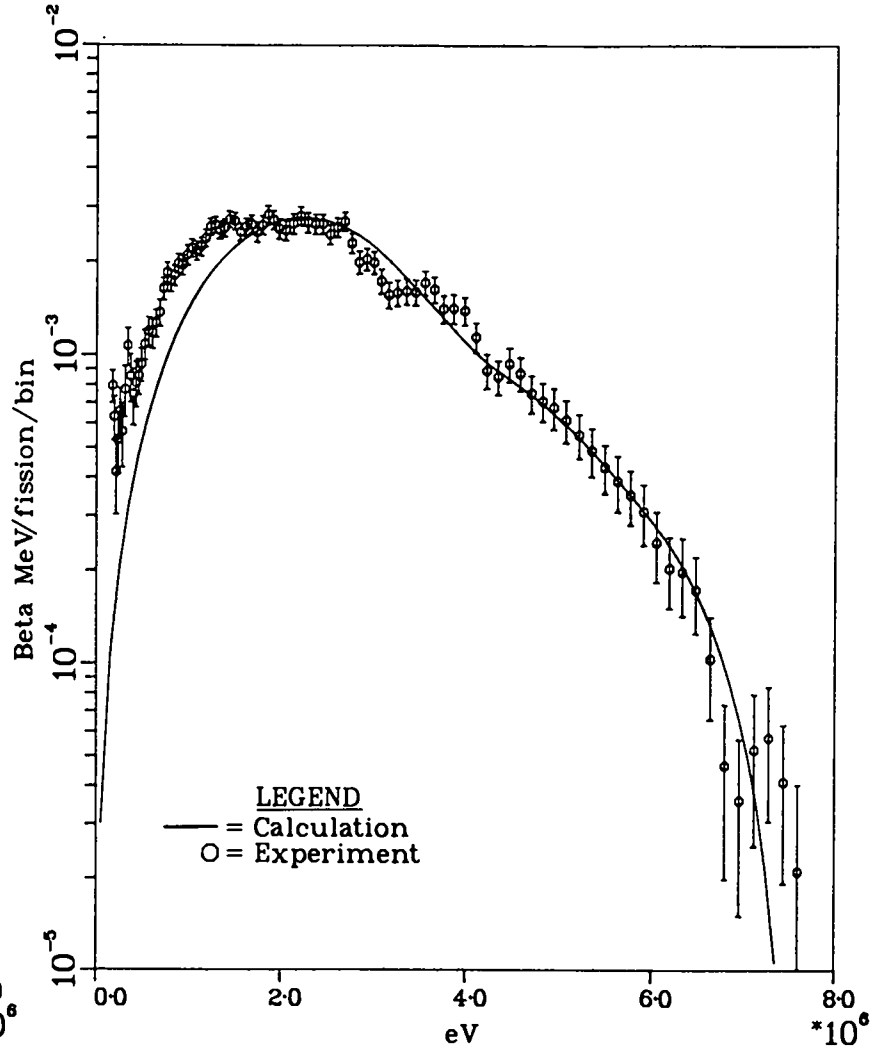

Fig. 56. Comparison of calculation with ORNL 1-s irradiation experiment, 8.2-s decay.

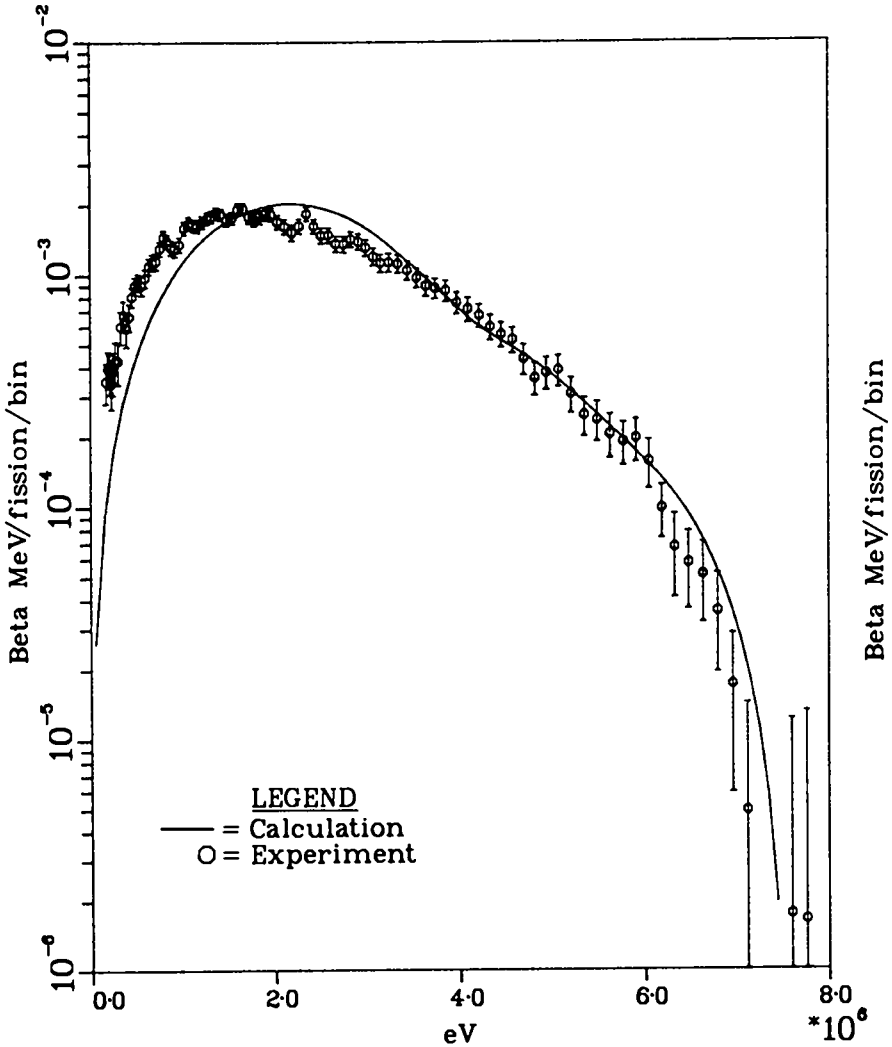

Fig. 57. Comparison of calculation with ORNL 1-s irradiation experiment, 12.2-s decay.

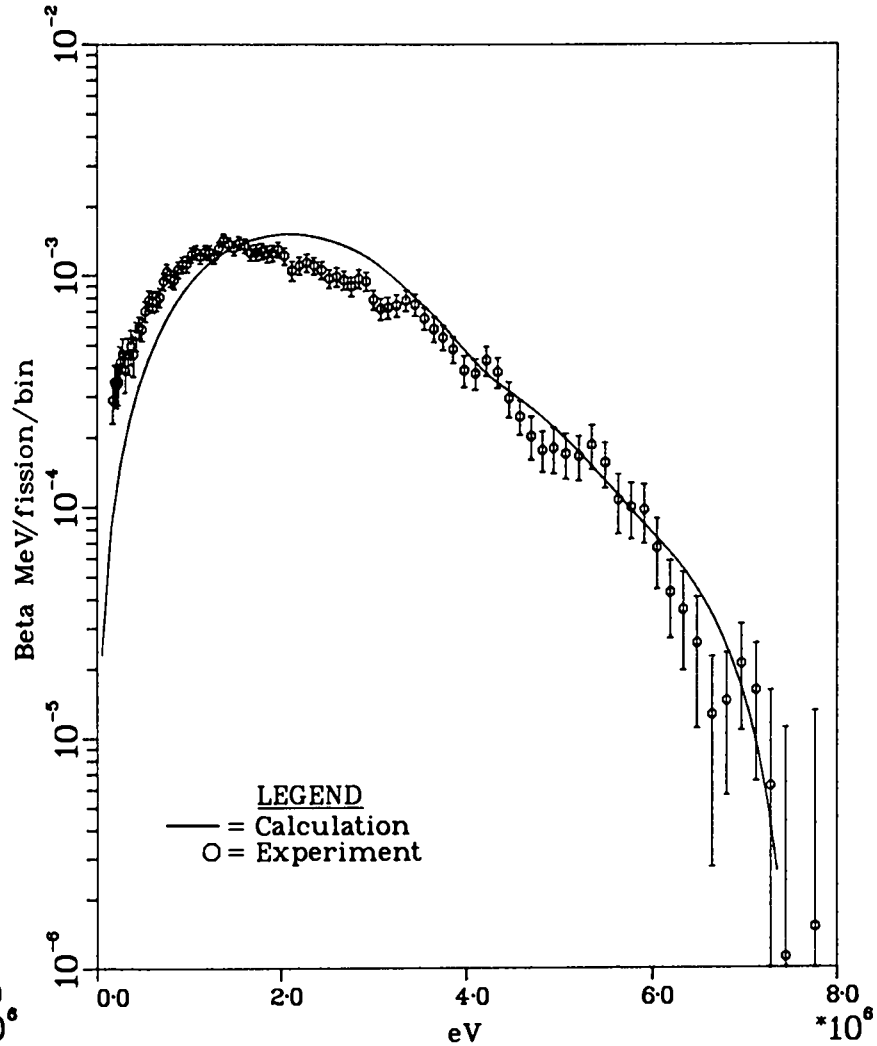

Fig. 58. Comparison of calculation with ORNL 1-s irradiation experiment, 17.2-s decay.

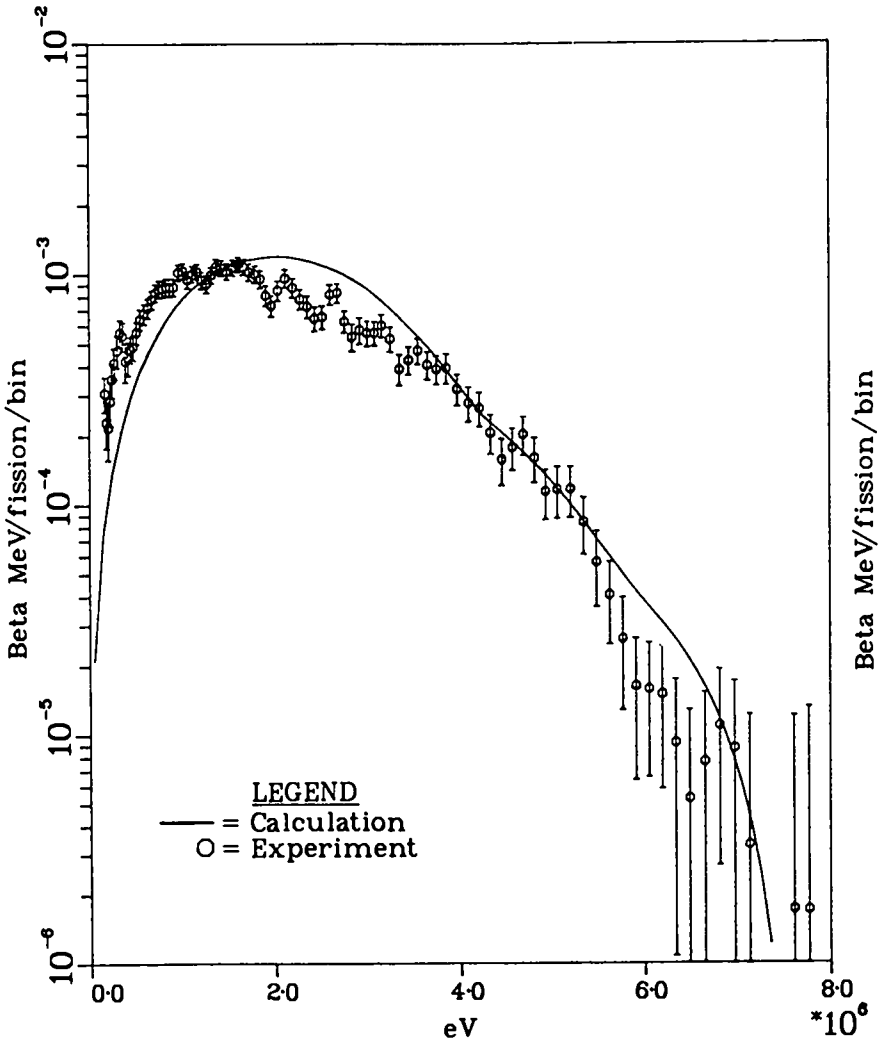

Fig. 59. Comparison of calculation with ORNL 1-s irradiation experiment, 22.2-s decay.

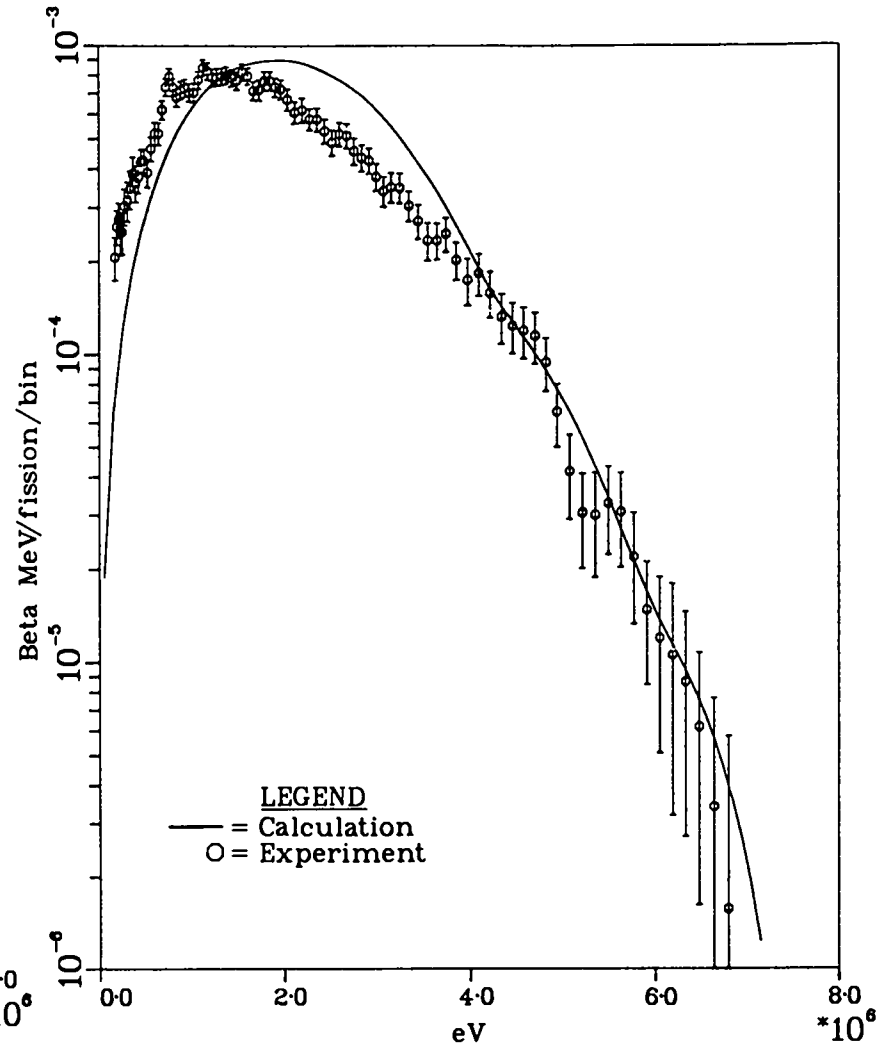

Fig. 60. Comparison of calculation with ORNL 1-s irradiation experiment, 29.7-s decay.

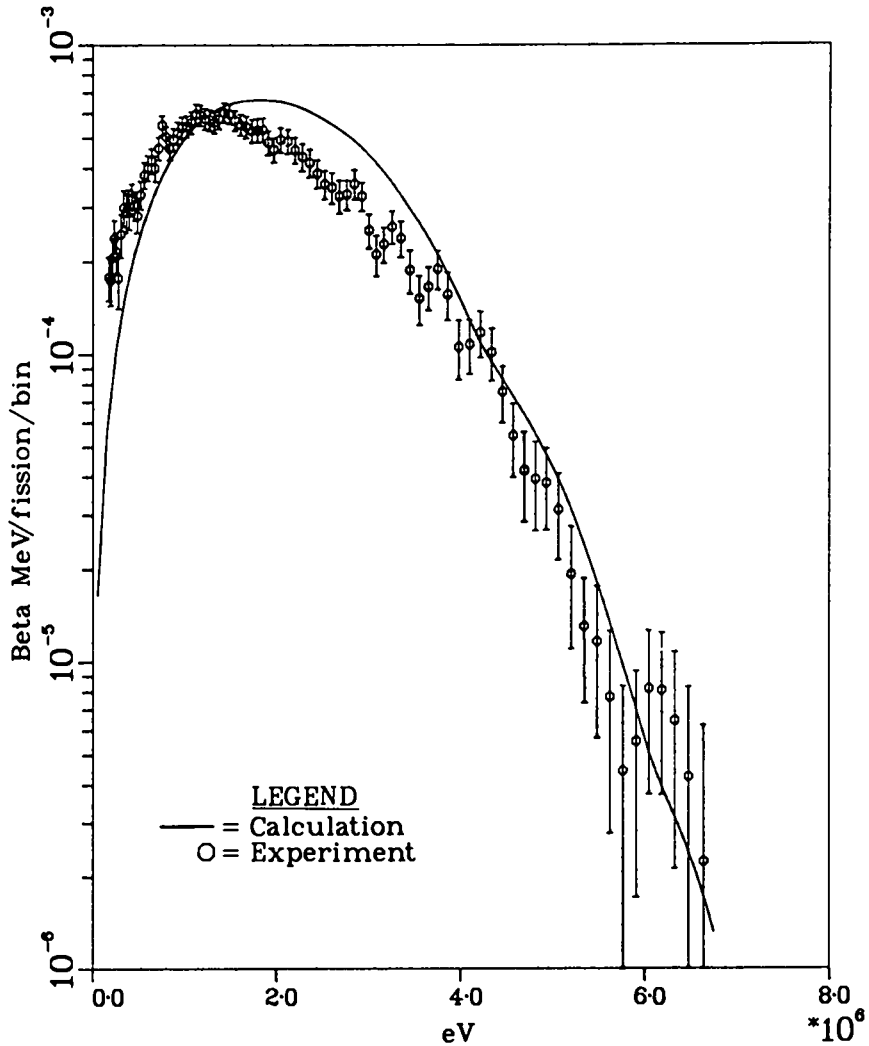

Fig. 61. Comparison of calculation with ORNL 1-s irradiation experiment, 39.7-s decay.

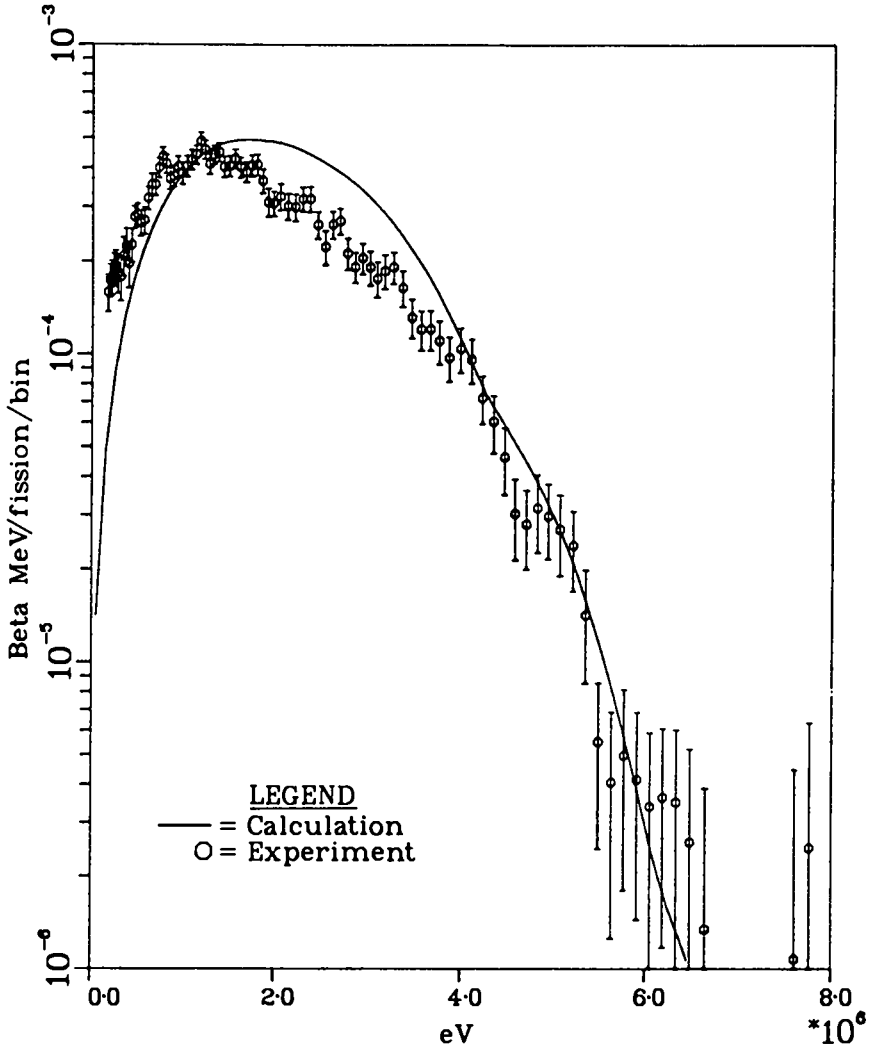

Fig. 62. Comparison of calculation with ORNL 1-s irradiation experiment, 52.2-s decay.

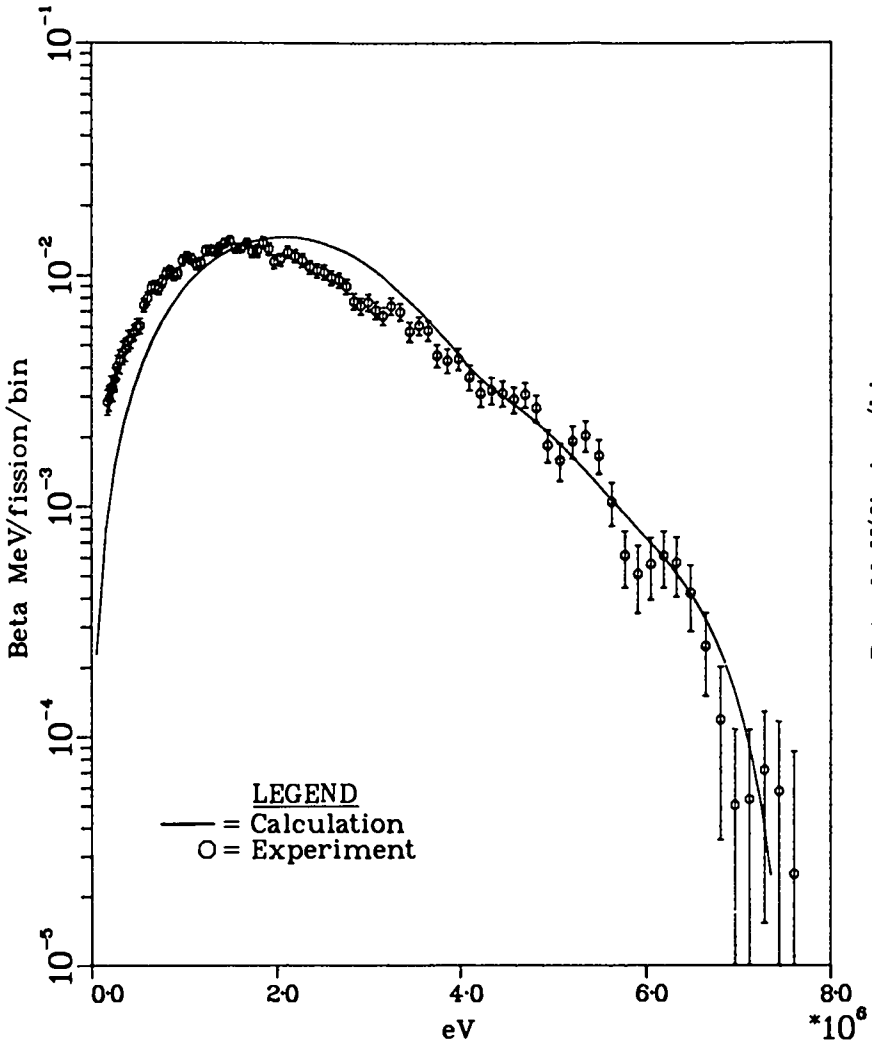

Fig. 63. Comparison of calculation with ORNL 10 s irradiation experiment, 13.7-s decay.

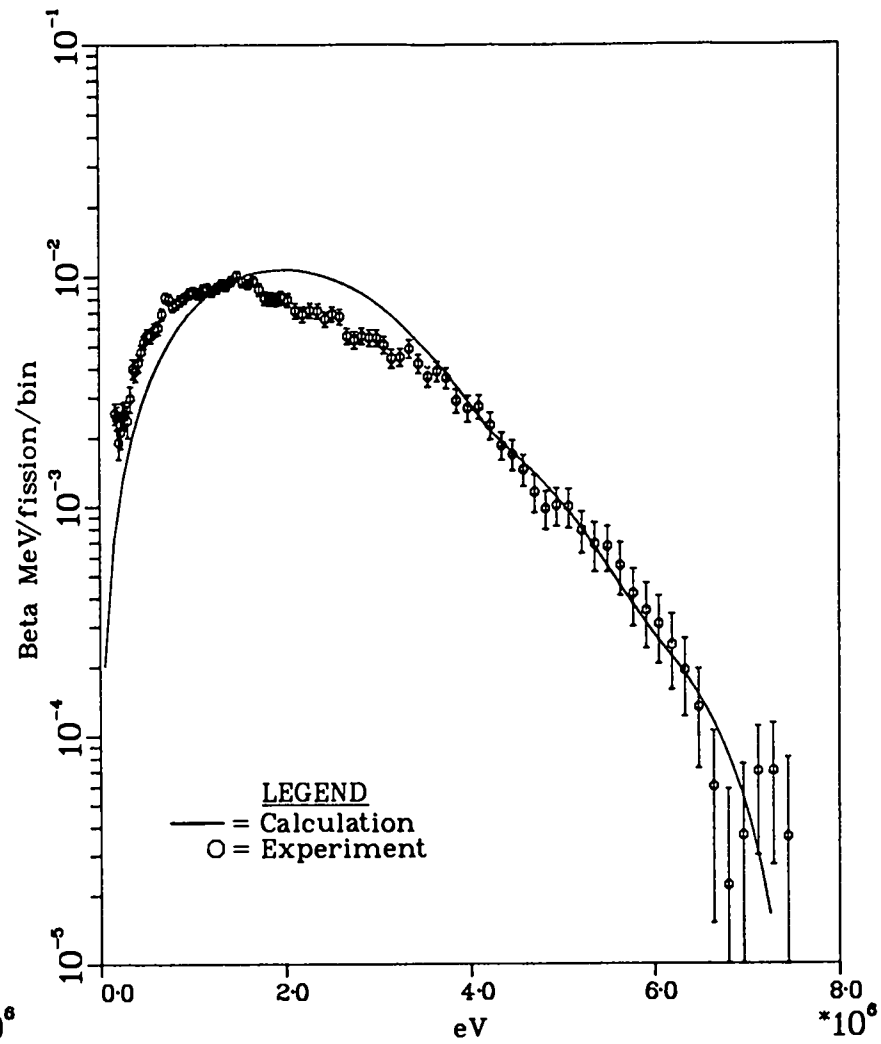

Fig. 64. Comparison of calculation with ORNL 10-s irradiation experiment, 20.7-s decay.

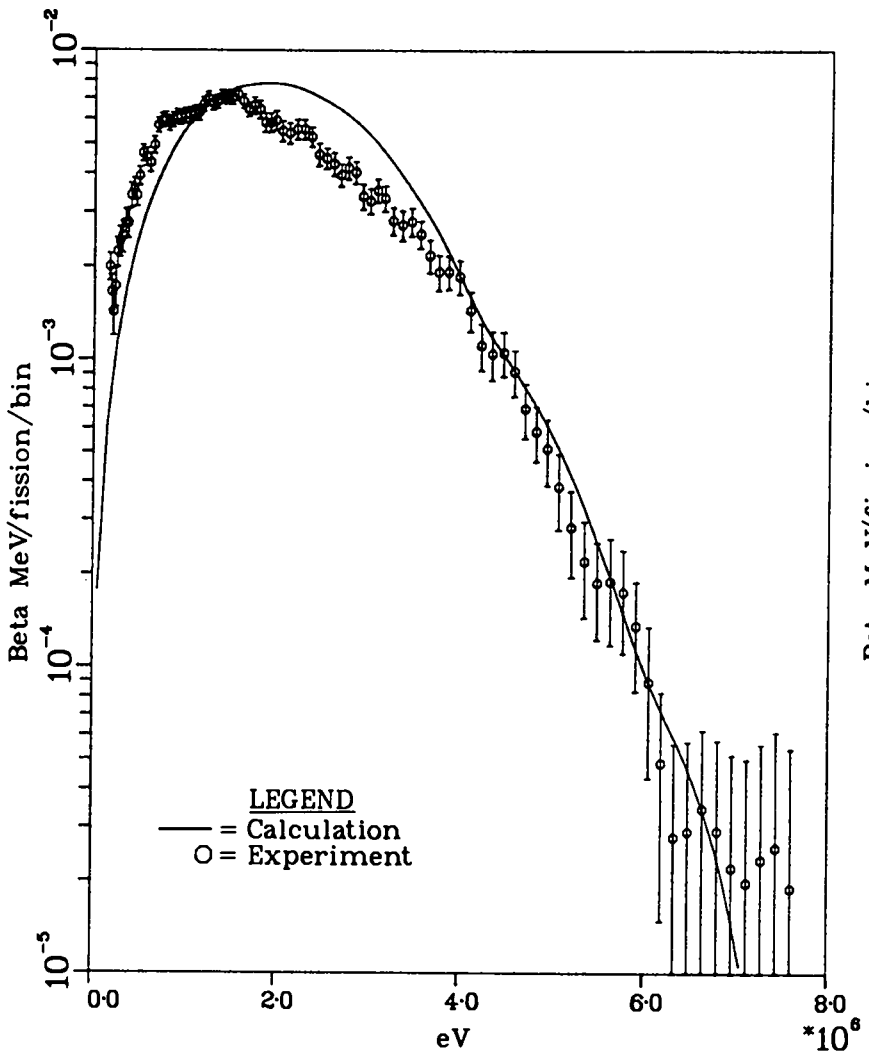

Fig. 65. Comparison of calculation with ORNL 10-s irradiation experiment, 29.7-s decay.

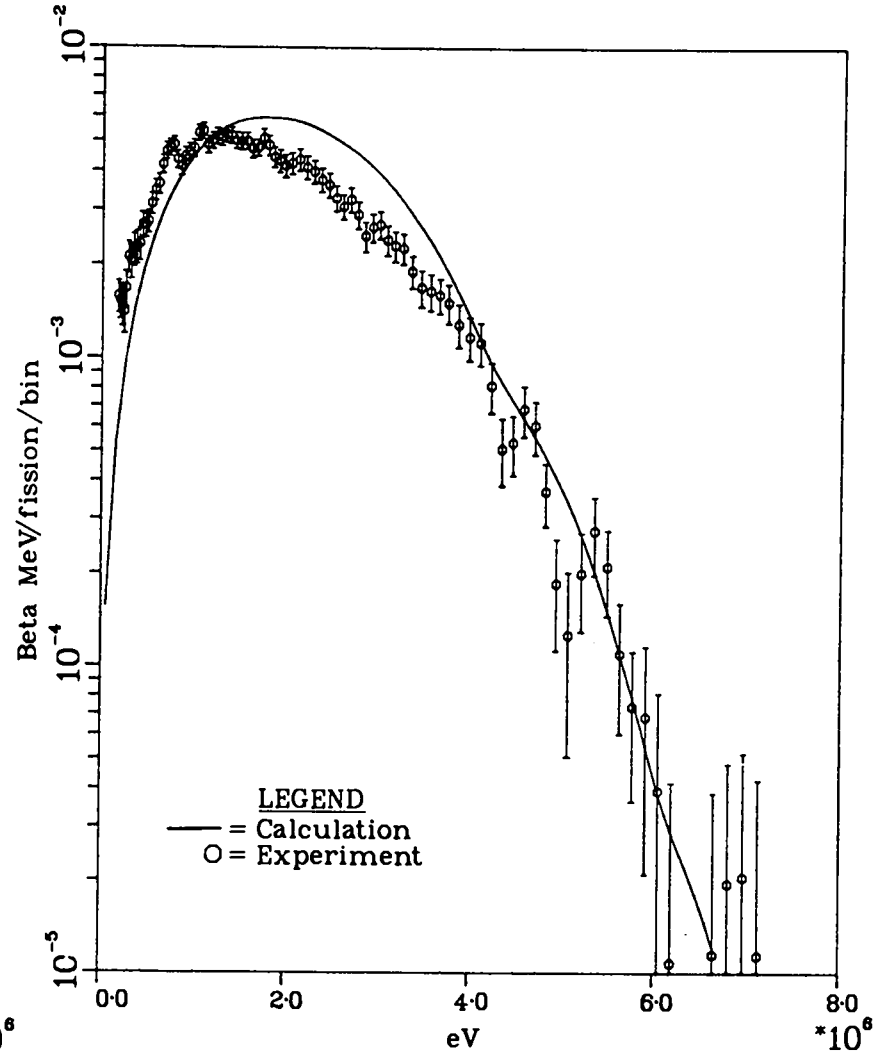

Fig. 66. Comparison of calculation with ORNL 10-s irradiation experiment, 39.7-s decay.

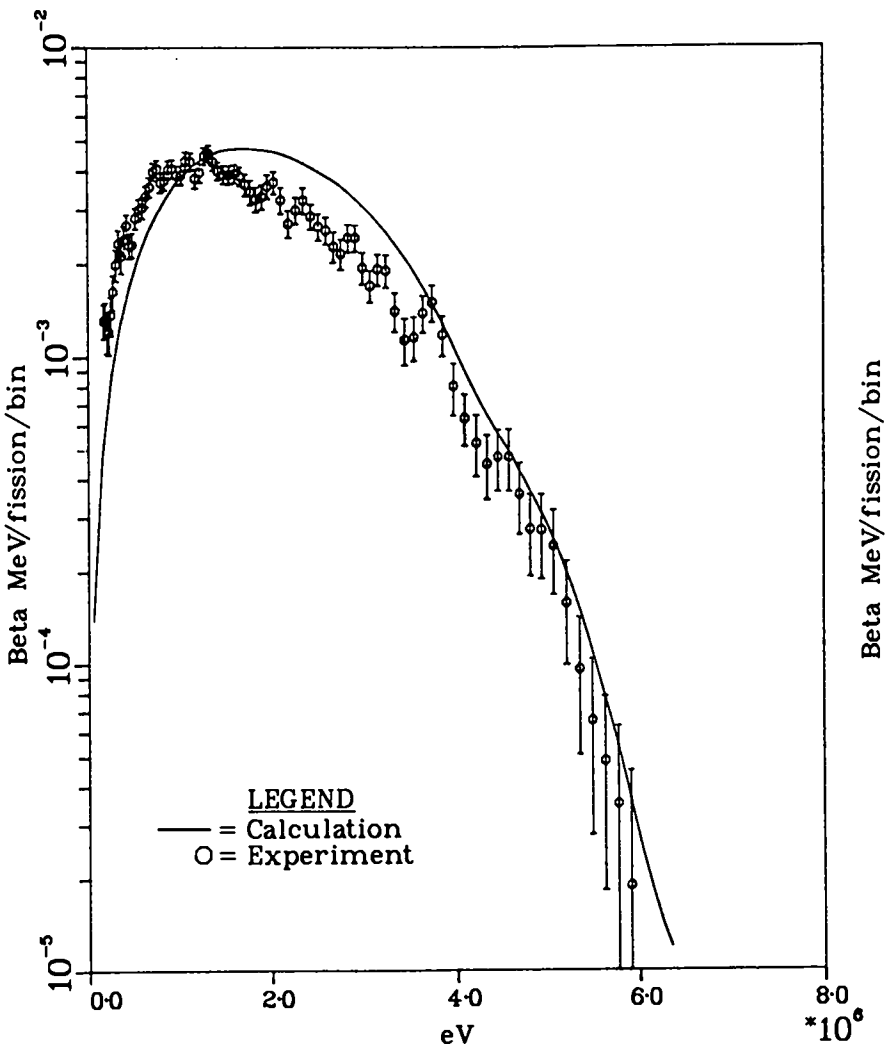

Fig. 67. Comparison of calculation with ORNL 10-s irradiation experiment, 49.7-s decay.

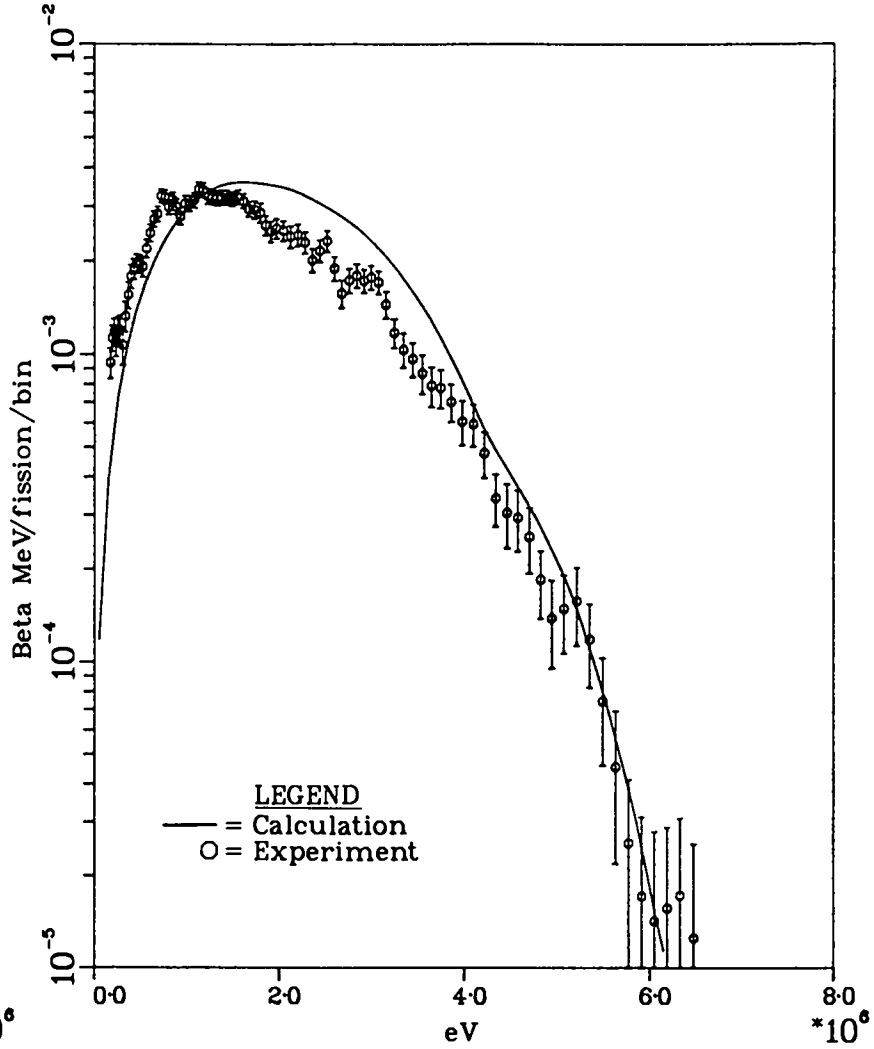

Fig. 68. Comparison of calculation with ORNL 10-s irradiation experiment, 64.7-s decay.

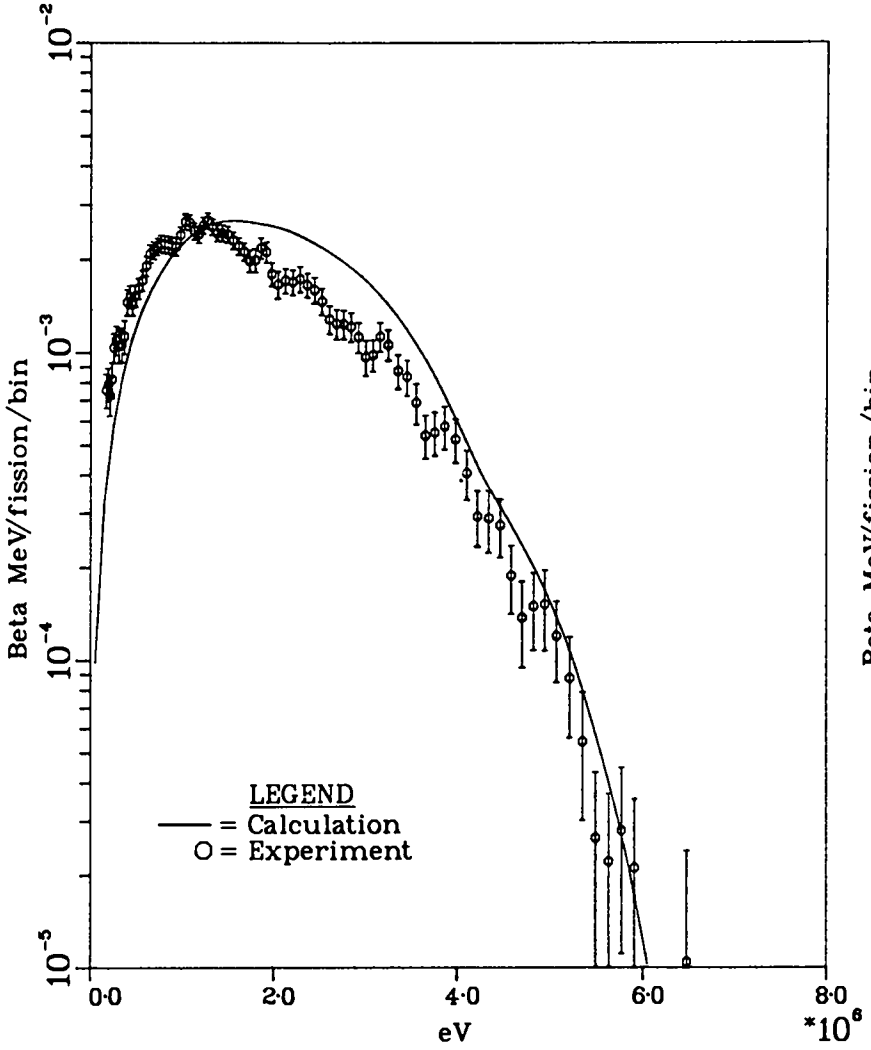

Fig. 69. Comparison of calculation with ORNL 10-s irradiation experiment, 84.7-s decay.

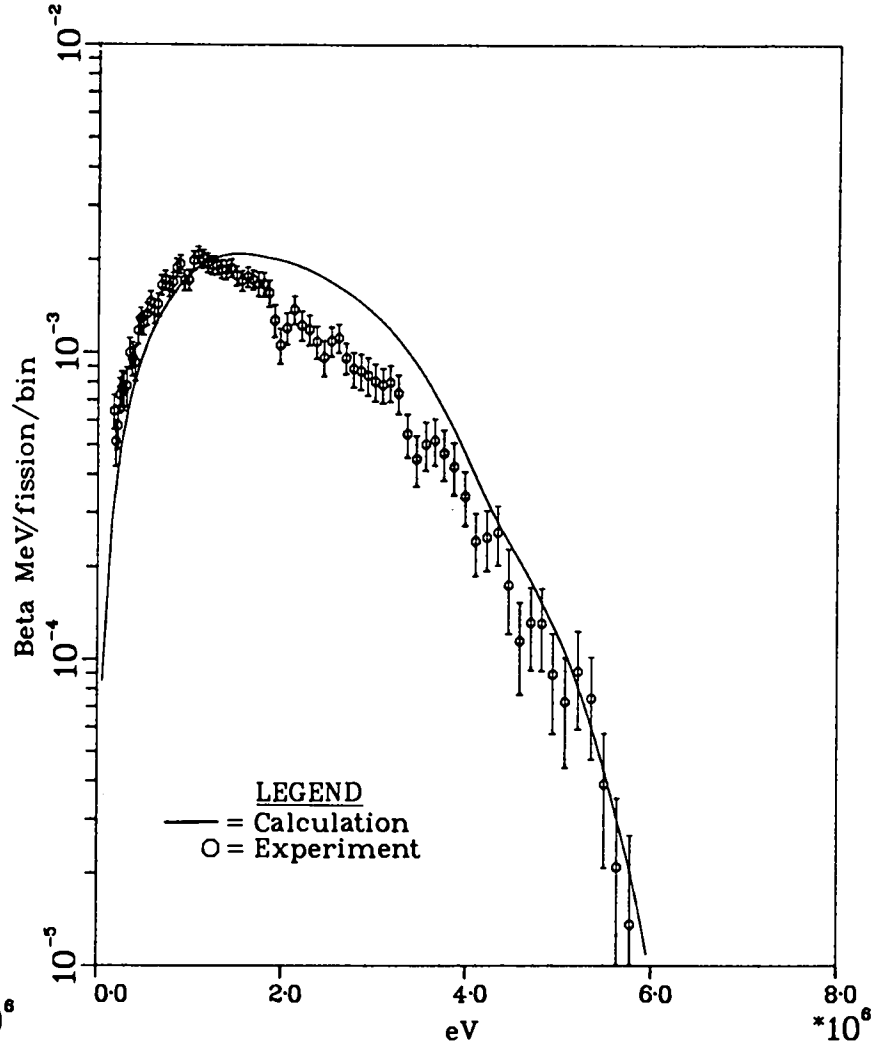

Fig. 70. Comparison of calculation with ORNL 10-s irradiation experiment, 104.7-s decay.

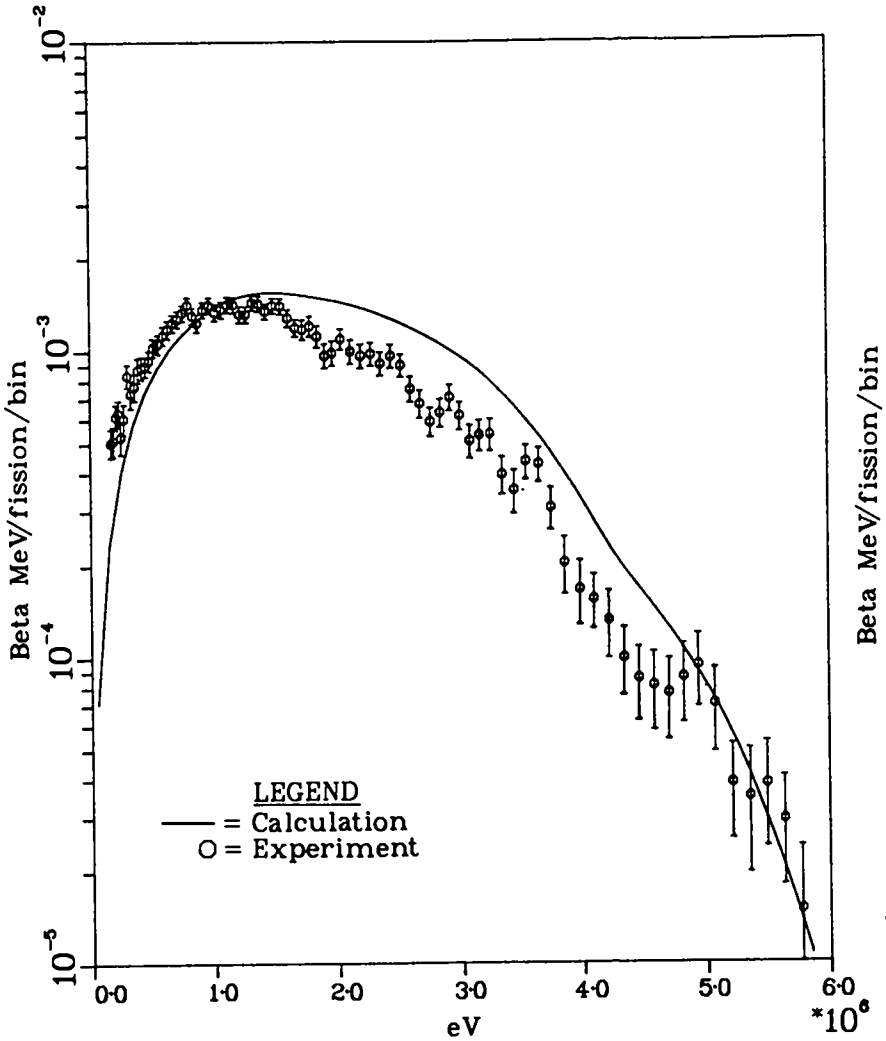

Fig. 71. Comparison of calculation with ORNL 10-s irradiation experiment, 134.7-s decay.

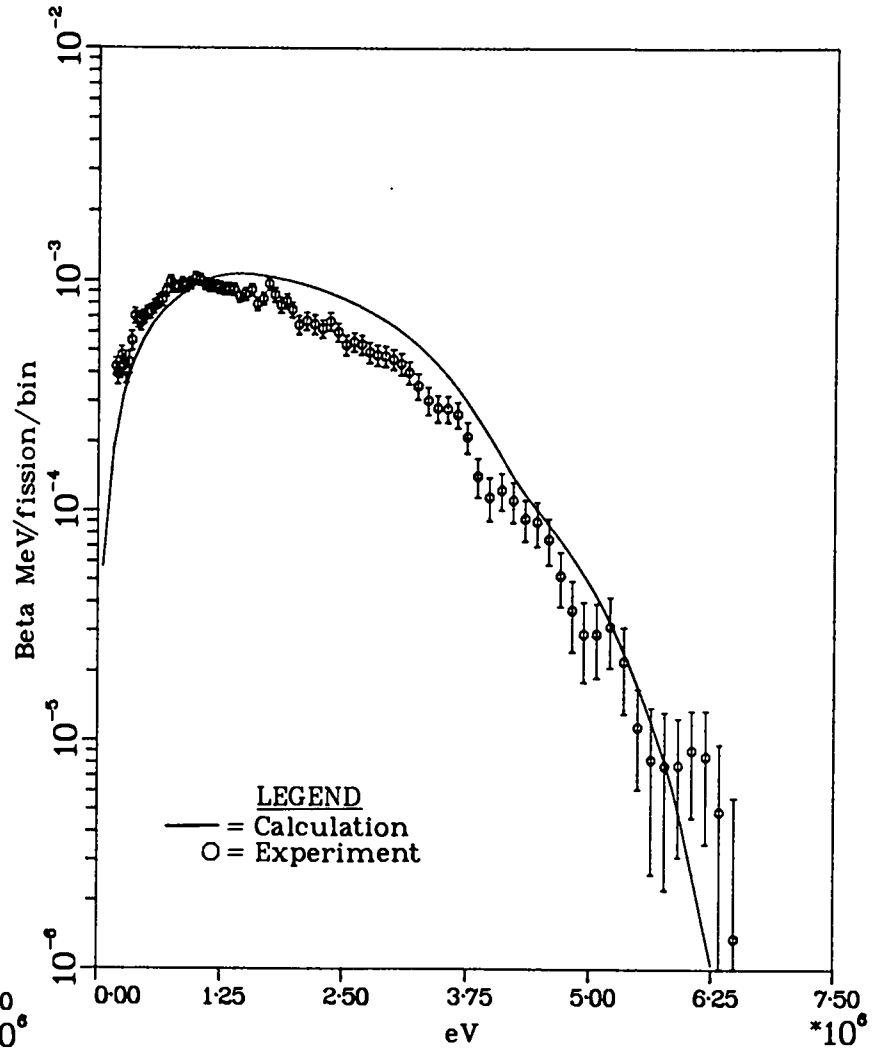

Fig. 72. Comparison of calculation with ORNL 10-s irradiation experiment, 184.7-s decay.

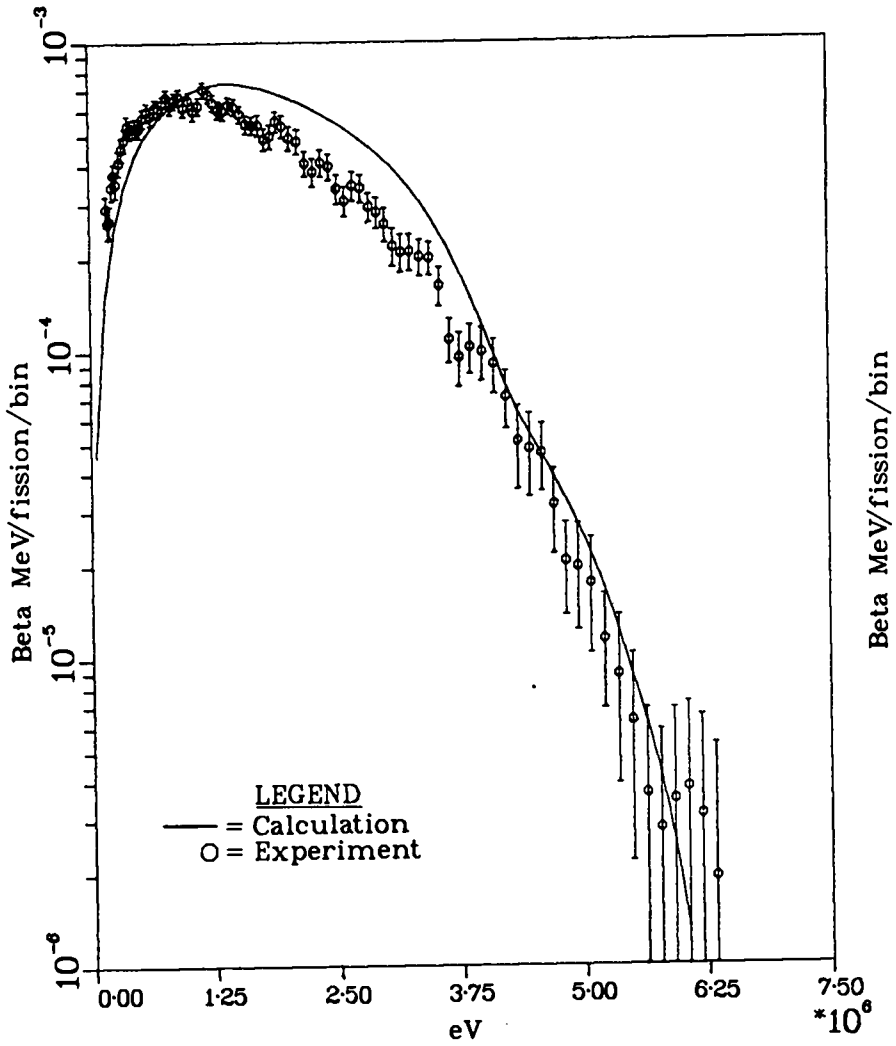

Fig. 73. Comparison of calculation with ORNL 10-s irradiation experiment, 254.7 s decay.

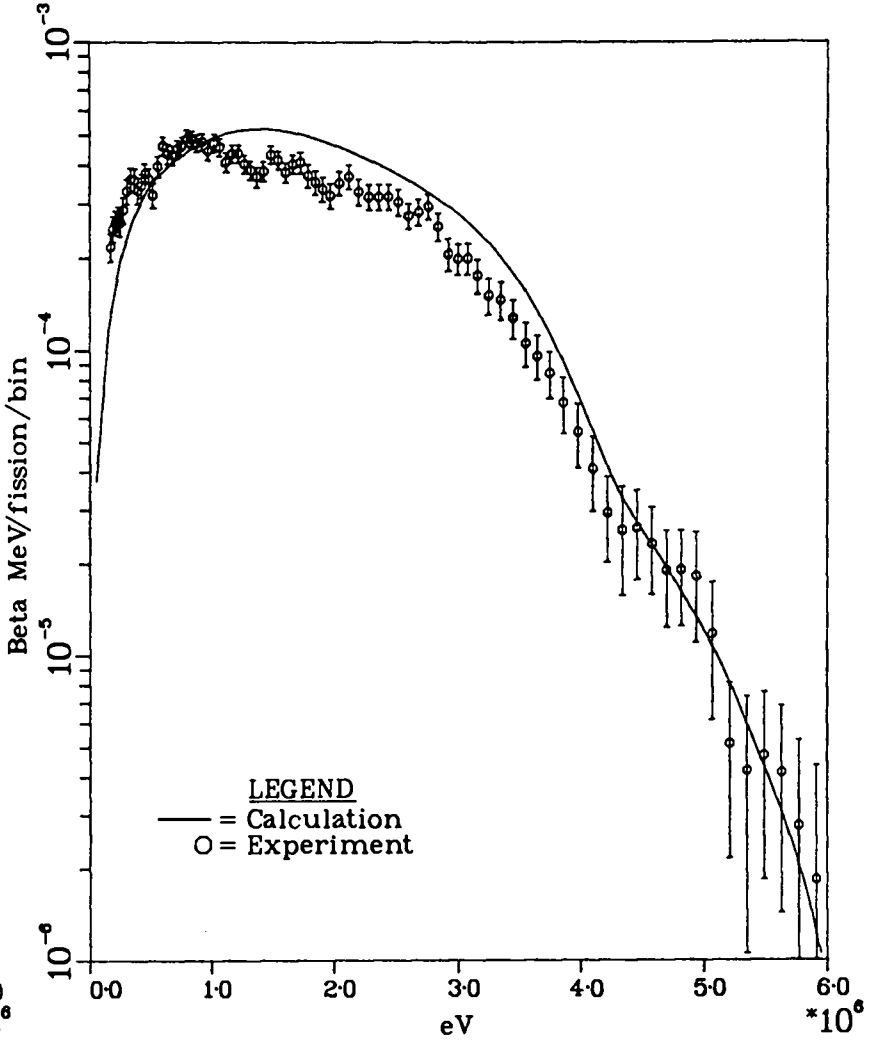

Fig. 74. Comparison of calculation with ORNL 10-s irradiation experiment, 344.7-s decay.

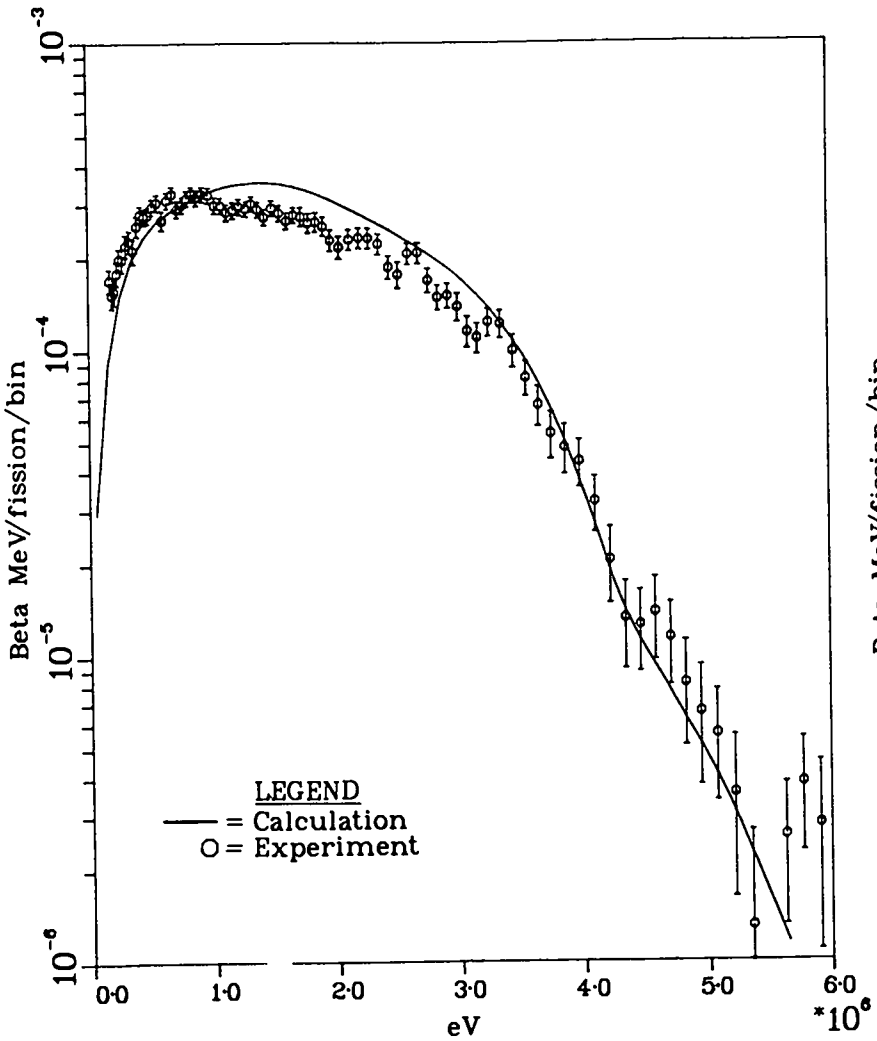

Fig. 75. Comparison of calculation with ORNL 10-s irradiation experiment, 194.7-s decay.

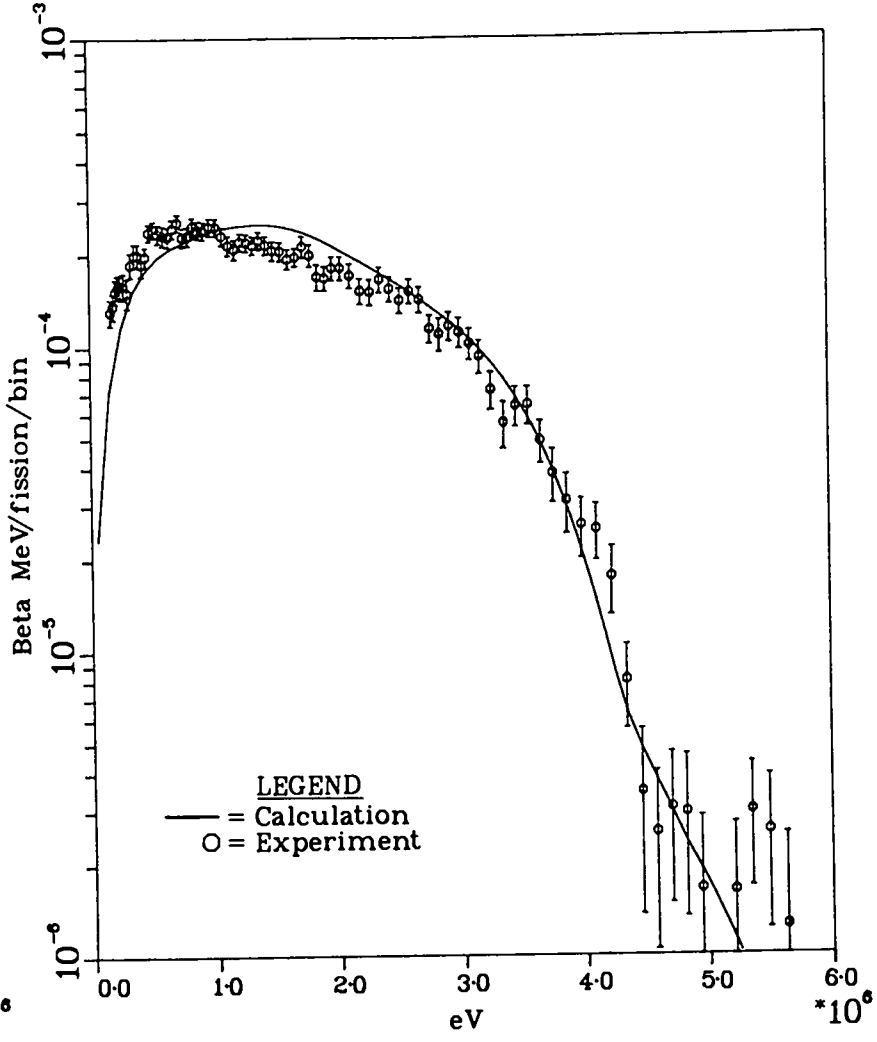

Fig. 76. Comparison of calculation with ORNL 10-s irradiation experiment, 694.7-s decay.

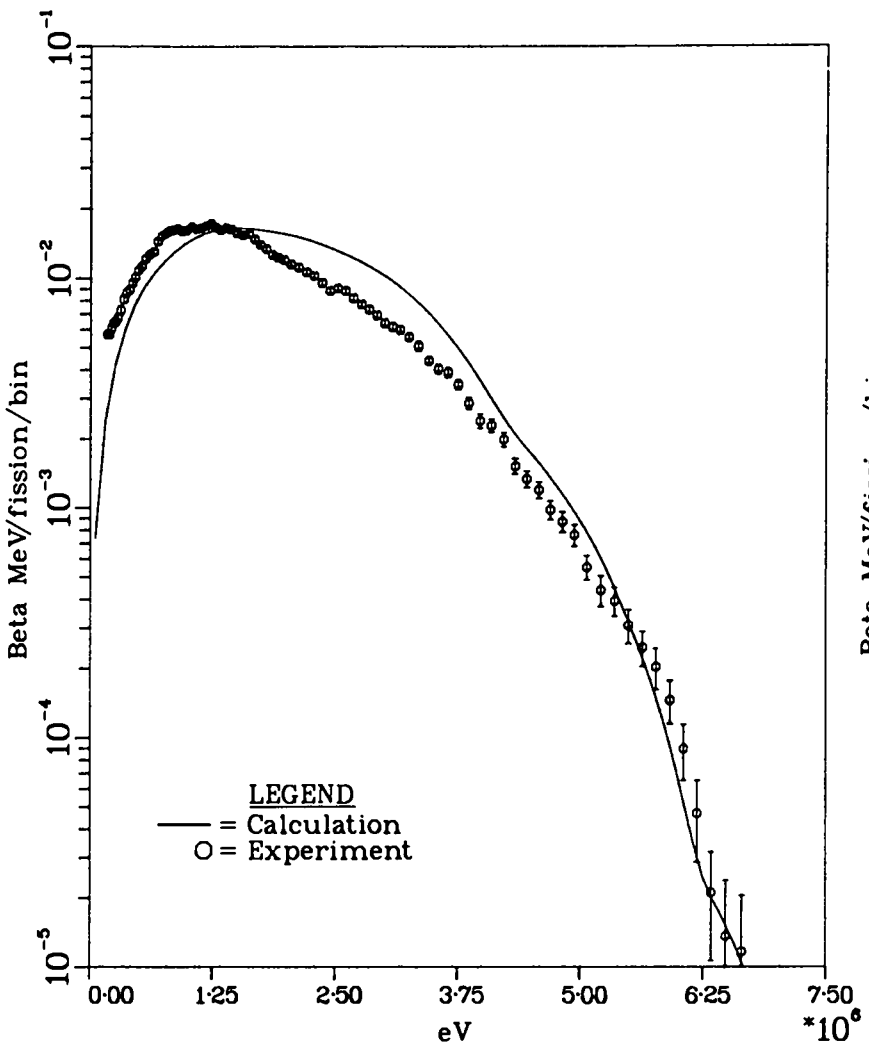

Fig. 77. Comparison of calculation with ORNL 100-s irradiation experiment, 90-s decay.

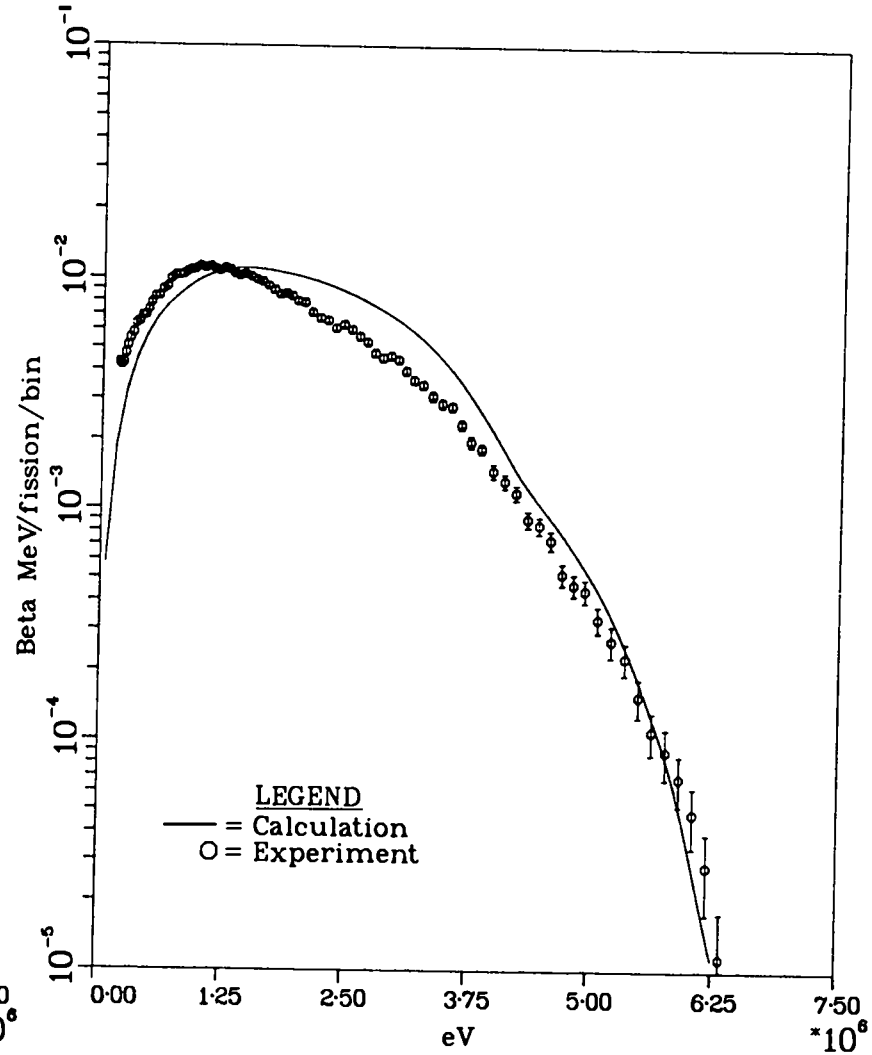

Fig. 78. Comparison of calculation with ORNL 100-s irradiation experiment, 140-s decay.

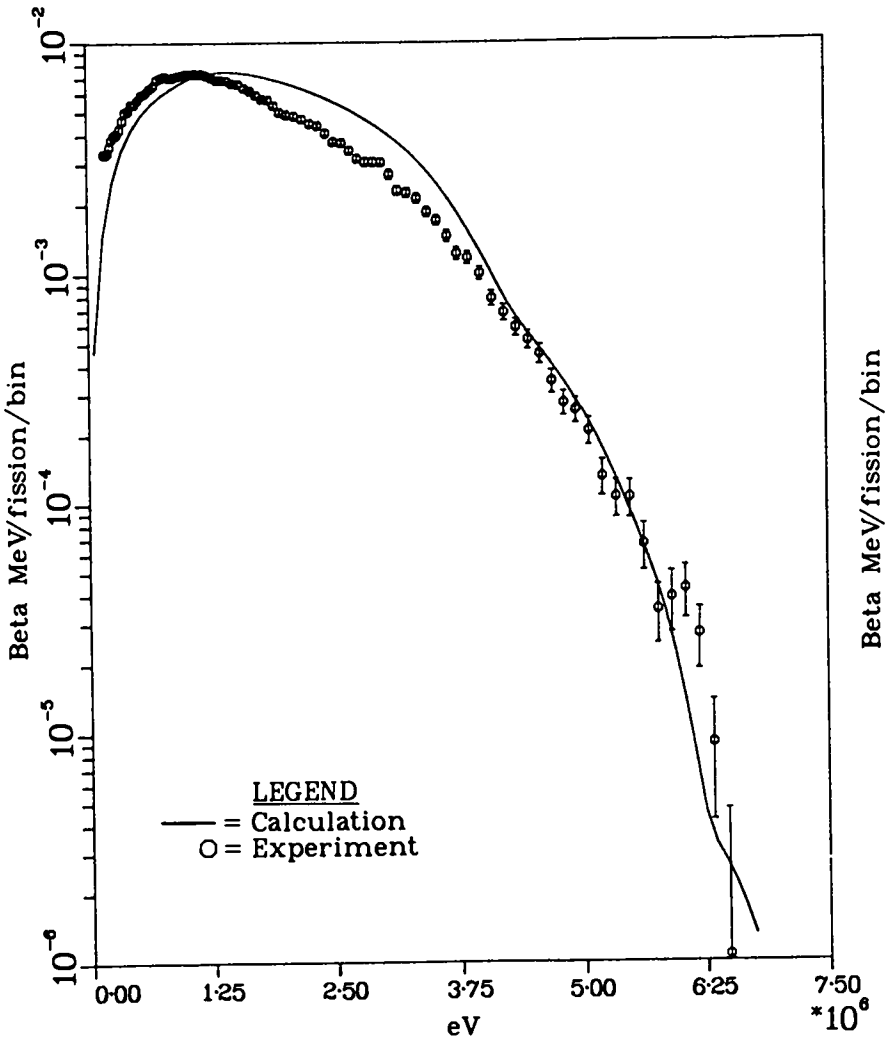

Fig. 79. Comparison of calculation with ORNL 100-s irradiation experiment, 210-s decay.

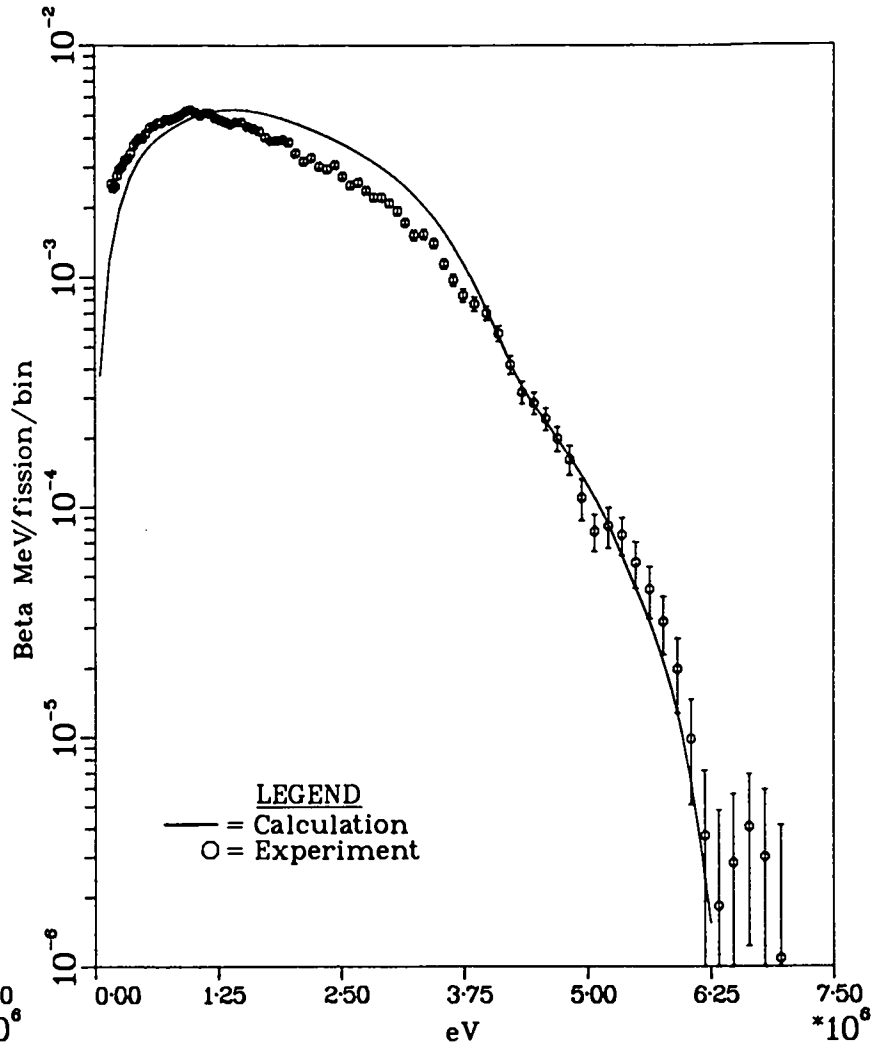

Fig. 80. Comparison of calculation with ORNL 100-s irradiation experiment, 300-s decay.

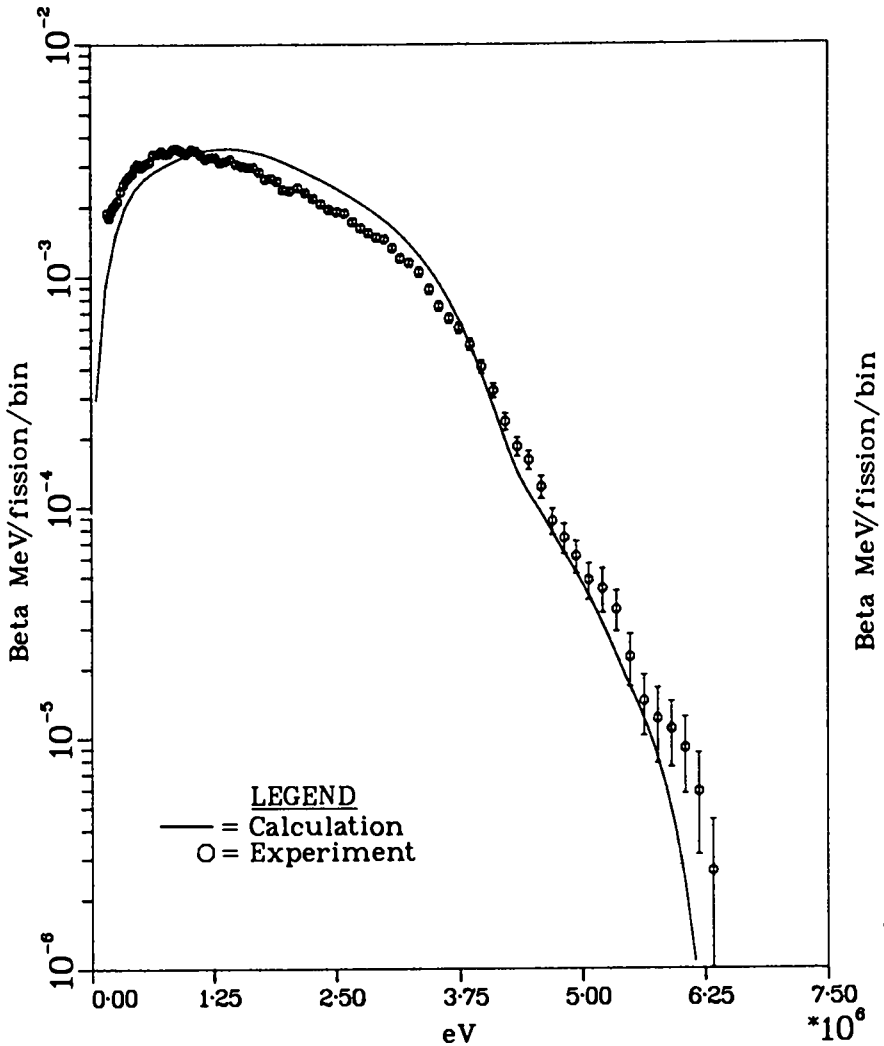

Fig. 81. Comparison of calculation with ORNL 100-s irradiation experiment, 450-s decay.

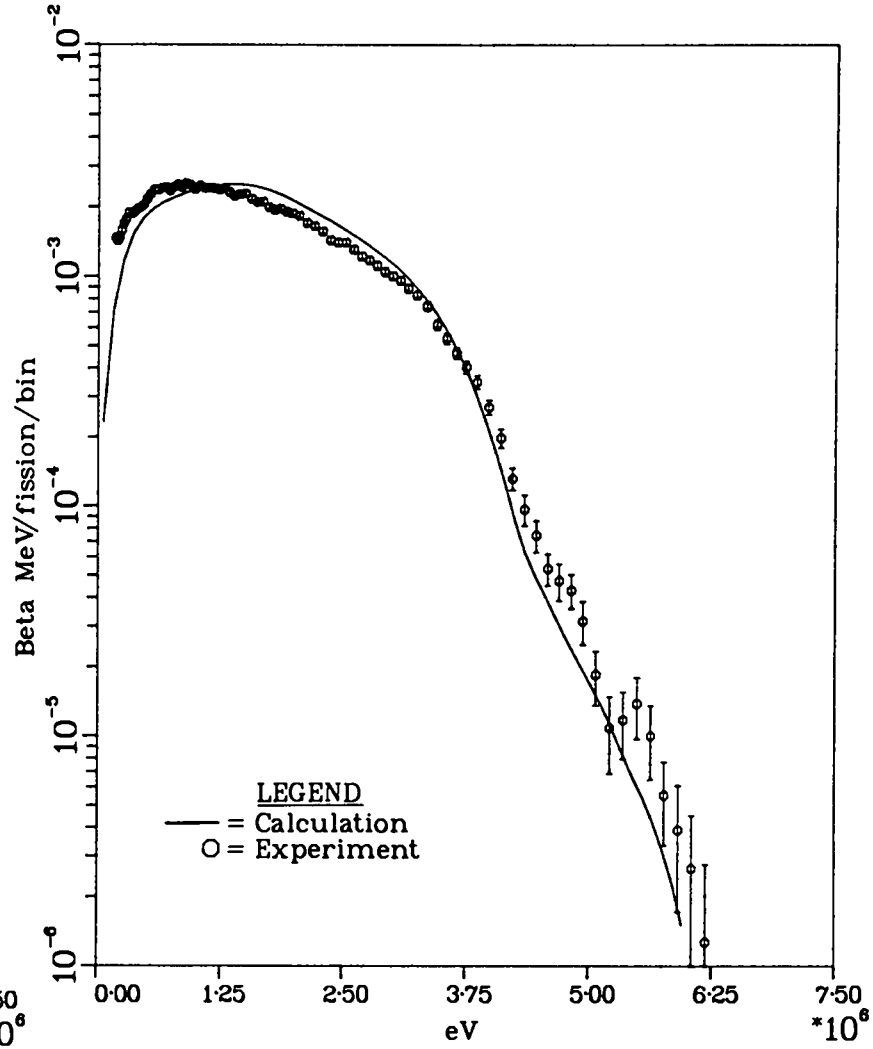

Fig. 82. Comparison of calculation with ORNL 100-s irradiation experiment, 650-s decay.

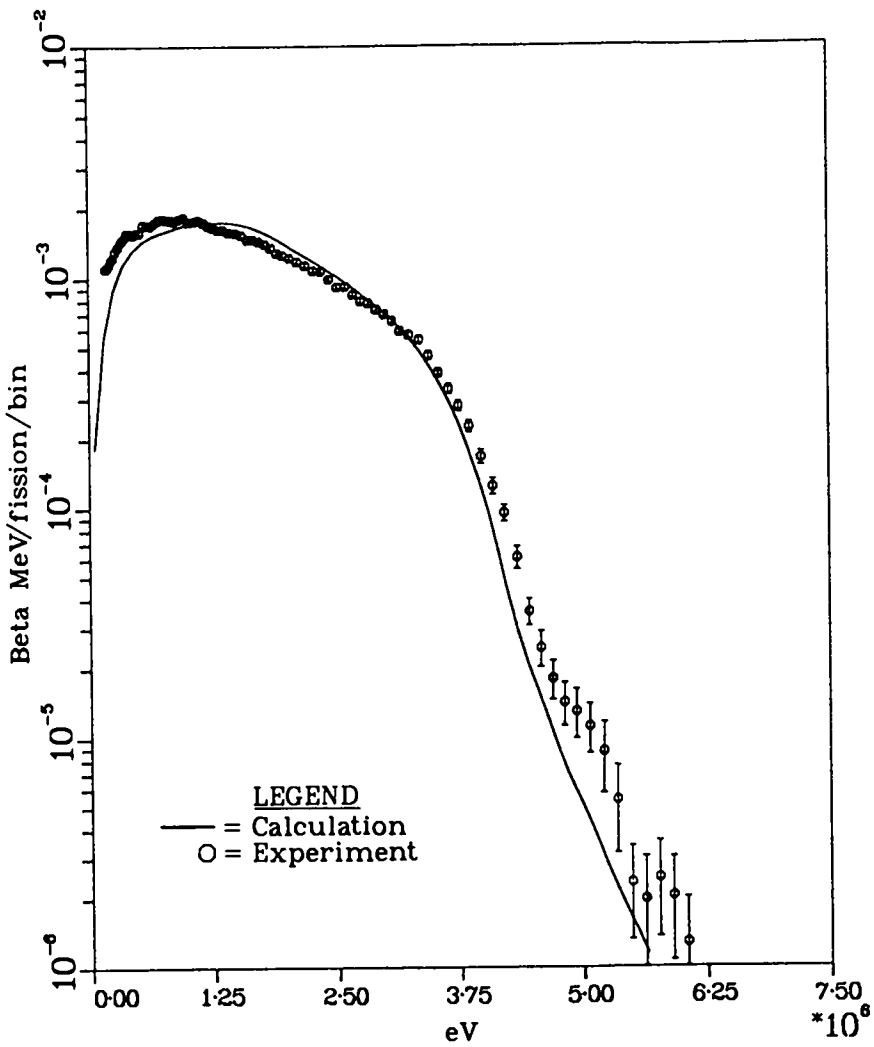

Fig. 83. Comporison of calculation with ORNL 100-s irradiation experiment, 950-s decay.

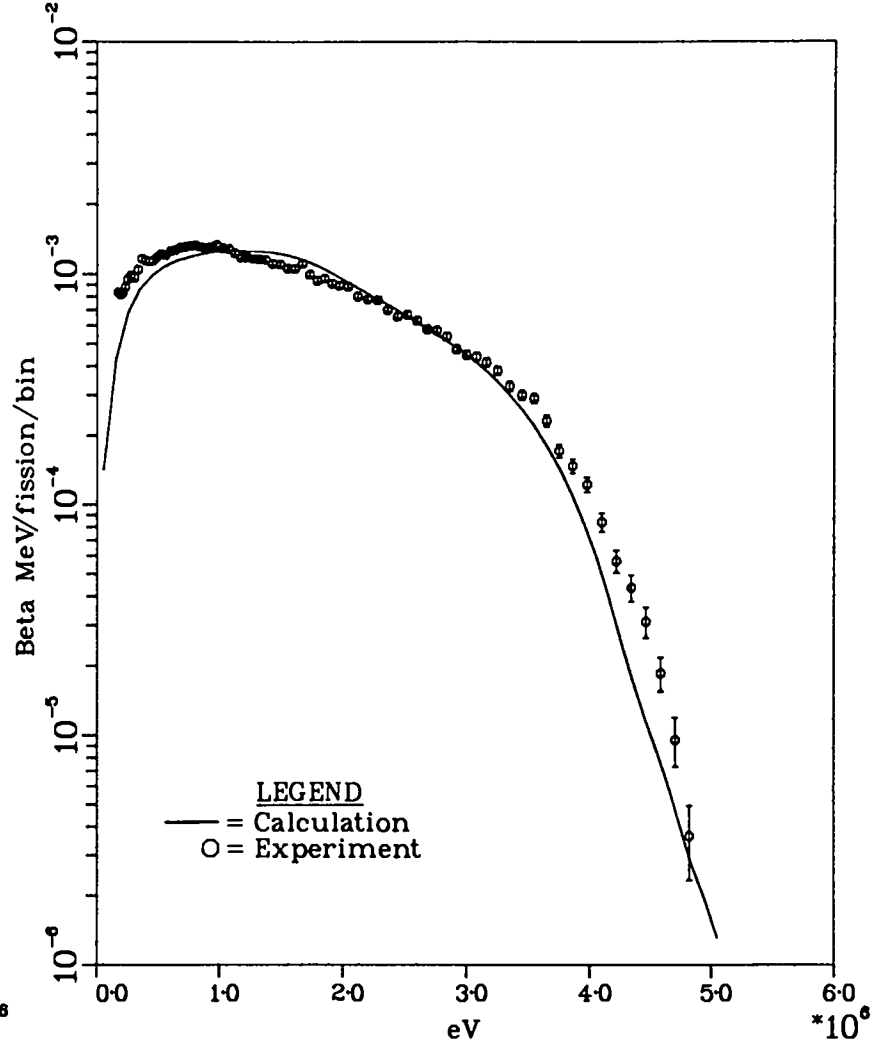

Fig. 84. Comparison of calculation with ORNL 100-s irradiation experiment, 1350-s decay.

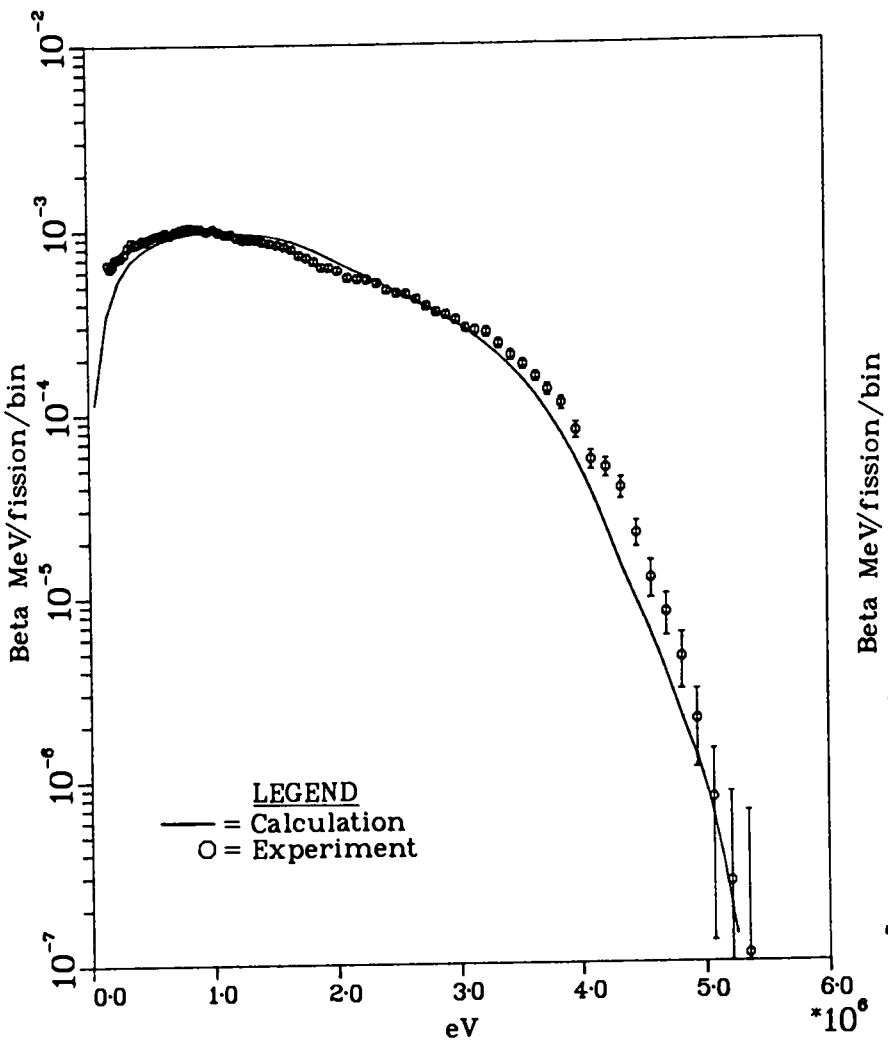

Fig. 85. Comparison of calculation with ORNL 100-s irradiation experiment, 1750-s decay.

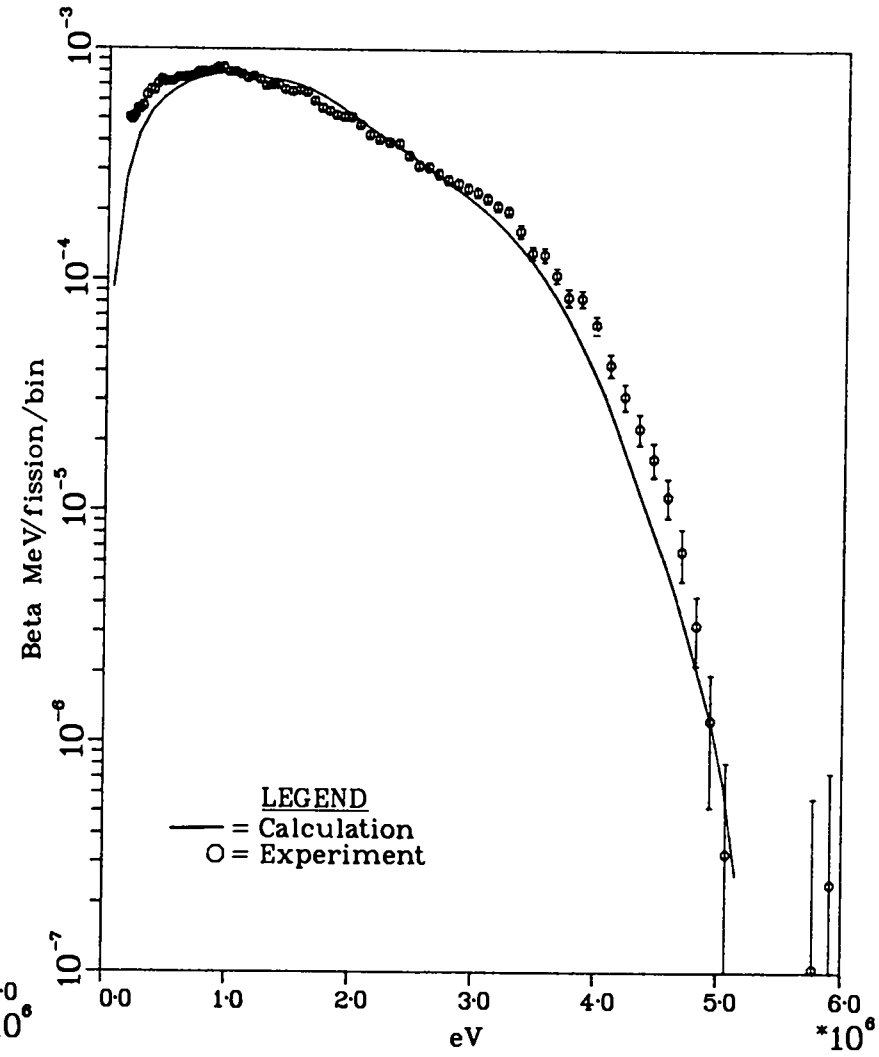

Fig. 86. Comparison of calculation with ORNL 100-s irradiation experiment, 2200-s decay.

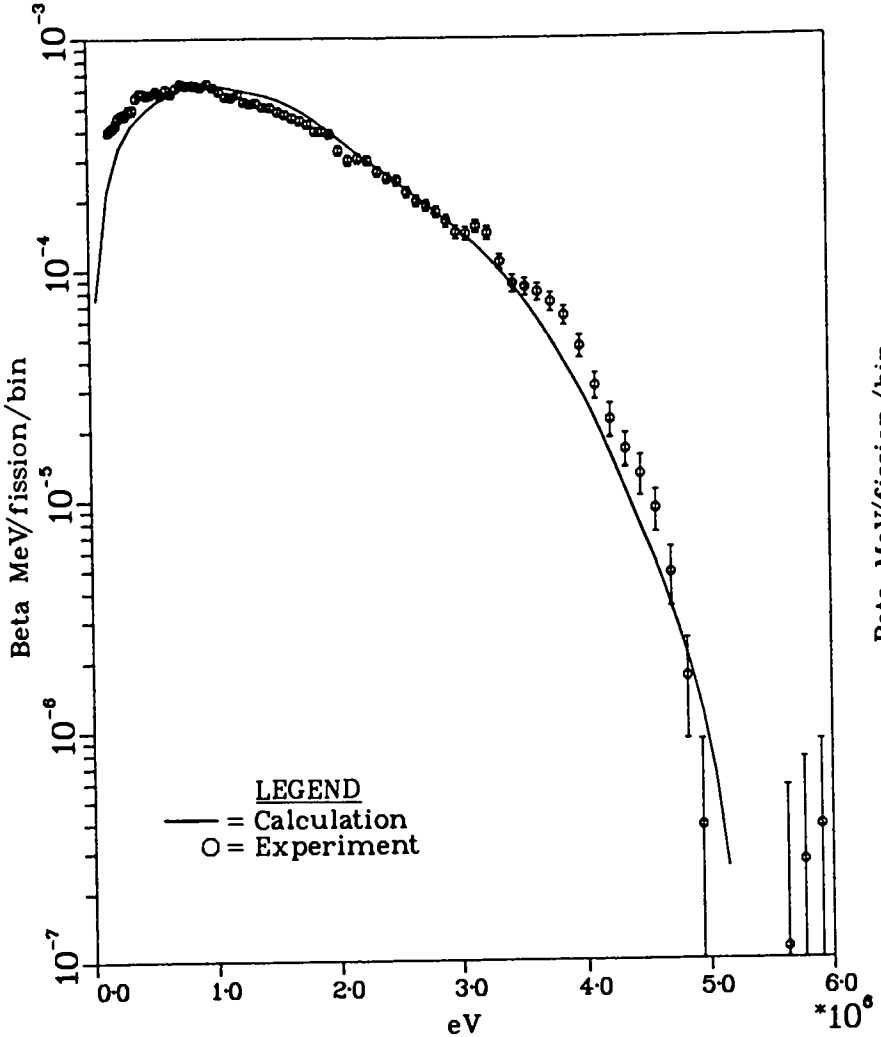

Fig. 87. Comparison of calculation with ORNL 100-s irradiation experiment, 2700-s decay.

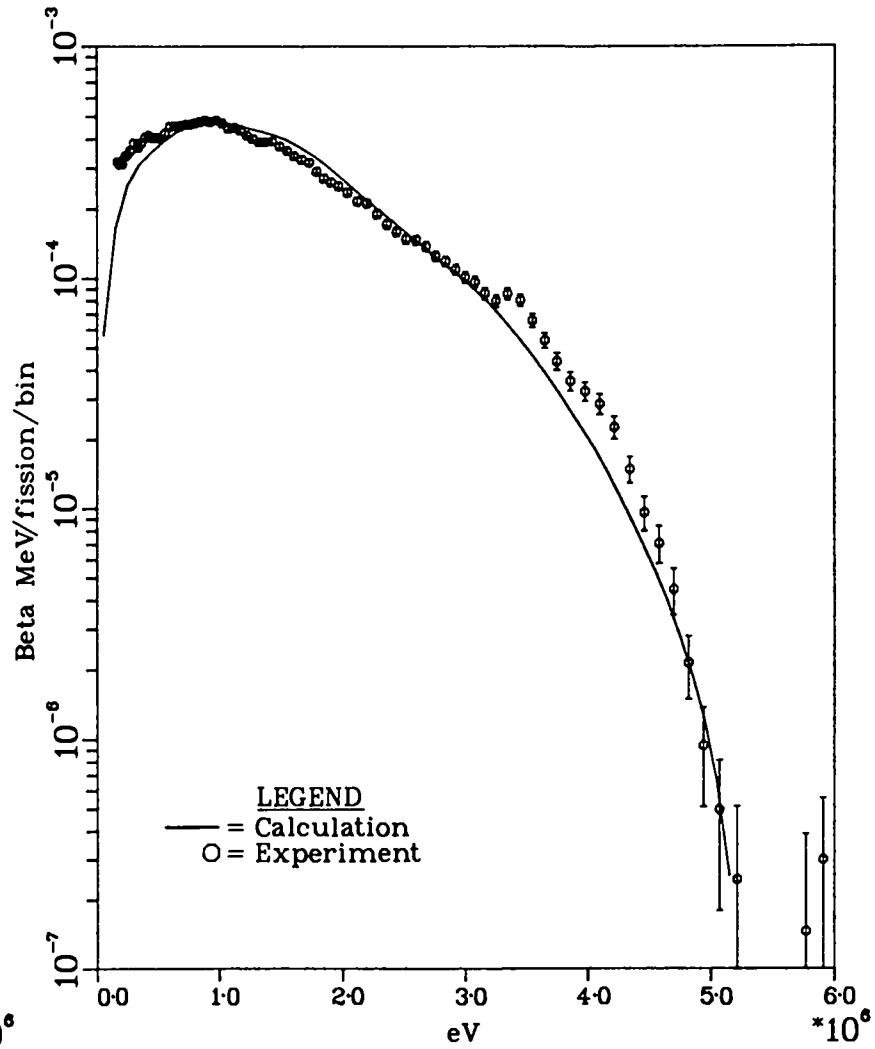

Fig. 88. Comparison of calculation with ORNL 100-s irradiation experiment, 3150-s decay.

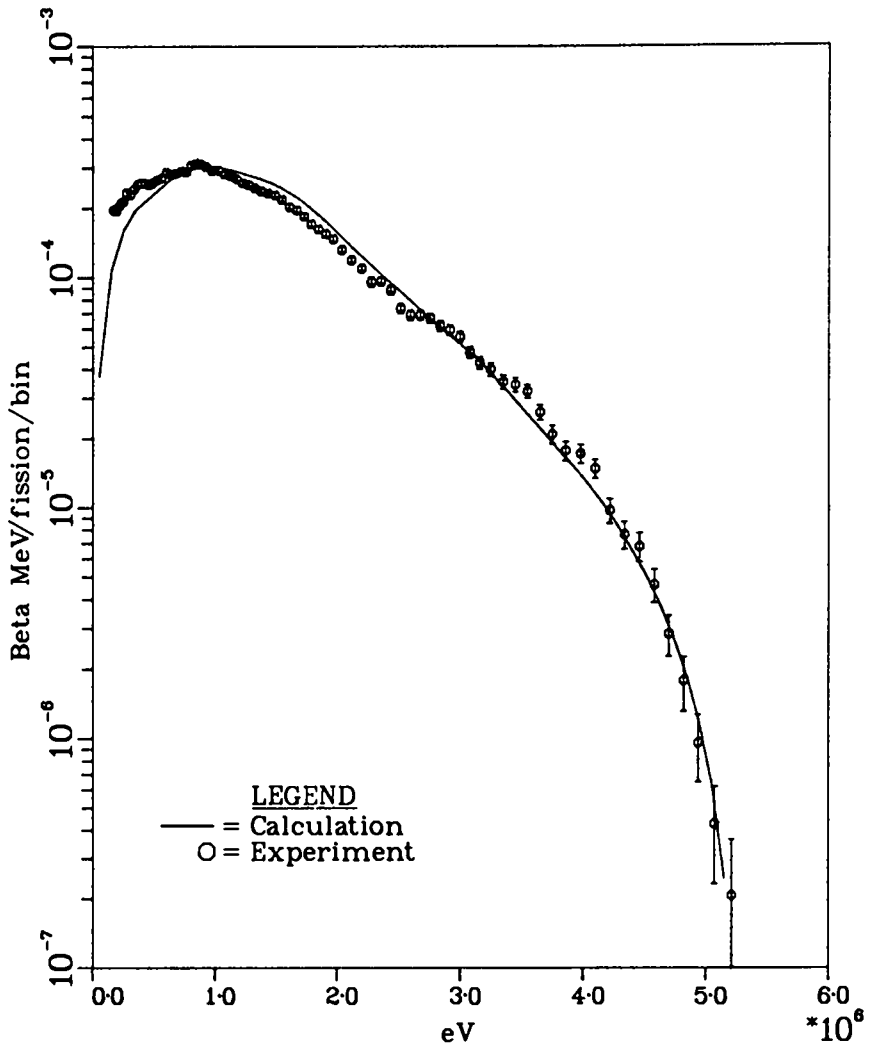

Fig. 89. Comparison of calculation with ORNL 100-s irradiation experiment, 4950-s decay.

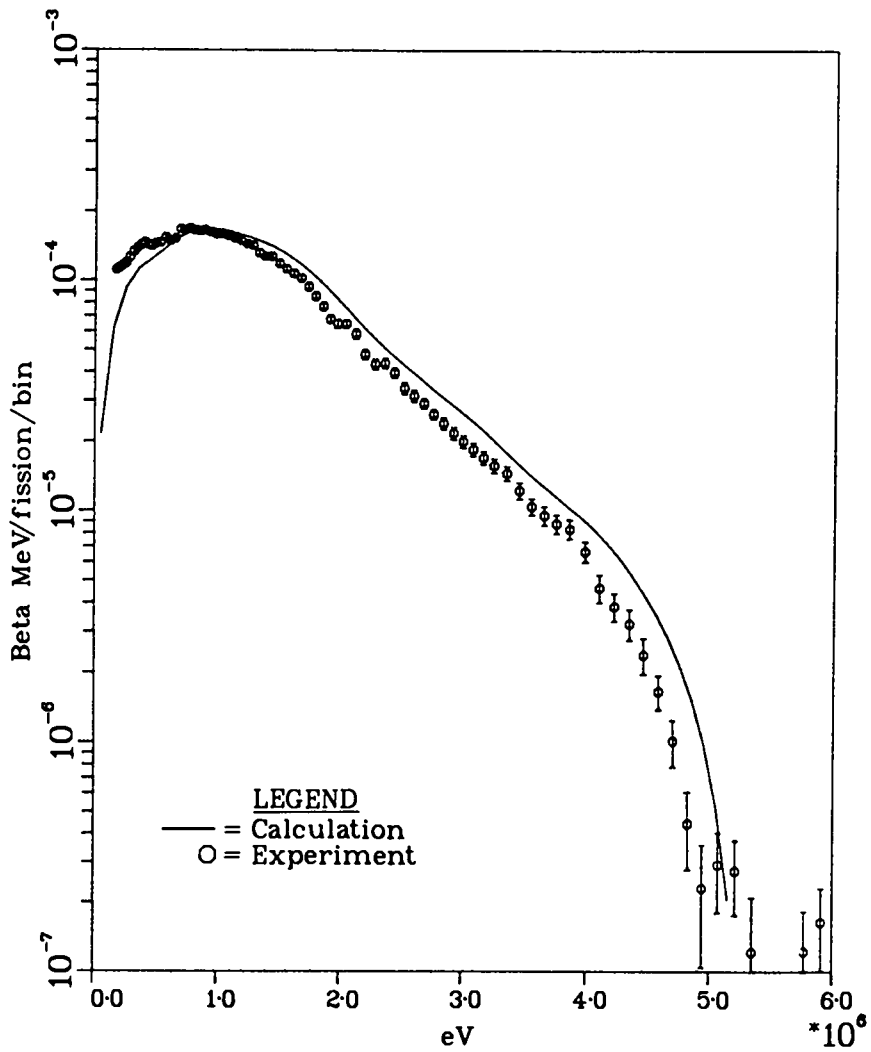

Fig. 90. Comparison of calculation with ORNL 100-s irradiation experiment, 7950-s decay.

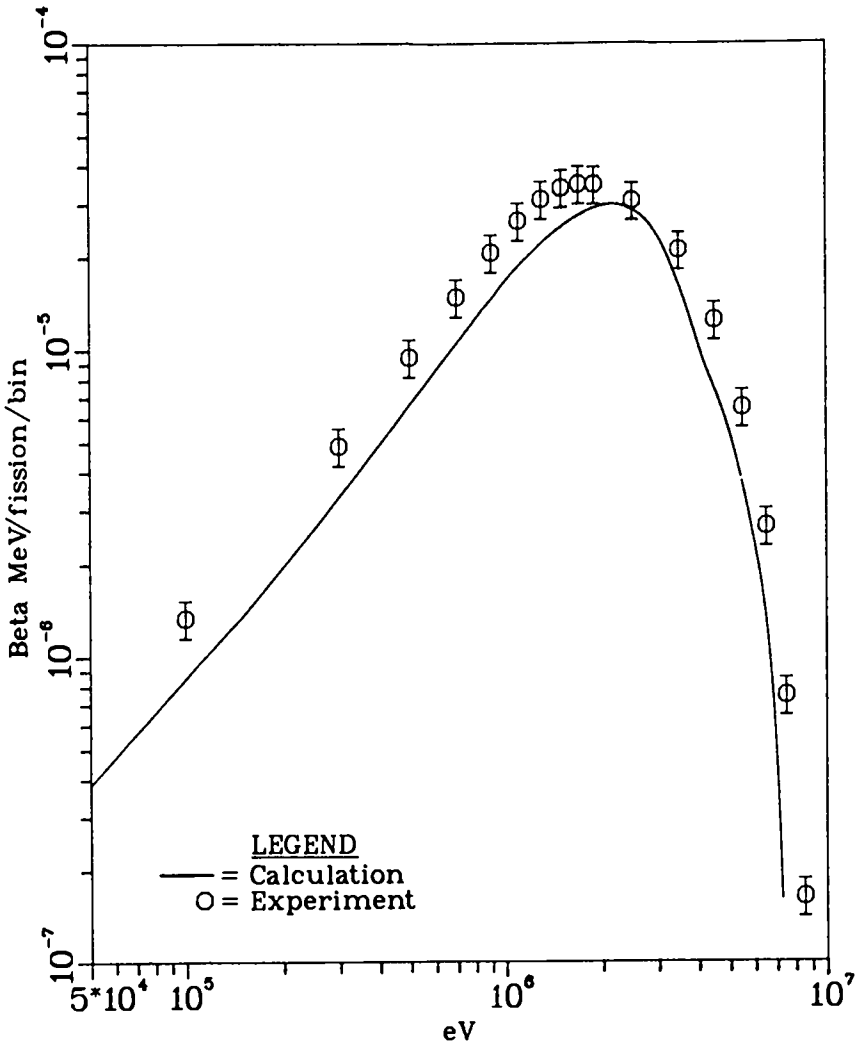

Fig.91. Comparison of calculation with UI 15-ms irradiation experiment, 13-s decay.

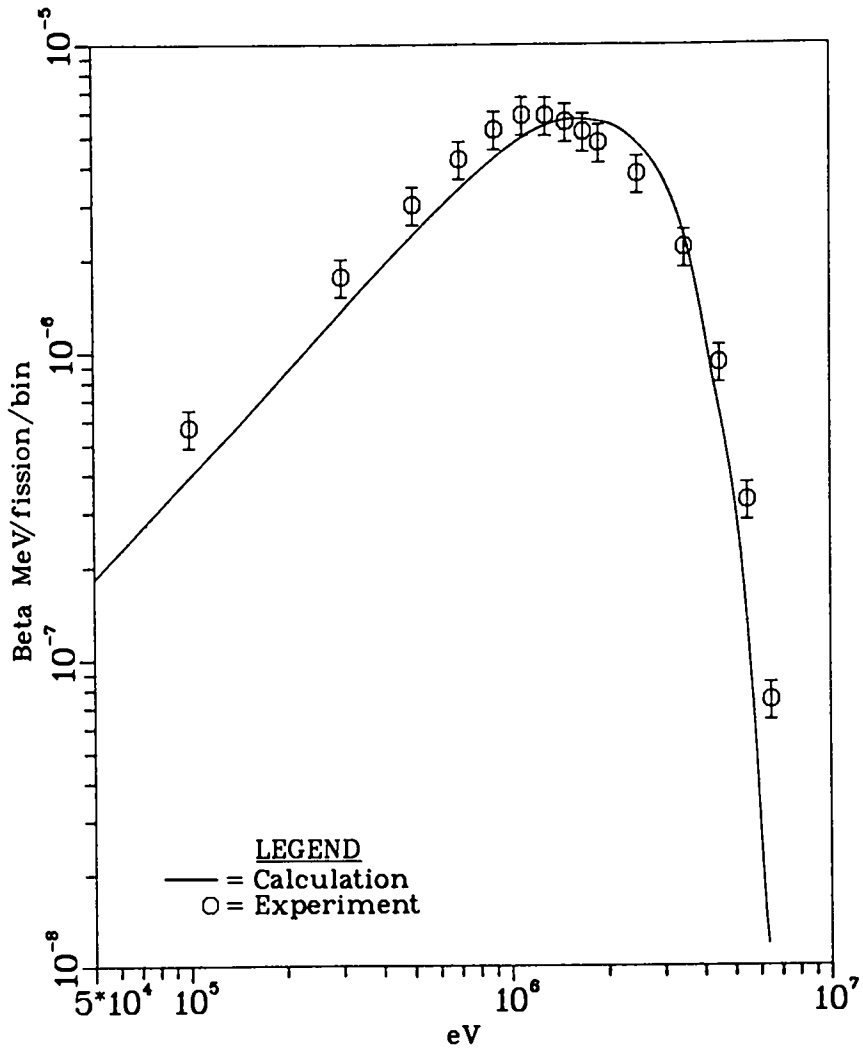

Fig. 92. Comparison of calculation with UI 15-ms irradiation experiment, 66-s decay.

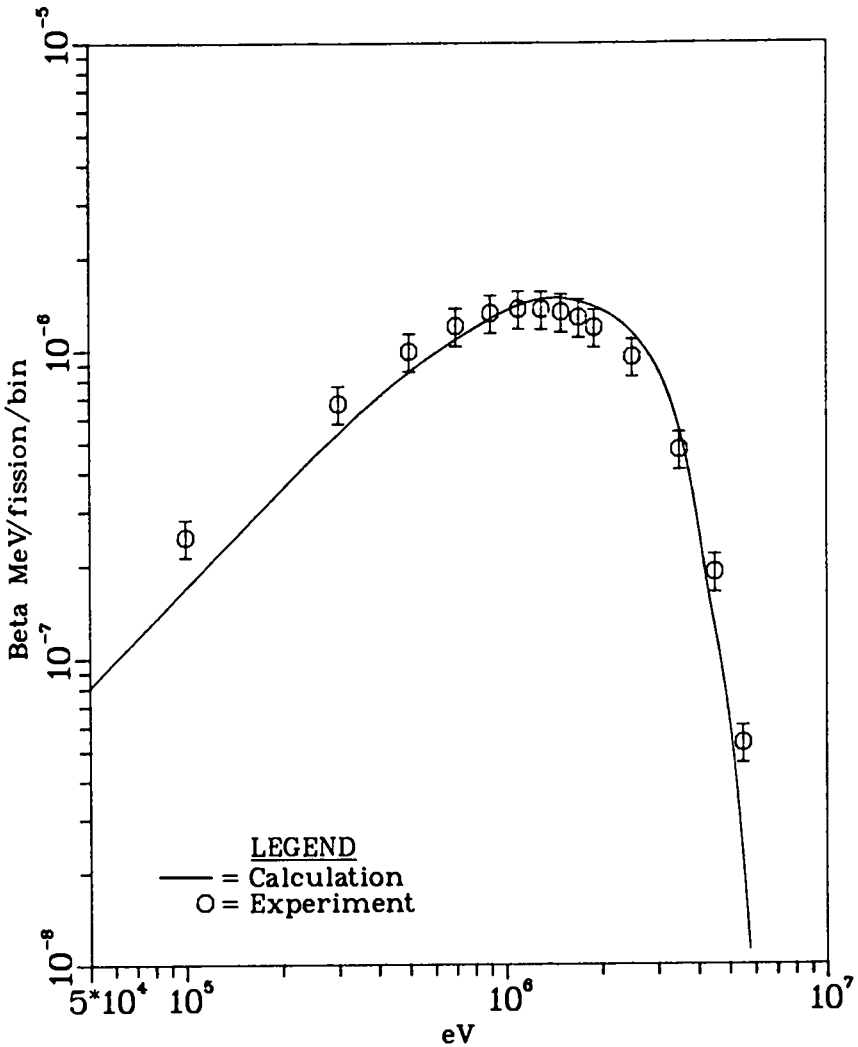

Fig.93. Comparison of calculation with UI 15-ms irradiation experiment, 204-s decay.

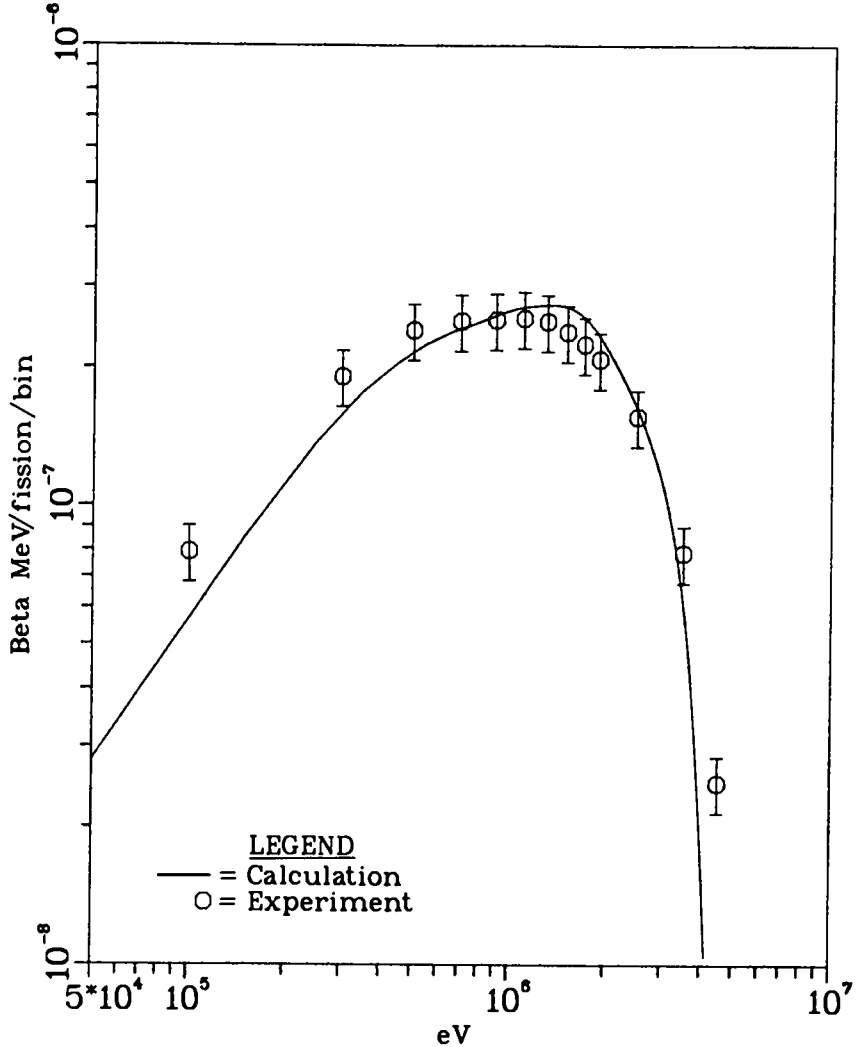

Fig.94. Comparison of calculation with UI 15-ms irradiation experiment, 960-s decay.

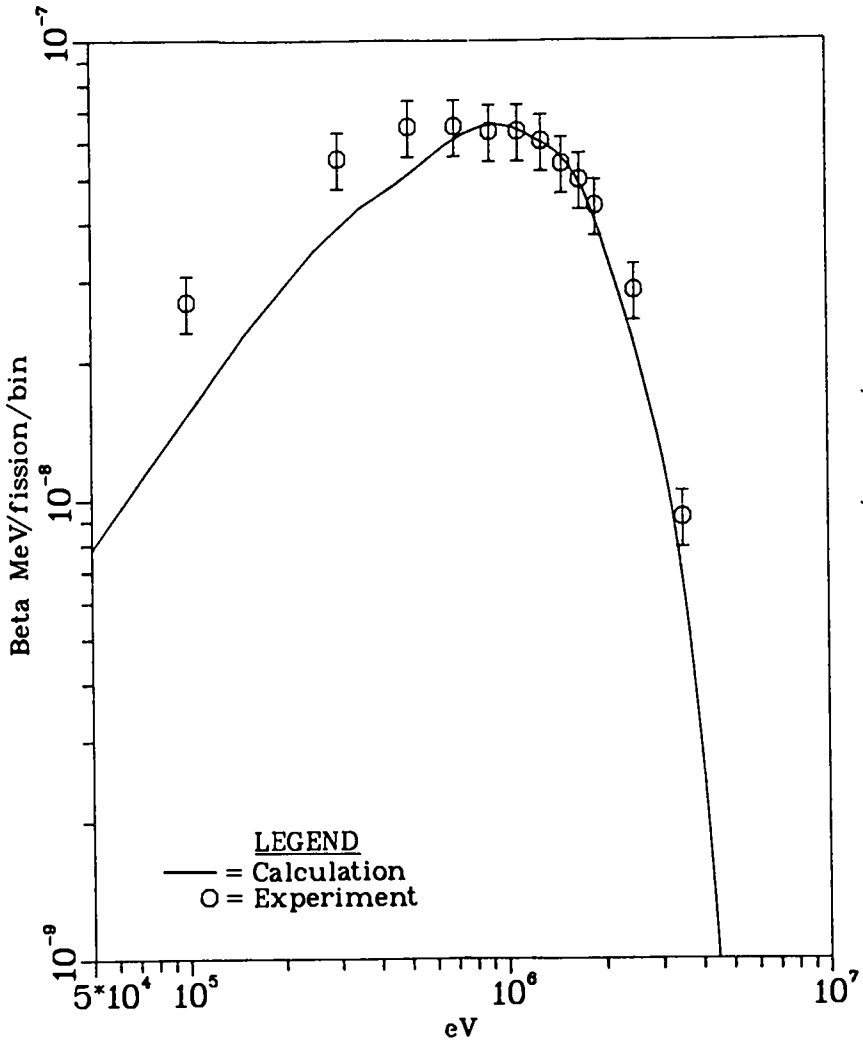

Fig.95. Comparison of calculation with UI 15 ms irradiation experiment, 3750-s decay.

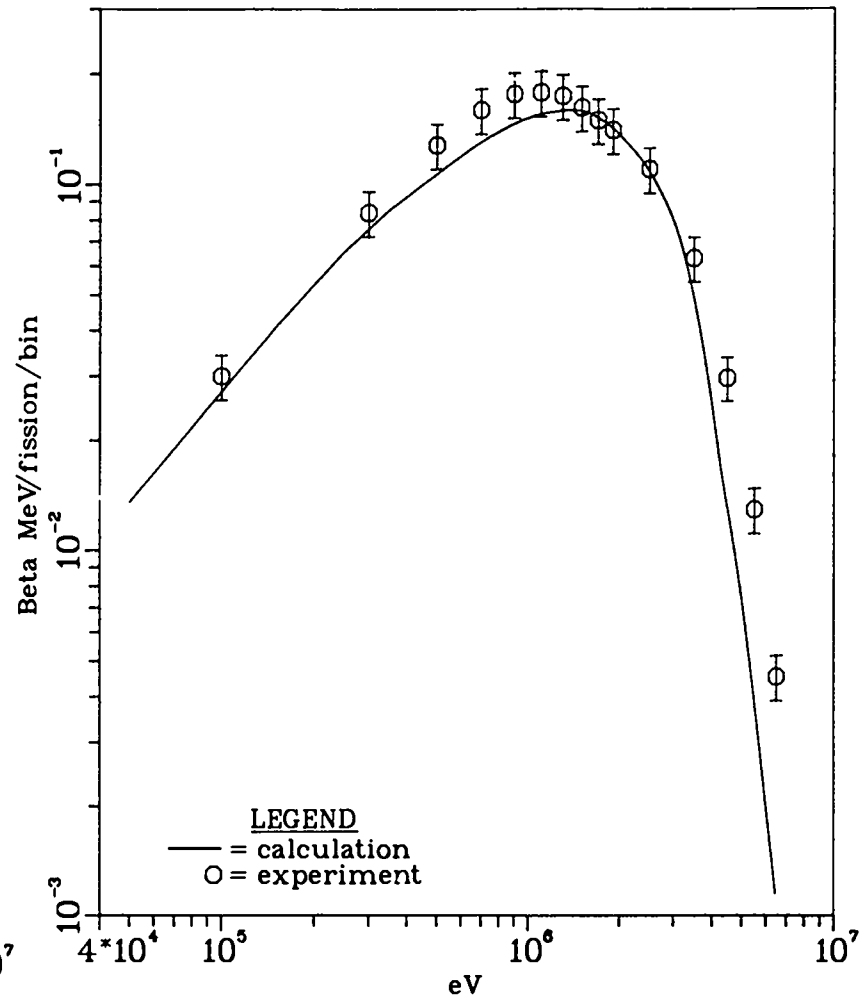

Fig.96. Comparison of calculation with UI 8-h irradiation, 6-s decay.

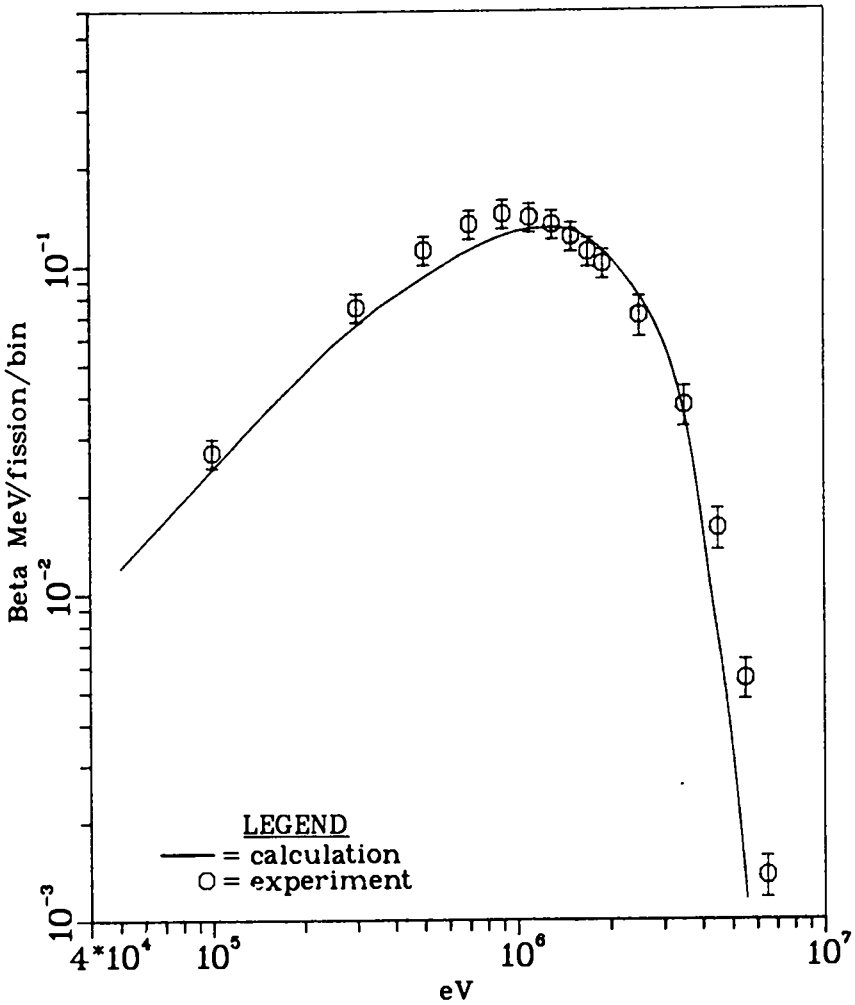

Fig.97. Comparison of calculation with Ul 8-h irradiation, 21-s decay.

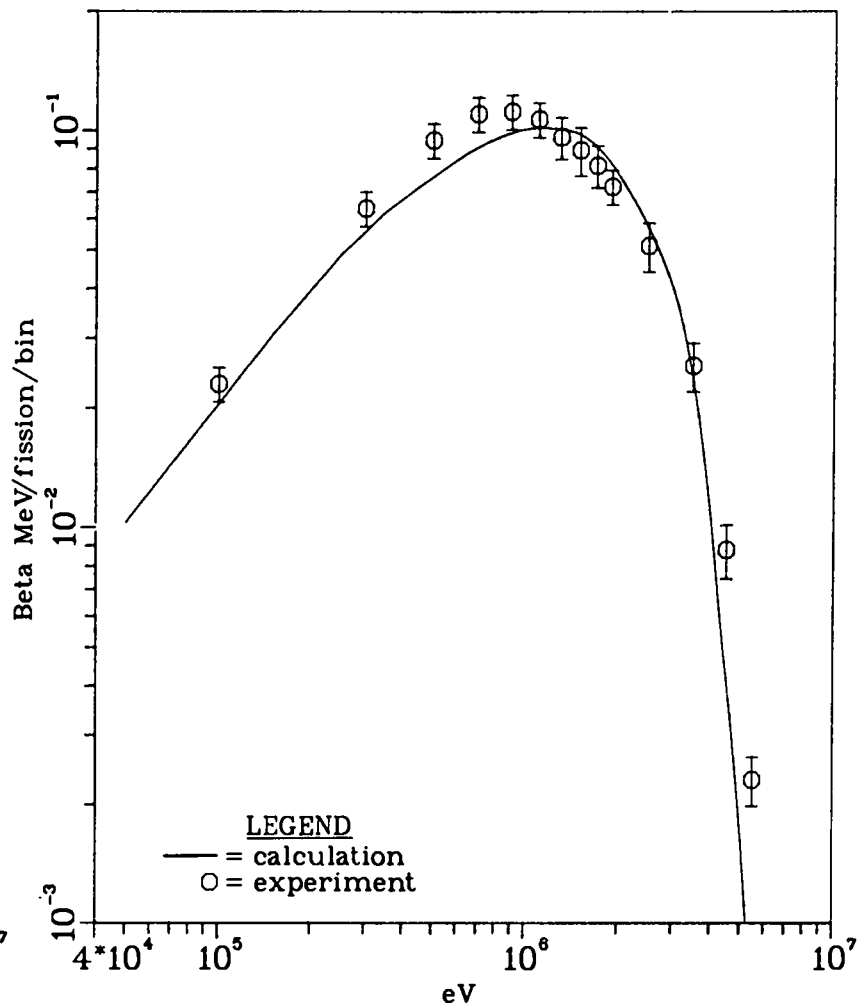

Fig.98. Comparision of calculation with Ul 8-h irradiation, 66-s decay.

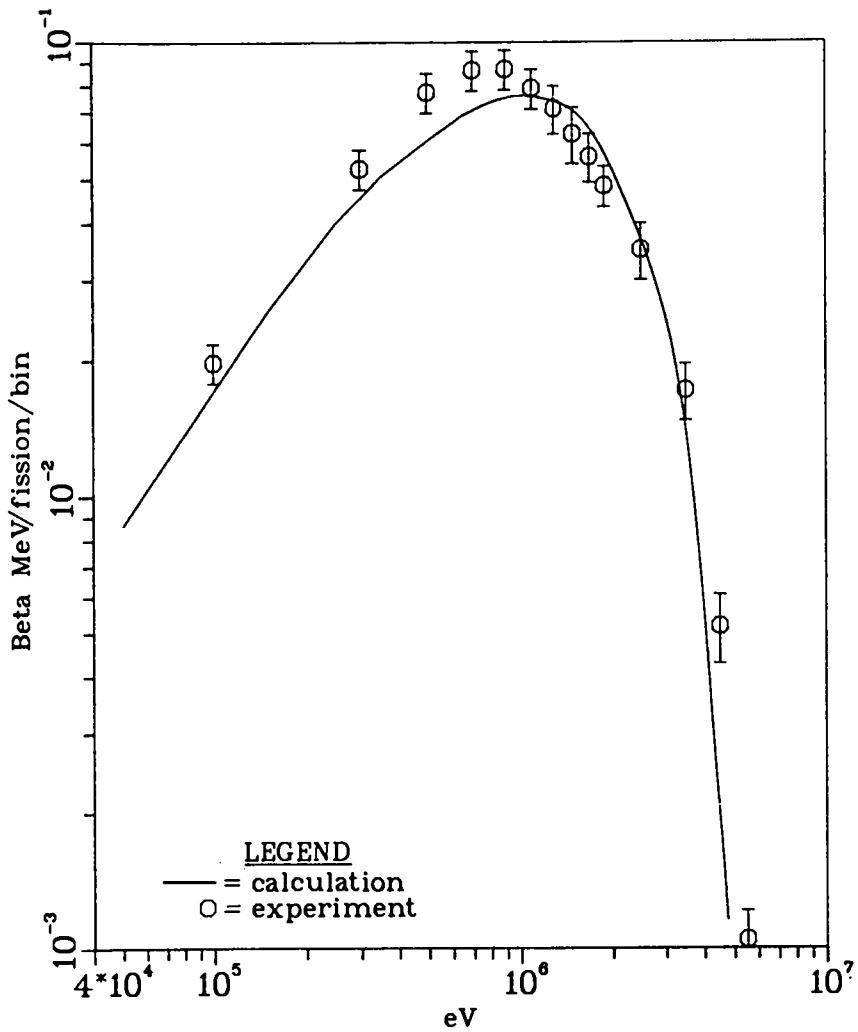

Fig99. Comparison of calculation with UI 8-h irradiation, 210-s decay.

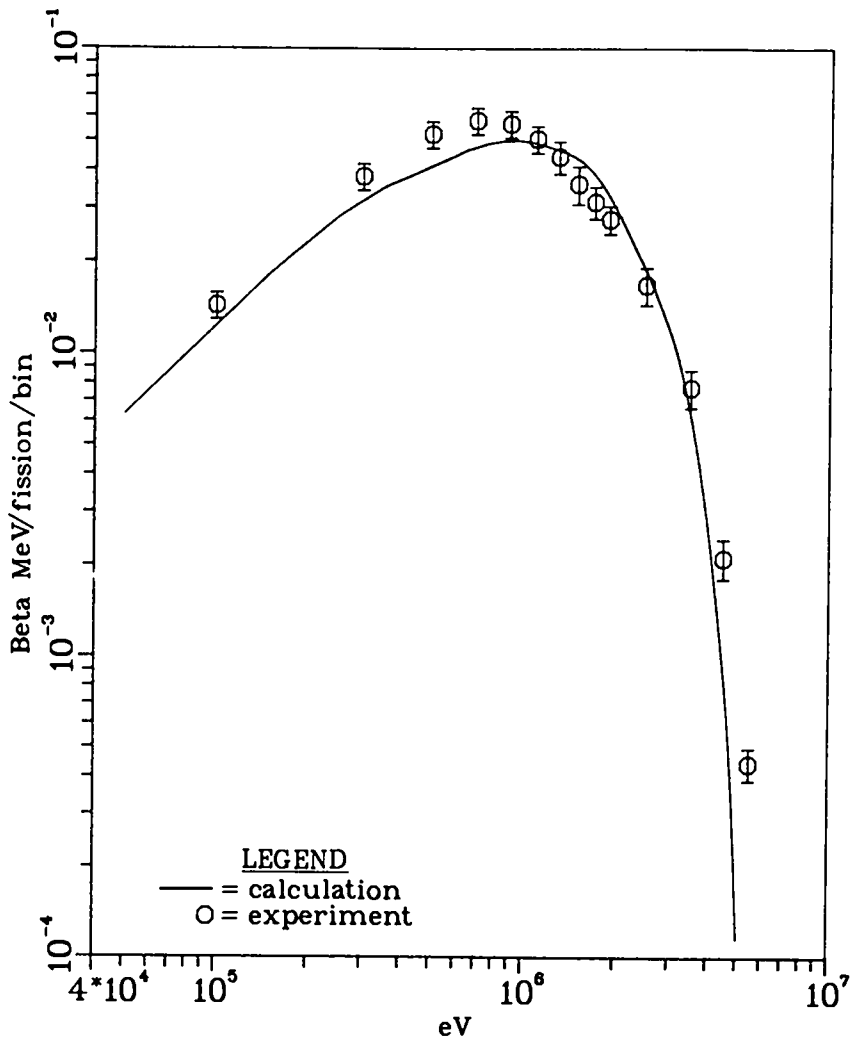

Fig100. Comparison of calculation with UI 8-h irradiation, 960-s decay.

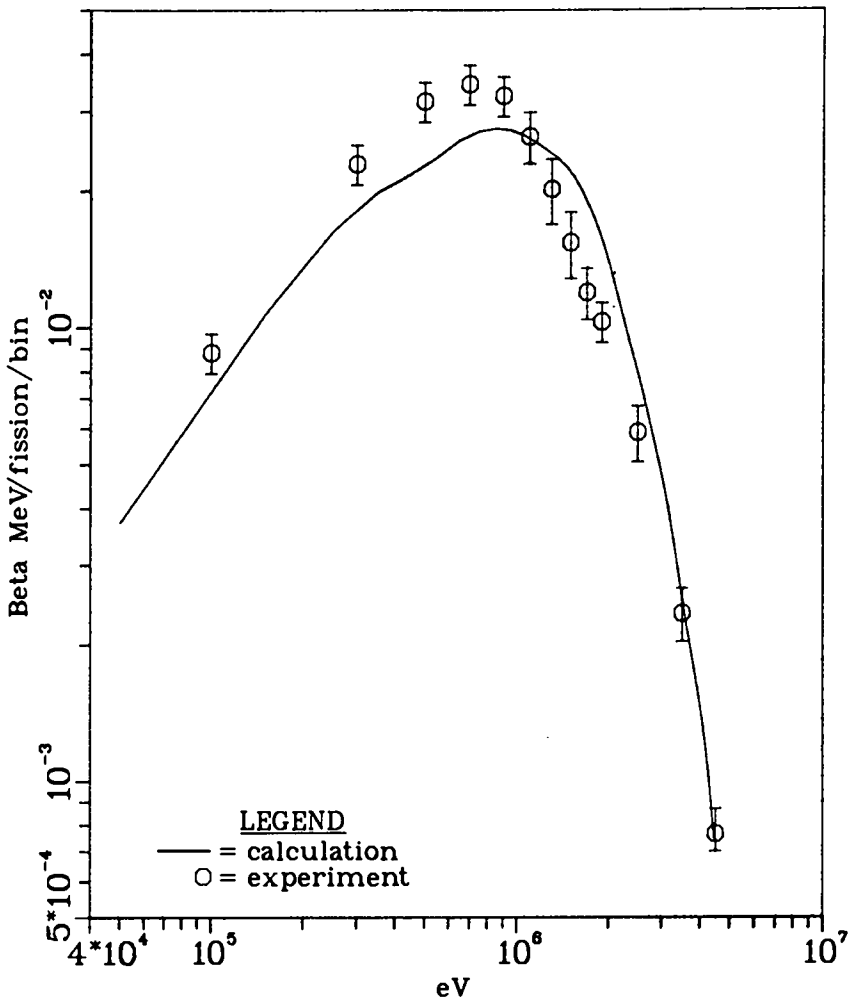

Fig101. Comparison of calculation with UI 8-h irradiation, 3750-s decay.

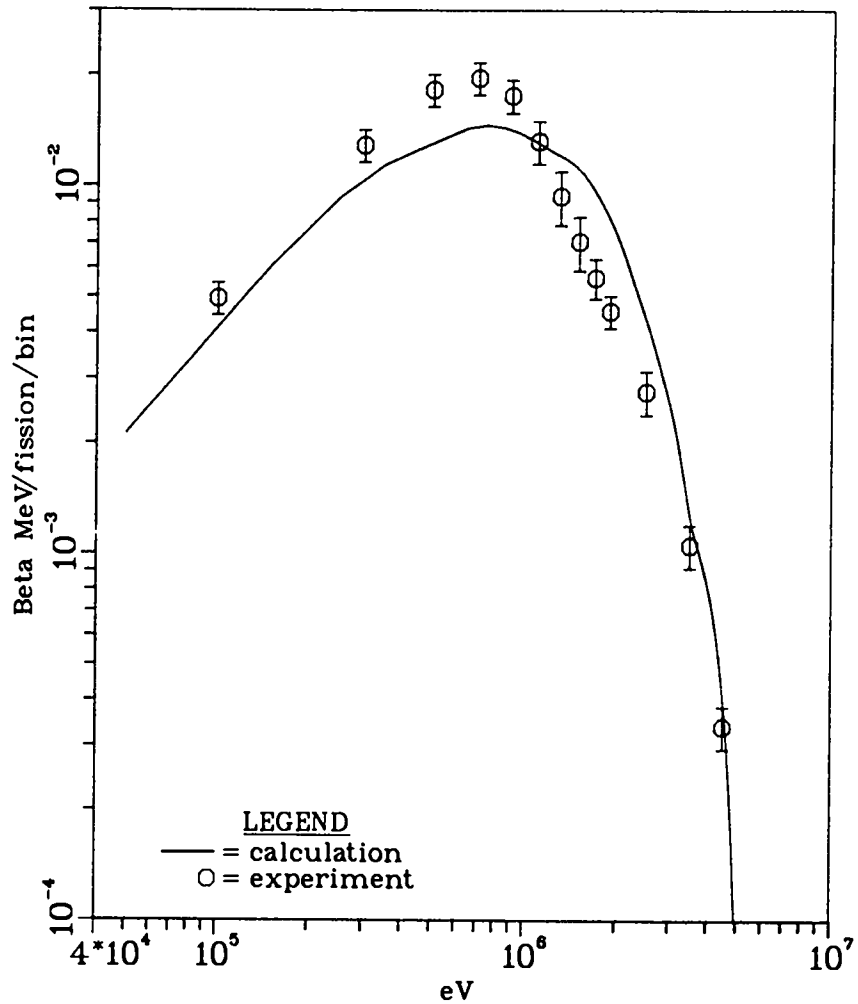

Fig.102. Comparison of calculation with UI 8-h irradiation, 10950-s decay.

☆ U.S. GOVERNMENT PRINTING OFFICE: 1977—777-018/102